Boronic acid with high oxidative stability and utility in biological contexts

Brian J. Graham, Ian W. Windsor, Brian Gold, and Ronald T. Raines

Department of Chemistry, Massachusetts Institute of Technology, Cambridge, MA 02139

Content	Page
Table of Contents	S1
Chemical Synthesis	S2–S8
Supplemental References	S8
Tables S1–S7. Crystallographic data for BOL·H_2O	S9–S12
Table S8. Values of $\Delta\varepsilon$ During Oxidation Reactions	S12
Table S9. Second-Order Rate Constants for the Oxidation of Boronic Acids	S13
Table S10. Calculated Energies of Substrates, Transition States, and Products	S13
Table S11. Calculated Energies of Activation and Reaction	S13
Table S12. Experimental and Computational Kinetic Parameters for Boronic Acid Oxidation	S14
Table S13. Boron–Oxygen and Competing Donor–Acceptor Interaction Energies	S14
Table S14. Inhibition of Transthyretin Fibril Formation by Stilbene **1**	S15
Table S15. Crystallographic Data-Collection and Refinement for the TTR·Stilbene **1** Complex	S16
Fig. S1. Representative ^{11}B-NMR spectra for the determination the pK_a values of 2-CPBA	S17–S19
Fig. S2. Crystal-packing diagram of hydrated BOL	S20
Fig. S3. UV-Spectroscopic basis for assays of the oxidation of boronic acids	S21
Fig. S4. Kinetic traces of the oxidation of boronic acids by hydrogen peroxide at pH 7.4	S22
Fig. S5. ^{1}H-NMR spectra acquired during the oxidation of boronic acids	S23–S26
Fig. S6. Optimized structures during the oxidation of boronic acids	S27
Fig. S7. Graph of k_{obs} values for the oxidation of PBA and representative derivatives	S28–S29
Fig. S8. ^{1}H-NMR spectra for the determination of the affinity of BOL for saccharides	S30
Fig. S9. ^{1}H-NMR spectra for the determination of the k_{on} value for PBA + nopoldiol-PEG	S31
Fig. S10. ^{1}H-NMR spectra for the determination of the affinity of BL for nopoldiol-PEG	S32
Fig. S11. Electron density of stilbene **1** bound to transthyretin	S33
Atomic Coordinates of Optimized Structures	S34–S38
NMR Spectra	S40–S54

Chemical Synthesis

General

Column chromatography was performed with a Biotage Isolera automated purification system using prepacked SNAP KP silica gel columns or SNAP Ultra HP-Sphere C18 columns for reversed-phase purification if specified. Preparative HPLC purification was performed on an Agilent Technologies 1260 Infinity II instrument with a VP250/21 Nucleosil 100-5 C18 column from Macherey–Nagel.

High-resolution mass spectra were obtained with an AccuTOF-DART 4G from JEOL by helium DART ionization. Low-resolution mass spectra were obtained with an ExpressionL CMS from Advion using APCI ionization.

The phrase "concentrated under reduced pressure" refers to the removal of solvents and other volatile materials with a rotary evaporator at water-aspirator pressure (<20 Torr) and a water bath at <40 °C. Residual solvent was removed from samples by the vacuum (<0.1 Torr) achieved by using a mechanical belt-drive oil pump.

All procedures were performed in air at ambient temperature (~22 °C) and pressure (1.0 atm) unless indicated otherwise.

Potassium Phenyltrifluoroborate. Phenylboronic acid (1.0575 g, 8.7 mmol, 1 equiv) was dissolved in 60 mL of methanol, and 8.7 mL of a 4.5 M aqueous solution of KHF_2 (4.5 equiv) was added slowly to the resulting solution. The reaction mixture was stirred for 30 min, then concentrated under reduced pressure. The residue was taken up in hot acetone, filtered, and rinsed with hot acetone. The filtrate was concentrated and allowed to crystallize from a minimum volume of acetone/diethyl ether. The product (1.6088 g, 8.7 mmol, quant) was isolated as a white crystalline solid. **^{1}H NMR** (400 MHz, acetone-d_6, δ): 7.48 (d, J = 7.2 Hz, 2H), 7.07 (dq, J = 14.1, 7.1 Hz, 3H). **^{13}C NMR** (101 MHz, acetone-d_6, δ): 130.56, 125.23, 124.16, 28.57, 28.37, 28.18, 27.99, 27.80, 27.61, 27.41. **^{11}B NMR** (128 MHz, acetone-d_6, δ): 3.43, 2.97, 2.50, 2.03. **^{19}F NMR** (376 MHz, acetone-d_6, δ): −143.42, −143.52, −143.68, −143.82. **HRMS** (DART–TOF) (m/z): [M^-] calcd for $C_6H_5BF_3^-$, 145.0442; found, 145.0493.

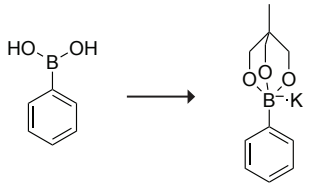

Phenylboronic Acid–Cyclictriol Complex. Phenylboronic acid (1.0672 g, 8.8 mmol, 1 equiv) and 1,1,1-tris(hydroxymethyl)ethane (1.0519 g, 8.8 mmol, 1 equiv) were dissolved in 50 mL of toluene. The resulting solution was heated at reflux with a Dean–Stark trap for 4 h, and then cooled and concentrated under reduced pressure. The residue was dissolved in 50 mL of toluene. Potassium hydroxide (0.4040 g, 7.92 mmol, 0.9 equiv) was added to the resulting solution, and the mixture was heated at reflux with a Dean–Stark trap for 4 h, then allowed to cool to room temperature. The resulting precipitate was isolated by filtration, rinsing with acetone. The product (1.4151 g, 5.8 mmol, 66%) was isolated as a white solid. **^{1}H NMR** (400 MHz, DMSO-d_6, δ): 7.36–7.29 (m, 2H), 7.00 (dd, J = 7.8, 6.3 Hz, 2H), 6.96–6.90 (m, 1H), 3.59 (s, 6H), 0.49 (s, 3H). **^{13}C**

NMR (101 MHz, DMSO-d_6, δ): 132.02, 125.58, 124.09, 73.50, 40.06, 39.86, 39.65, 39.44, 39.23, 39.02, 38.81, 34.38, 16.20. **^{11}B NMR** (128 MHz, DMSO-d_6, δ): 1.32. **HRMS** (DART–TOF) (*m*/*z*): [M^-] calcd for $C_{11}H_{14}BO_3^-$, 205.1041; found, 205.1139.

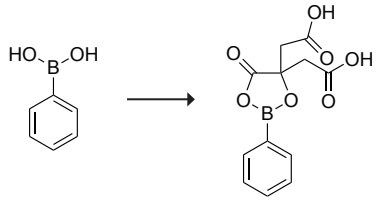

Phenylboronic Acid–Citrate Complex. Phenylboronic acid (0.6157 g, 5.1 mmol, 1 equiv) and citric acid monohydrate (1.0614 g, 5.1 mmol, 1 equiv) were dissolved in 15 mL of ethyl acetate, and the resulting solution was stirred at 70 °C for 10 min. The solution was then concentrated under reduced pressure, resulting in crystallization. Crystals were rinsed with hexanes, then dried under high vacuum. The product (1.1054 g, 4.0 mmol, 78%) was isolated as a white crystalline solid. **^{1}H NMR** (400 MHz, DMSO-d_6, δ): 11.60 (s, 3H), 7.52–7.38 (m, 2H), 7.27–7.10 (m, 3H), 2.71 (d, J = 15.6 Hz, 2H), 2.60 (d, J = 15.6 Hz, 2H). **^{13}C NMR** (101 MHz, DMSO-d_6, δ): 178.93, 171.17, 132.17, 127.29, 76.47, 42.03. **^{11}B NMR** (128 MHz, DMSO-d_6, δ): 8.66. **HRMS** (DART–TOF) (*m*/*z*): [M − H^+] calcd for $C_{12}H_{10}BO_7^-$, 277.0525; found, 277.0719.

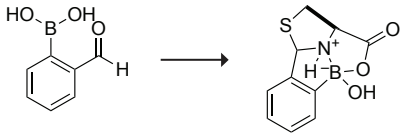

2-Formylphenylboronic Acid–Cysteine Complex (S1)**.** 2-Formylphenylboronic acid (0.3043 g, 2.03 mmol, 1 equiv) was dissolved in 15 mL of water. A solution of L-cysteine (0.2460 g, 2.03 mmol, 1 equiv) in 2 mL of water was added, and the mixture was allowed to stand for 30 min. The resulting crystals were isolated by filtration, rinsed with water, and dried under high vacuum. The product (0.4237 g, 1.8 mmol, 89%) was isolated as a white crystalline solid. **^{1}H NMR** (400 MHz, DMSO-d_6, δ): 8.67 (s, 1H), 7.36 (dd, J = 5.4, 3.1 Hz, 1H), 7.24 (dt, J = 7.3, 3.7 Hz, 2H), 7.15 (dd, J = 5.4, 3.3 Hz, 1H), 6.10 (s, 1H), 4.71 (s, 1H), 4.67 (dd, J = 6.0, 2.7 Hz, 1H), 3.47 (dd, J = 12.2, 5.9 Hz, 1H), 3.38 (dd, J = 12.3, 2.7 Hz, 1H), 3.34 (s, 2H). **^{13}C NMR** (101 MHz, DMSO-d_6, δ): 172.01, 142.59, 129.59, 127.96, 127.87, 122.41, 72.00, 64.65, 37.33. **^{11}B NMR** (128 MHz, DMSO-d_6, δ): 11.03. **HRMS** (DART–TOF) (*m*/*z*): [M − H^+] calcd for $C_{10}H_9BNO_3S^-$, 234.0402; found, 234.0544.

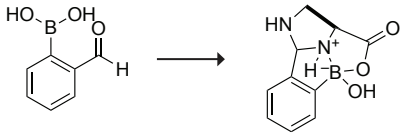

2-Formylphenylboronic Acid–Diaminopropionic Acid Complex (S2)**.** 2-Formylphenylboronic acid (0.3536 g, 2.35 mmol, 1 equiv) and 3-amino-L-alanine hydrochloride (0.3317 g, 2.35 mmol, 1 equiv) were dissolved in 5 mL of water, and the pH of the resulting solution was adjusted to 7.4 with aliquots of 10 M sodium hydroxide. Methanol (5 mL) was added, and the resulting solution was allowed to stand overnight. Solvent was removed by lyophilization. The resulting solid was dissolved in a minimum volume of methanol and allowed to crystallize. The product (0.1507 g, 0.69 mmol, 29%) was isolated as a white crystalline solid. **^{1}H NMR** (400 MHz, DMSO-d_6, δ): 7.33 (dd, J = 5.6, 2.9 Hz, 1H), 7.22 (ddd, J = 9.8, 5.8, 3.4 Hz, 3H), 5.64 (d, J

= 8.8 Hz, 1H), 4.10 (dd, *J* = 7.2, 4.9 Hz, 1H), 3.42 (q, *J* = 9.3 Hz, 1H), 3.37–3.24 (m, 1H), 3.01–2.88 (m, 1H). **^{13}C NMR** (101 MHz, DMSO-d_6, δ): 173.19, 142.77, 129.12, 127.85, 127.53, 123.35, 83.94, 60.90, 51.45. **^{11}B NMR** (128 MHz, DMSO-d_6, δ): 10.64. **HRMS** (DART–TOF) (*m*/*z*): [M − H$^+$] calcd for $C_{10}H_{10}BN_2O_3^-$, 217.0790, found, 217.0927.

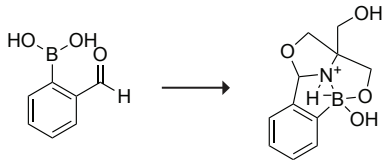

2-Formylphenylboronic Acid–Tris Base Complex (S3)**.** 2-Formylphenylboronic acid (0.3131 g, 2.09 mmol, 1 equiv) and Tris base (0.2530 g, 2.09 mmol, 1 equiv) were dissolved in 16 mL of 3/1 acetonitrile:water. The resulting solution was allowed to stand for 1 week. Solvent was removed by lyophilization. The resulting white solid was dissolved in a minimum volume of 1:1 acetonitrile/acetone and allowed to crystallize. The product (0.4238 g, 1.8 mmol, 86%) was isolated as a white solid. **^{1}H NMR** (400 MHz, DMSO-d_6, δ): 7.32–7.14 (m, 4H), 6.93 (d, *J* = 6.5 Hz, 1H), 5.99 (d, *J* = 6.4 Hz, 1H), 5.29 (t, *J* = 5.6 Hz, 1H), 3.92 (d, *J* = 8.8 Hz, 1H), 3.86 (s, 1H), 3.77 (d, *J* = 9.5 Hz, 1H), 3.74–3.59 (m, 3H), 3.10 (d, *J* = 9.5 Hz, 1H). **^{13}C NMR** (101 MHz, DMSO-d_6, δ): 142.45, 129.36, 128.36, 126.88, 123.09, 92.91, 71.97, 70.45, 66.21, 60.40. **^{11}B NMR** (128 MHz, DMSO-d_6, δ): 13.09. **HRMS** (DART–TOF) (*m*/*z*): [M − H$^+$] calcd for $C_{11}H_{13}BNO_4^-$, 234.0943; found, 234.1109.

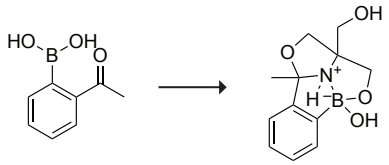

2-Acetylphenylboronic Acid–Tris Base Complex (S3)**.** 2-Acetylphenylboronic acid (0.3457 g, 2.1 mmol, 1 equiv) and Tris base (0.2554 g, 2.1 mmol, 1 equiv) were dissolved in 16 mL of 3/1 acetonitrile:water. The resulting solution was stirred for 1 h. Solvent was removed by lyophilization. The resulting white solid was suspended in 3 mL of acetonitrile overnight, then solid isolated by filtration, rinsed with acetonitrile, and dried under high vacuum. The product (0.2345 g, 0.94 mmol, 45%) was isolated as a white solid. **^{1}H NMR** (400 MHz, DMSO-d_6, δ): 7.38–7.11 (m, 4H), 6.44 (s, 1H), 5.23 (t, *J* = 5.9 Hz, 1H), 3.96 (d, *J* = 8.8 Hz, 1H), 3.87 (s, 1H), 3.71 (d, *J* = 9.5 Hz, 1H), 3.60 (dd, *J* = 5.8, 1.9 Hz, 2H), 3.45 (d, *J* = 8.8 Hz, 1H), 3.32 (s, 1H), 3.09 (d, *J* = 9.5 Hz, 1H), 1.68 (s, 3H). **^{13}C NMR** (101 MHz, DMSO-d_6, δ): 146.11, 128.88, 128.02, 127.06, 121.59, 100.43, 71.69, 70.91, 66.84, 61.34, 25.39. **^{11}B NMR** (128 MHz, DMSO-d_6, δ): 13.02. **HRMS** (DART–TOF) (*m*/*z*): [M − H$^+$] calcd for $C_{12}H_{15}BNO_4^-$, 248.1100; found, 248.1286.

Synthesis of (−)-Nopoldiol–PEG

(−)-Nopol–PEG

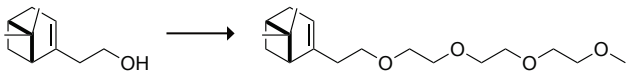

13-((1*R*,5*S*)-6,6-Dimethylbicyclo[3.1.1]hept-2-en-2-yl)-2,5,8,11-tetraoxatridecane (6). Triethyleneglycol monomethyl ether (8 mL, 50 mmol, 1 equiv) was dissolved in 100 mL of dry DCM. Triethylamine (8.4 mL, 60 mmol, 1.2 equiv) and *p*-toluenesulfonyl chloride (11.4390 g, 60

mmol, 1.2 equiv) were added, and the reaction mixture was allowed to stir overnight and then concentrated under reduced pressure. The residue was suspended in 50 mL of EtOAc, and the resulting triethylammonium chloride crystals were removed by filtration. The filtrate was concentrated, passed through a short silica plug eluting 3:1 EtOAc/hexanes, and concentrated to a pale yellow liquid, which was used without further purification (17.1290 g, quant). In a dry flask at 0 °C under N_2(g), NaH (60% w/w in mineral oil, 0.9152 g, 22.1 mmol, 1.3 equiv) was suspended in 20 mL of dry DMF. (−)-Nopol (3 mL, 17.6 mmol, 1 equiv) was added dropwise, and the resulting mixture was allowed to stir at 0 °C for 30 min. Triethyleneglycol monomethyl ether tosylate (14.0087 g, 44 mmol, 2.5 equiv) was added slowly, and the reaction mixture was allowed to warm to room temperature and stir overnight. The reaction mixture was diluted with 50 mL of saturated aqueous NH_4Cl and extracted with EtOAc (3 × 50 mL). The combined organics were washed with water (2 × 50 mL) and brine, dried over $MgSO_4$(s), filtered, and concentrated, and purified by chromatography on silica gel (EtOAc/hexanes; product eluted at 40% v/v EtOAc) to yield (−)-nopol–PEG as a pale yellow liquid (2.2406 g, 7.17 mmol, 41%). (7.6779 g of unreacted triethyleneglycol monomethyl ether tosylate was also recovered, eluting in a broad band from 50–100% v/v EtOAc). **^{1}H NMR** (400 MHz, chloroform-*d*, *δ*): 5.25 (dt, 1H, *J* = 3.2, 1.6), 3.71–3.61 (m, 8H), 3.56 (ddd, 4H, *J* = 9.7, 6.0, 3.9 Hz), 3.53–3.42 (m, 2H), 3.38 (s, 3H), 2.34 (dt, 1H, *J* = 8.6, 5.7 Hz), 2.31–2.14 (m, 4H), 2.05 (tdd, 2H, *J* = 11.3, 4.9, 1.9 Hz), 1.26 (s, 3H), 1.14 (d, 1H, *J* = 8.5 Hz), 0.82 (s, 3H). **^{13}C NMR** (101 MHz, chloroform-*d*, *δ*): 145.12, 117.89, 72.02, 70.71, 70.70, 70.68, 70.60, 70.10, 69.85, 59.09, 45.95, 40.83, 38.06, 37.15, 31.70, 31.41, 26.41, 21.24. **HRMS** (DART–TOF) (*m*/*z*): $[M + H]^+$ calcd for $C_{18}H_{33}O_4$, 313.2379; found, 313.2377.

(−)-Nopoldiol–PEG

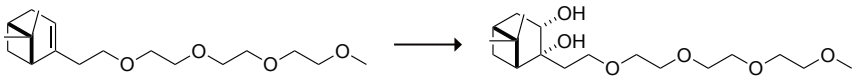

(1*R*,2*R*,3*S*,5*R*)-6,6-Dimethyl-2-(2,5,8,11-tetraoxatridecan-13-yl)bicyclo[3.1.1]heptane-2,3-diol (7). (−)-Nopol-PEG (1.7313 g, 5.54 mmol, 1 equiv) was dissolved in 20 mL of *i*PrOH. 2,6-Lutidine (0.78 mL, 6.7 mmol, 1.2 equiv) and NMO (50% w/v in water, 1.5 mL, 7.2 mmol, 1.3 equiv) were added, followed by $K_2OsO_4 \cdot 2H_2O$ from Millipore–Sigma (0.0405 g, 0.11 mmol, 0.02 equiv). The reaction mixture was heated at reflux (95 °C) under ambient atmosphere overnight, then concentrated under reduced pressure and diluted with 50 mL of EtOAc. The solution was washed with 10 mL of 1 N HCl, water, and brine, dried over $MgSO_4$(s), filtered, and purified by chromatography on silica gel (EtOAc/hexanes; product eluted at 100% v/v EtOAc) to yield (−)-nopoldiol–PEG as a dark yellow liquid (0.6179 g, 1.78 mmol, 30%). **^{1}H NMR** (400 MHz, chloroform-*d*, *δ*): 4.37 (s, 1H), 4.19 (dt, 1H, *J* = 9.6, 5.9 Hz), 4.11 (d, 1H, *J* = 6.3 Hz), 3.86 (td, 1H, *J* = 9.6, 2.6 Hz), 3.72–3.51 (m, 14H), 3.38 (s, 4H), 2.40 (dddd, 1H, *J* = 13.5, 9.6, 3.8, 2.5 Hz), 2.15 (dtd, 1H, *J* = 10.1, 6.1, 2.4 Hz), 2.03–1.94 (m, 2H), 1.93–1.84 (m, 1H), 1.64 (ddd, 1H, *J* = 13.9, 5.7, 2.3 Hz), 1.53 (ddd, 1H, *J* = 14.8, 5.2, 2.7 Hz), 1.46 (d, 1H, *J* = 10.2 Hz), 1.26 (s, 3H), 0.95 (s, 3H).**^{13}C NMR** (101 MHz, chloroform-*d*, *δ*): 74.35, 71.96, 70.56, 70.09, 70.05, 67.77, 67.42, 59.06, 54.34, 41.80, 40.57, 38.61, 37.41, 28.15, 28.06, 24.38 (missing carbon peaks are likely hidden under the solvent peak, as reported previously (S4)). **HRMS** (DART–TOF) (*m*/*z*): $[M + H]^+$ calcd for $C_{18}H_{35}O_6$, 347.2434; found, 347.2449.

Synthesis of Stilbene 1

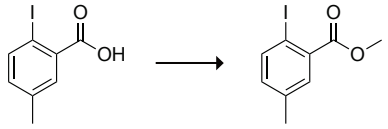

2

Methyl 2-Iodo-5-methylbenzoate (2). To a solution of 5.0040 g (19.1 mmol) 2-iodo-5-methylbenzoic acid in 100 mL methanol was added 1 mL concentrated sulfuric acid. The mixture was heated at reflux 19 h, then allowed to cool to room temperature. The solution was diluted with 100 mL of 1 N NaOH and extracted with DCM (3 × 100 mL). The organic layers were combined, washed with brine, dried with $MgSO_4$(s), filtered, and concentrated under reduced pressure to yield compound **2** as a pale yellow liquid (4.9182 g, 93%) which was used without further purification. **^{1}H NMR** (600 MHz, chloroform-*d*, *δ*): 7.81 (d, 1H, *J* = 8.1 Hz), 7.60 (d, 1H, *J* = 2.4 Hz), 6.94 (dd, 1H, *J* = 8.3, 2.3 Hz), 3.91 (s, 3H), 2.30 (s, 3H). **^{13}C NMR** (151 MHz, chloroform-*d*, *δ*): 167.0, 141.0, 138.1, 134.8, 133.7, 131.7, 90.0, 52.4, 20.8. **HRMS** (DART–TOF) (*m*/*z*) $[M + H]^+$ calcd for $C_9H_{10}IO_2$, 276.9725; found, 276.9794.

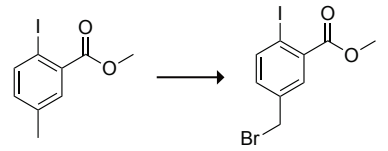

2 **3**

Methyl 5-(Bromomethyl)-2-iodobenzoate (3). To a solution of methyl 2-iodo-5-methylbenzoate (4.6517 g, 16.9 mmol) in dry acetonitrile was added 1,3-dibromo-5,5-dimethylhydantoin (2.8878 g, 10.1 mmol, 0.6 equiv) and AIBN (0.2775 g, 1.69 mmol, 0.1 equiv). The mixture was heated at reflux under N_2(g) for 4 h, then allowed to cool, diluted with 50 mL DCM, washed with a dilute aqueous solution of sodium bisulfite and brine, and dried over $MgSO_4$(s), filtered, and concentrated under reduced pressure. Residue was passed through a short silica plug eluting with DCM, and the eluant concentrated under reduced pressure, then crystallized from DCM/hexanes to yield compound **3** as a pale orange solid (3.0459 g, 8.6 mmol, 51%) of sufficient purity to carry forward. **^{1}H NMR** (600 MHz, chloroform-*d*, *δ*): 7.99 (d, 1H, *J* = 8.1 Hz), 7.85 (d, 1H, *J* = 2.4 Hz), 7.21 (dd, 1H, *J* = 8.1, 2.3 Hz), 4.45 (s, 2H), 3.97 (s, 3H). **^{13}C NMR** (151 MHz, chloroform-*d*, *δ*): 166.37, 141.96, 138.04, 135.48, 133.09, 131.45, 93.95, 52.63, 31.47. **HRMS** (DART–TOF) (*m*/*z*): $[M + H]^+$ calcd for $C_9H_9BrIO_2$, 354.8831; found, 354.8840.

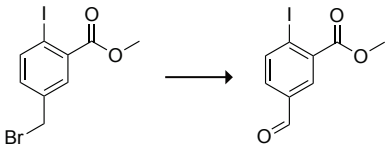

3 **4**

Methyl 5-Formyl-2-iodobenzoate (4). 4-Methylmorpholine *N*-oxide (4.4048 g, 37.6 mmol, 4 equiv) was dissolved in 40 mL of dry THF under N_2(g), compound **3** (3.3495 g, 9.4 mmol) was added, and the mixture was stirred at reflux for 4 h, cooled to room temperature, and diluted with 50 mL of water. The mixture was extracted with EtOAc (3 × 50 mL), the organic layers were combined, washed with water and brine, dried over $MgSO_4$(s), filtered, and concentrated under reduced pressure. The product was purified by chromatography on silica gel (EtOAc/hexanes; product eluted at 25% v/v EtOAc) to yield compound **4** as a white solid of sufficient purity to carry

forward (2.4140 g, 8.3 mmol, 88%). **^{1}H NMR** (600 MHz, chloroform-*d*, *δ*): 10.01 (s, 1H), 8.27 (d, 1H, *J* = 2.1 Hz), 8.21 (d, 1H, *J* = 8.1 Hz), 7.64 (dd, J = 8.1, 2.1 Hz, 1H), 3.99 (s, 3H). **^{13}C NMR** (151 MHz, chloroform-*d*, *δ*): 190.56, 165.95, 142.57, 135.50, 132.68, 131.94, 131.90, 102.38, 52.86. **HRMS** (DART–TOF) (*m*/*z*): $[M + H]^+$ calcd for $C_9H_8IO_3$, 290.9518; found, 290.9521.

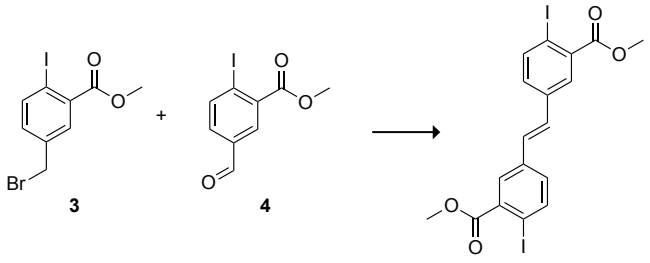

3 **4** **5**

Dimethyl 5,5′-(Ethene-1,2-diyl)(*E*)-bis(2-iodobenzoate) (5). Compound **3** (1.0102 g, 3.48 mmol, 1 equiv) was dissolved in 0.72 mL triethyl phosphite (4.18 mmol, 1.2 equiv), and the resulting solution was heated at 150 °C for 4 h, then cooled in an ice water bath, and diluted with 10 mL dry DMF. NaH (60% w/w in mineral oil; 0.1948 g, 4.87 mmol, 1.4 equiv) was added, and the mixture was stirred for 20 min at 0 °C to produce an orange solution. A solution of compound **4** in 5 mL dry DMF was added dropwise, and the mixture was stirred at room temperature overnight. The mixture was diluted with EtOAc, washed with saturated aqueous NH_4Cl and brine, dried over $MgSO_4$(s), filtered, concentrated under reduced pressure, and then crystallized twice from EtOAc to yield compound **5** as pale yellow-brown crystals of sufficient purity to carry forward (0.5968 g, 1.09 mmol, 32%). **^{1}H NMR** (600 MHz, chloroform-*d*, *δ*): 8.00 (d, 2H, *J* = 8.3 Hz), 7.93 (d, 2H, *J* = 2.2 Hz), 7.52 (dd, 2H, *J* = 8.3, 2.3 Hz), 7.40 (s, 2H), 3.89 (s, 6H). **^{13}C NMR** (151 MHz, DMSO-d_6, *δ*): 167.41, 141.42, 137.28, 136.82, 130.87, 128.85, 128.75, 93.65, 53.04. **HRMS** (DART–TOF) (*m*/*z*): $[M + H]^+$ calcd for $C_{18}H_{15}I_2O_4$, 548.9060; found, 548.9076.

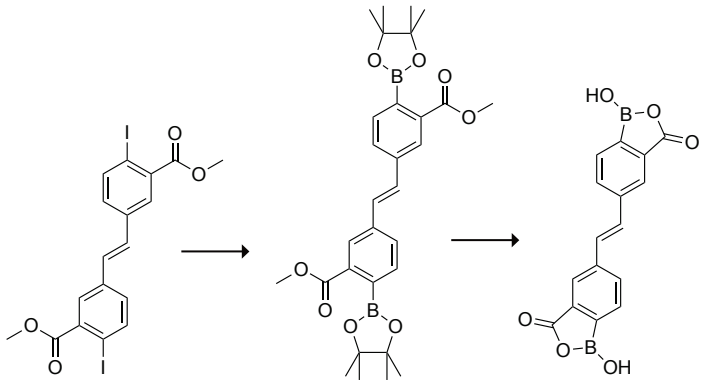

5 **1**

(*E*)-5,5′-(Ethene-1,2-diyl)bis(1-hydroxybenzo[*c*][1,2]oxaborol-3(*1*H)-one) (1). Compound **4** (0.2357 g, 0.43 mmol, 1 equiv) and 2-isopropoxy-4,4,5,5-tetramethyl-1,3,2-dioxaborolane (0.36 mL, 1.3 mmol, 3 equiv) were dissolved in 3 mL of dry THF at 0 °C. A solution of isopropylmagnesium chloride lithium chloride complex (1.3 M in THF, 0.79 mL, 1.03 mmol, 2.4 equiv) was added dropwise over 5 min, and the resulting solution was stirred for 10 min at 0 °C, then quenched by the addition of 20 mL of saturated aqueous NH_4Cl. The resulting solution was extracted with 20 mL of EtOAc. The organic layers were combined and washed with 10 mL of saturated aqueous NH_4Cl. The combined aqueous layers were extracted with EtOAc (2 × 20 mL).

The combined organic layers were dried over $MgSO_4$(s), filtered, concentrated under reduced pressure, and passed through a short silica plug, eluting with DCM, and concentrated to a pale yellow oil. The oil was dissolved in 5 mL of 1:1 H_2O/THF, and 10 equiv of $LiOH \cdot H_2O$ was added (0.1762 g, 4.2 mmol, 10 equiv). The mixture was stirred at room temperature overnight, then cooled to 0 °C and acidified to pH < 2 with concentrated aqueous HCl. The mixture was extracted with EtOAc (3 × 10 mL), washed with brine, dried over $MgSO_4$(s), filtered, and concentrated under reduced pressure. The resulting solid was dissolved in 5.5 mL of 10:1 THF/H_2O and $NaIO_4$ (0.2781 g, 1.3 mmol, 3 equiv) was added. The resulting mixture was stirred 20 min, then 1 mL of 1 N HCl was added, and the mixture was stirred for 2 h, then concentrated under reduced pressure and separated by reversed-phase column chromatography (water/acetonitrile, product eluted at 40% v/v CH_3CN in H_2O). The product was isolated by lyophilization to yield a white solid that exhibited blue fluorescence under UV illumination. The product was purified further by preparative HPLC (0.1% v/v TFA in H_2O/CH_3CN; product eluted at 40%), taking only the central peak fractions to yield stilbene **1** as a fluffy white solid (0.0076 g, 0.024 mmol, 6%). **^{1}H NMR** (400 MHz, methanol-d_4, δ): 8.16 (d, 2H, J = 1.6 Hz), 7.83 (dd, 2H, J = 7.7, 1.6 Hz), 7.47 (d, 2H, J = 7.6 Hz), 7.35 (s, 2H). **^{13}C NMR** (101 MHz, methanol-d_4, δ): 170.95, 137.57, 134.42, 130.28, 130.22, 128.48, 125.38. The carbon bonded directly to the boron was not observed due to quadrupolar broadening. **^{11}B NMR** (128 MHz, methanol-d_4, δ): 24.13. **HRMS** (DART–TOF) (m/z): $[M - H]^-$ calcd for $C_{16}H_9B_2O_6$, 319.0591; found, 319.0432.

Supplemental References

S1. A. Bandyopadhyay, S. Cambray, J. Gao, Fast and selective labeling of N-terminal cysteines at neutral pH via thiazolidino boronate formation. *Chem. Sci.* **7**, 4589–4593 (2016).
S2. K. Li, C. Weidman, J. Gao, Dynamic formation of imidazolidino boronate enables design of cysteine-responsive peptides. *Org. Lett.* **20**, 20–23 (2017).
S3. K. Li, M. A. Kelly, J. Gao, Biocompatible conjugation of Tris base to 2-acetyl and 2-formyl phenylboronic acid. *Org. Biomol. Chem.* **17**, 5908–5912 (2019).
S4. B. Akgun, D. G. Hall, Fast and tight boronate formation for click bioorthogonal conjugation. *Angew. Chem. Int. Ed.* **55**, 3909–3913 (2016).

Table S1. Crystal Data and Structure Refinement for BOL·H_2O.

Identification code	CCDC ID 1953993
Empirical formula	$C_7H_7BO_4$
Formula weight	165.94
Temperature	100(2) K
Wavelength	0.71073 Å
Crystal system	Monoclinic
Space group	$P2_1/c$
Unit cell dimensions	a = 13.3947(5) Å α = 90° b = 7.9080(3) Å β = 95.3376(12)° c = 7.0529(2) Å γ = 90°
Volume	743.84(4) $Å^3$
Z	4
Density (calculated)	1.482 Mg/m^3
Absorption coefficient	0.119 mm^{-1}
F_{000}	344
Crystal size	0.450 × 0.400 × 0.080 mm^3
Theta range for data collection	1.527 to 36.330°
Index ranges	$-22 \le h \le 22$, $-13 \le k \le 13$, $-11 \le l \le 11$
Reflections collected	51761
Independent reflections	3598 [R_{int} = 0.0680]
Completeness to theta = 25.242°	99.9%
Absorption correction	Semi-empirical from equivalents
Refinement method	Full-matrix least-squares on F^2
Data / restraints / parameters	3598 / 3 / 118
Goodness-of-fit on F^2	1.072
Final R indices [I > 2sigma(I)]	$R1$ = 0.0365, $wR2$ = 0.0990
R indices (all data)	$R1$ = 0.0388, $wR2$ = 0.1012
Extinction coefficient	n/a
Largest diff. peak and hole	0.629 and −0.320 e.$Å^{-3}$

Table S2. Atomic Coordinates (×10^4) and Equivalent Isotropic Displacement Parameters (Å^2 × 10^3) for BOL·H_2O. U_{eq} is defined as one third of the trace of the orthogonalized U_{IJ} tensor.

Atom	*x*	*y*	*z*	U_{eq}
B(1)	1461(1)	3951(1)	4044(1)	9(1)
O(1)	1110(1)	2160(1)	3907(1)	10(1)
O(2)	1382(1)	4478(1)	5992(1)	11(1)
O(3)	741(1)	5015(1)	2725(1)	9(1)
O(4)	796(1)	7021(1)	518(1)	13(1)
C(1)	2511(1)	4345(1)	3192(1)	9(1)
C(2)	2315(1)	5593(1)	1804(1)	10(1)
C(3)	3055(1)	6373(1)	848(1)	13(1)
C(4)	4041(1)	5863(1)	1323(1)	15(1)
C(5)	4263(1)	4622(1)	2713(1)	16(1)
C(6)	3506(1)	3857(1)	3654(1)	13(1)
C(7)	1227(1)	5960(1)	1592(1)	9(1)

Table S3. Anisotropic Displacement Parameters (Å^2 × 10^3) for BOL·H_2O. The anisotropic displacement factor exponent takes the form: $-2\pi^2[h^2a^*U_{11} + ... + 2hka^*b^*U_{12}]$.

Atom	U_{11}	U_{22}	U_{33}	U_{23}	U_{13}	U_{12}
B(1)	10(1)	8(1)	9(1)	1(1)	3(1)	0(1)
O(1)	11(1)	8(1)	10(1)	0(1)	4(1)	–1(1)
O(2)	15(1)	9(1)	9(1)	0(1)	5(1)	1(1)
O(3)	9(1)	9(1)	10(1)	2(1)	3(1)	0(1)
O(4)	13(1)	11(1)	14(1)	4(1)	3(1)	2(1)
C(1)	9(1)	9(1)	10(1)	0(1)	3(1)	0(1)
C(2)	10(1)	9(1)	10(1)	1(1)	4(1)	0(1)
C(3)	13(1)	13(1)	15(1)	3(1)	6(1)	–1(1)
C(4)	11(1)	16(1)	19(1)	1(1)	7(1)	–2(1)
C(5)	10(1)	19(1)	19(1)	1(1)	4(1)	1(1)
C(6)	10(1)	16(1)	14(1)	3(1)	2(1)	2(1)
C(7)	10(1)	8(1)	10(1)	0(1)	3(1)	0(1)

Table S4. Bond Lengths for BOL·H_2O.

Atom	Atom	Length (Å)
B1	O2	1.4487(7)
B1	O1	1.4934(7)
B1	O3	1.5284(7)
B1	C1	1.6095(8)
O1	H1A	0.927(10)
O1	H1B	0.890(10)
O2	H2	0.819(10)
O3	C7	1.3109(7)
O4	C7	1.2377(7)
C1	C6	1.3964(8)
C1	C2	1.3976(8)
C2	C3	1.3931(8)
C2	C7	1.4797(8)
C3	C4	1.3914(9)
C3	H3	0.9500
C4	C5	1.3996(9)
C4	H4	0.9500
C5	C6	1.3996(8)
C5	H5	0.9500
C6	H6	0.9500

Table S5. Bond Angles for BOL·H_2O.

Atom	Atom	Atom	Angle (°)
O2	B1	O1	106.48(4)
O2	B1	O3	108.72(4)
O1	B1	O3	107.76(4)
O2	B1	C1	116.22(5)
O1	B1	C1	116.14(4)
O3	B1	C1	100.97(4)
B1	O1	H1A	118.5(7)
B1	O1	H1B	111.3(7)
H1A	O1	H1B	108.4(10)
B1	O2	H2	110.6(8)
C7	O3	B1	111.30(4)
C6	C1	C2	118.09(5)
C6	C1	B1	135.00(5)
C2	C1	B1	106.54(4)
C3	C2	C1	123.81(5)
C3	C2	C7	127.02(5)
C1	C2	C7	109.14(4)
C4	C3	C2	117.17(5)
C4	C3	H3	121.4
C2	C3	H3	121.4
C3	C4	C5	120.46(5)
C3	C4	H4	119.8
C5	C4	H4	119.8
C6	C5	C4	121.27(5)
C6	C5	H5	119.4
C4	C5	H5	119.4
C1	C6	C5	119.19(5)
C1	C6	H6	120.4
C5	C6	H6	120.4
O4	C7	O3	121.97(5)
O4	C7	C2	126.50(5)
O3	C7	C2	111.53(5)

Table S6. Hydrogen Coordinates ($\times 10^4$) and Isotropic Displacement Parameters ($Å^2 \times 10^3$) for BOL·H_2O.

Atom	*x*	*y*	*z*	U_{eq}
H(1A)	1204(8)	1554(14)	2813(14)	14
H(1B)	468(8)	2077(14)	4129(15)	14
H(2)	1207(9)	5469(13)	6029(16)	16
H(3)	2893	7217	-89	16
H(4)	4567	6361	700	18
H(5)	4940	4292	3024	19
H(6)	3667	3017	4596	16

Table S7. Hydrogen Bonds for BOL·H_2O.[a]

D-H···A	$d_{D\text{-}H}$ (Å)	$d_{H\cdots A}$ (Å)	$d_{D\cdots A}$ (Å)	∠$_{DHA}$ (°)
O(1)-H(1A)···O(2)#1	0.927(10)	1.559(10)	2.4860(6)	178.9(11)
O(1)-H(1B)···O(3)#2	0.890(10)	2.569(11)	3.1332(6)	122.0(9)
O(1)-H(1B)···O(4)#2	0.890(10)	1.734(10)	2.6230(6)	176.7(11)
O(2)-H(2)···O(4)#3	0.819(10)	2.082(10)	2.8885(6)	168.0(11)

[a]Symmetry transformations used to generate equivalent atoms: #1: $x, -y + ½, z - ½$; #2: −x, $y - ½, -z + ½$; #3: $x, -y + {}^3/_2, z + ½$

Table S8. Values of $\Delta\varepsilon$ During Oxidation Reactions ($M^{-1}cm^{-1}$).

pH	Buffer	PBA	BL	BOL	BN	BON
3.2	sodium citrate	1069 ± 2	1336 ± 3	3386 ± 15	1421 ± 10	1819 ± 40
5.0	sodium acetate	962 ± 2	1448 ± 3	3364 ± 9	961 ± 9	1753 ± 11
6.2	sodium citrate	816 ± 5	1521 ± 7	2830 ± 7	1443 ± 45	1746 ± 17
7.3	sodium phosphate	1220 ± 8	1474 ± 9	3332 ± 10	1120 ± 8	1721 ± 45
9.0	sodium borate	1210 ± 6	2025 ± 9	3147 ± 46	1449 ± 9	1602 ± 24
10.5	sodium citrate	1791 ± 9	1940 ± 9	3469 ± 40	822 ± 13	1724 ± 14
7.3	PBS	1029 ± 33	1516 ± 35	2568 ± 266	852 ± 14	1689 ± 17

Table S9. Second-Order Rate Constants for the Oxidation of Boronic Acids ($M^{-1}s^{-1}$).[a]

pH	PBA	BL	BOL	BN	BON
3.2	$(1.3 \pm 0.1) \times 10^{-2}$	$(3.8 \pm 0.2) \times 10^{-3}$	$(2.2 \pm 0.1) \times 10^{-4}$	$(3.7 \pm 0.4) \times 10^{-3}$	$(1.5 \pm 0.5) \times 10^{-2}$
5.0	$(1.2 \pm 0.1) \times 10^{-2}$	$(2.4 \pm 0.1) \times 10^{-2}$	$(1.7 \pm 0.1) \times 10^{-4}$	$(3.8 \pm 0.4) \times 10^{-2}$	$(5.5 \pm 0.6) \times 10^{-2}$
6.2	$(1.8 \pm 0.1) \times 10^{-1}$	$(2.0 \pm 0.1) \times 10^{-1}$	$(1.4 \pm 0.1) \times 10^{-4}$	$(3.2 \pm 0.4) \times 10^{-1}$	$(3.4 \pm 0.2) \times 10^{-2}$
7.3	2.4 ± 0.2	2.4 ± 0.2	$(1.5 \pm 0.1) \times 10^{-4}$	8.1 ± 0.4	$(4.1 \pm 0.2) \times 10^{-2}$
9.0	24 ± 3	4.5 ± 0.4	$(7.1 \pm 2.6) \times 10^{-4}$	40 ± 5	$(6.2 \pm 0.2) \times 10^{-2}$
10.5	53 ± 1	4.7 ± 0.2	$(4.1 \pm 0.1) \times 10^{-2}$	55 ± 5	$(3.9 \pm 0.2) \times 10^{-2}$
7.3[b]	6.5 ± 0.2	3.5 ± 0.1	$(2.8 \pm 0.5) \times 10^{-4}$	48 ± 7	$(4.4 \pm 0.2) \times 10^{-2}$

[a]Each value is the mean ± SD from initial-velocity experiments performed in triplicate with at least three different concentrations of boronic acid and peroxide in the buffers listed in Table S8. [b]Second-order rate constants determined in PBS.

Table S10. Calculated Energies of Starting Materials, Transition States, and Products (Hartrees).

Structure	HF	Zero Point	H	G	Imaginary Frequency
PBA_SM	–559.3340606	–559.192210	–559.181182	–559.227363	—
PBA_TS	–559.2857740	–559.147518	–559.135260	–559.184357	–748.1166
PBA_Prod	–483.4941140	–483.364085	–483.354294	–483.399097	—
2-BL _SM	–597.4252050	–597.275288	–597.263948	–597.311131	—
2-BL_TS	–597.3757670	–597.229576	–597.217704	–597.26600	–743.2438
2-BL_Prod	–521.5891240	–521.450972	–521.441425	–521.485137	—
2-BOL _SM	–671.4918544	–671.360385	–671.348323	–671.397383	—
2-BOL _TS	–671.4329050	–671.305185	–671.292760	–671.342679	–757.4783
2-BOL_Prod	–595.6372030	–595.517838	–595.507956	–595.552297	—
2-BON_SM	–710.797109	–710.637070	–710.623881	–710.675409	—
2-BON_TS	–710.742195	–710.585665	–710.572201	–710.624321	–745.60
2-BON_Prod	–634.933105	–634.784857	–634.773849	–634.820964	—

Table S11. Calculated Free Energies of Activation and Reaction (kcal/mol).

Boronic Acid	$\Delta G^{\ddagger}$	$\Delta G_{reaction}$
PBA	27.0	−61.0
BL	28.3	−62.4
BOL	34.3	−50.4
BON	32.1	−44.6

Table S12. Experimental and Computational Kinetic Parameters for Boronic Acid Oxidation.

	Experimental		Computational	
	$k_{monoanion}$[a] ($M^{-1}s^{-1}$)	$k_{monoanion}$ (rel)	$\Delta\Delta G^{\ddagger}$ (kcal/mol)	$k_{monoanion}$ (rel)
PBA	49 ± 4	1	0.0	1
BL	4.2 ± 0.2	8.6×10^{-2}	1.3	3.5×10^{-2}
BON	0.041 ± 0.017	8.4×10^{-4}	5.1	2.3×10^{-4}
BOL	0.00016 ± 0.00001	3.3×10^{-6}	7.3	8.5×10^{-7}

[a]Values of $k_{monoanion}$ (which is k_2 for PBA and 2-HMPBA, and k_1 for 2-CPBA) are derived from the data in Fig. 2B and refer to the monoanionic species depicted in Fig. 2A.

Table S13. Boron–Oxygen and Competing Donor–Acceptor Interaction Energies in Transition States.

Boronic Acid	Donor[a]	Acceptor	$E^{(2)}$ (kcal/mol)	$F_{i,j}$	S
PBA	$n_{O1,p}$	p_B	35.2	0.118	0.29
	$n_{O2,p}$	p_B	37.4	0.122	0.30
BL	$n_{O1,p}$	p_B	20.4	0.089	0.23
	$n_{O2,p}$	p_B	43.9	0.131	0.30
	$n_{O1,p}$	σ^*_{C-H}	9.8	0.080	0.20
BON	$n_{O1,sp^{2.8}}$	p_B	6.0	0.056	0.15
	$n_{O1,p}$	p_B	14.8	0.077	0.20
	$n_{O2,p}$	p_B	39.2	0.125	0.29
	$n_{O1,p}$	$\pi^*_{C=O}$	67.3	0.153	0.32
BOL	$n_{O1,sp^{2.2}}$	p_B	9.1	0.069	0.19
	$n_{O1,p}$	p_B	4.0	0.039	0.11
	$n_{O2,p}$	p_B	47.7	0.136	0.30
	$n_{O1,p}$	$\pi^*_{C=O}$	66.3	0.151	0.31

[a]In BL, BON, and BOL, "O1" refers to the ring oxygen; "O2" refers to an acyclic oxygen.

Table S14. Inhibition of Transthyretin Aggregation by Stilbene **1**.

Ratio	% Fibril Formation[a]
1:1	92 ± 10
1:2	64 ± 12
1:5	43 ± 9
1:10	24 ± 9
1:50	1 ± 8

[a]**Procedure:** Human transthyretin (TTR) tetramers (7.2 μM) were incubated with varying molar ratios (1:1 to 50:1) of stilbene **1** in 10 mM sodium phosphate buffer, pH 7.6, containing KCl (100 mM) for 30 min at 37 °C. The solutions were acidified by a twofold dilution with 50 mM sodium acetate buffer, pH 5.5, containing KCl (100 mM). Solutions were plated (200 μL) in a clear, flat-bottomed, 96-well plate in quadruplicate. Absorbances at 400 nm were measured with a Tecan M1000 plate reader initially after plating and following a 96-h incubation at 37 °C sealed under foil. Fibril formation was quantified with the equation: % fibril formation = $(A_{\text{ligand,96h}} - A_{\text{ligand,0h}})/A_{\text{control,96h}} - A_{\text{control,0h}})$, where the control is buffer.

Table S15. Crystallographic Data-Collection and Refinement for the TTR·Stilbene **1** Complex.[a]

Ligand (PDB ID)	**1** (6u0q)
Data Collection	
Space group	$P2_12_12$
a, b, c (Å)	43.09, 64.25, 85.84
α, β, γ (°)	90, 90, 90
Wavelength (Å)	1.54178
Resolution (Å)	30.41–1.75 (1.81–1.75)
Total Reflections	83345 (6929)
Unique Reflections	24767 (2431)
Multiplicity	3.4 (2.9)
Completeness (%)	100.0 (100.0)
Mean $I/\sigma(I)$	17.8 (2.5)
Wilson B factor (Å^2)	17.05
R_{merge}	0.049 (0.388)
R_{meas}	0.058 (0.481)
$R_{p.i.m.}$	0.031 (0.278)
$CC_{1/2}$	0.999 (0.794)
Refinement	
Reflections	24740 (2432)
Work set	23185 (2278)
Test set	1555 (154)
R_{work}	0.1784 (0.2400)
R_{free}	0.2218 (0.2865)
RMSD, bond lengths (Å)	0.010
RMSD, bond angles (Å)	0.96
No. of atoms	
Total	2083
Protein	1857
Ligand	48
Water	178
Average B factor (Å^2)	
Overall	20.37
Protein	19.20
Ligand	32.80
Water	29.19
Ramachandran statistics	
Favored (%)	97.8
Allowed (%)	2.2
Outliers (%)	0.0

[a]Values in parentheses are for the highest resolution shell.

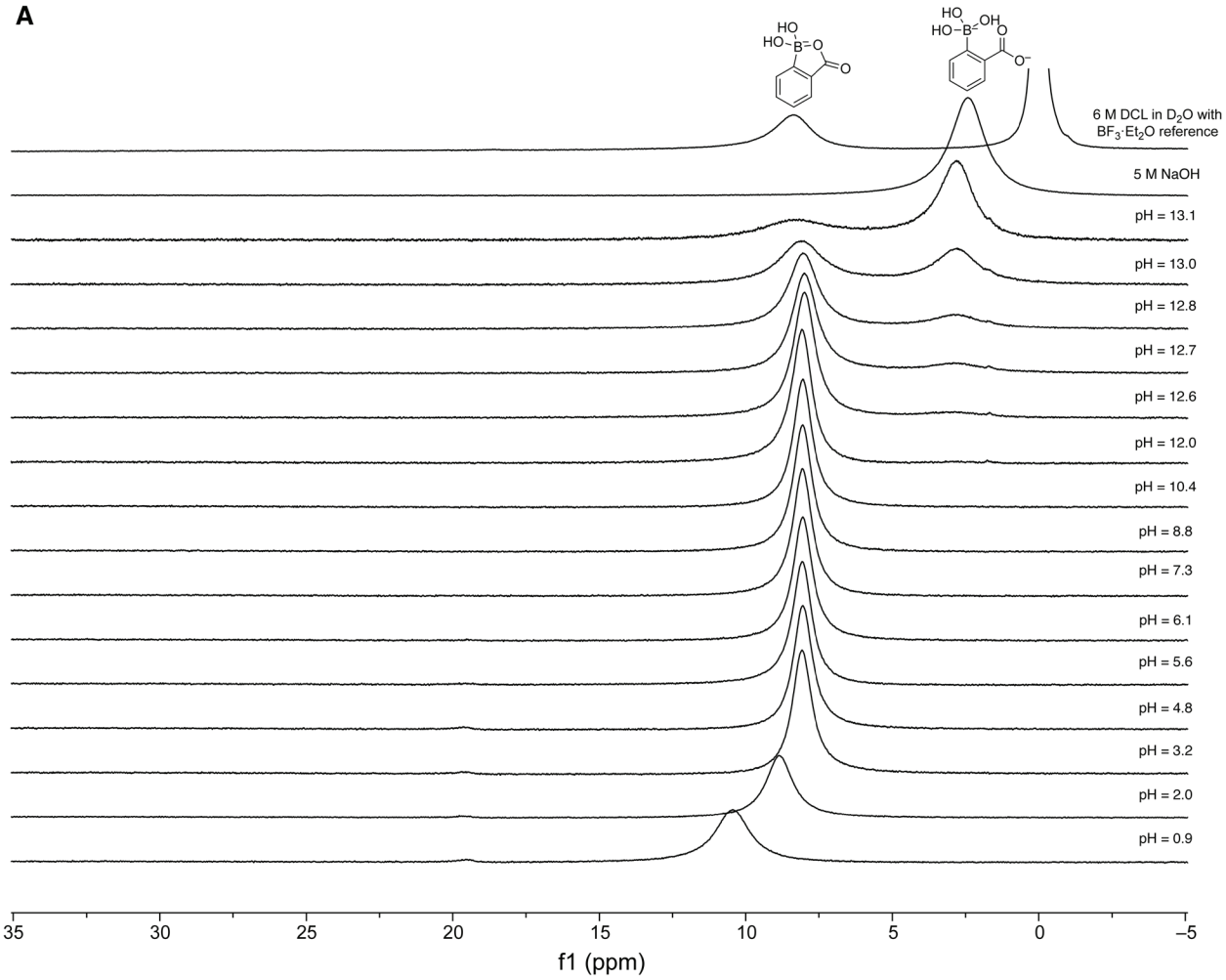
A
6 M DCL in D2O with BF3·Et2O reference
5 M NaOH
pH = 13.1
pH = 13.0
pH = 12.8
pH = 12.7
pH = 12.6
pH = 12.0
pH = 10.4
pH = 8.8
pH = 7.3
pH = 6.1
pH = 5.6
pH = 4.8
pH = 3.2
pH = 2.0
pH = 0.9
35
30
25
20
15
10
5
0
–5
f1 (ppm)

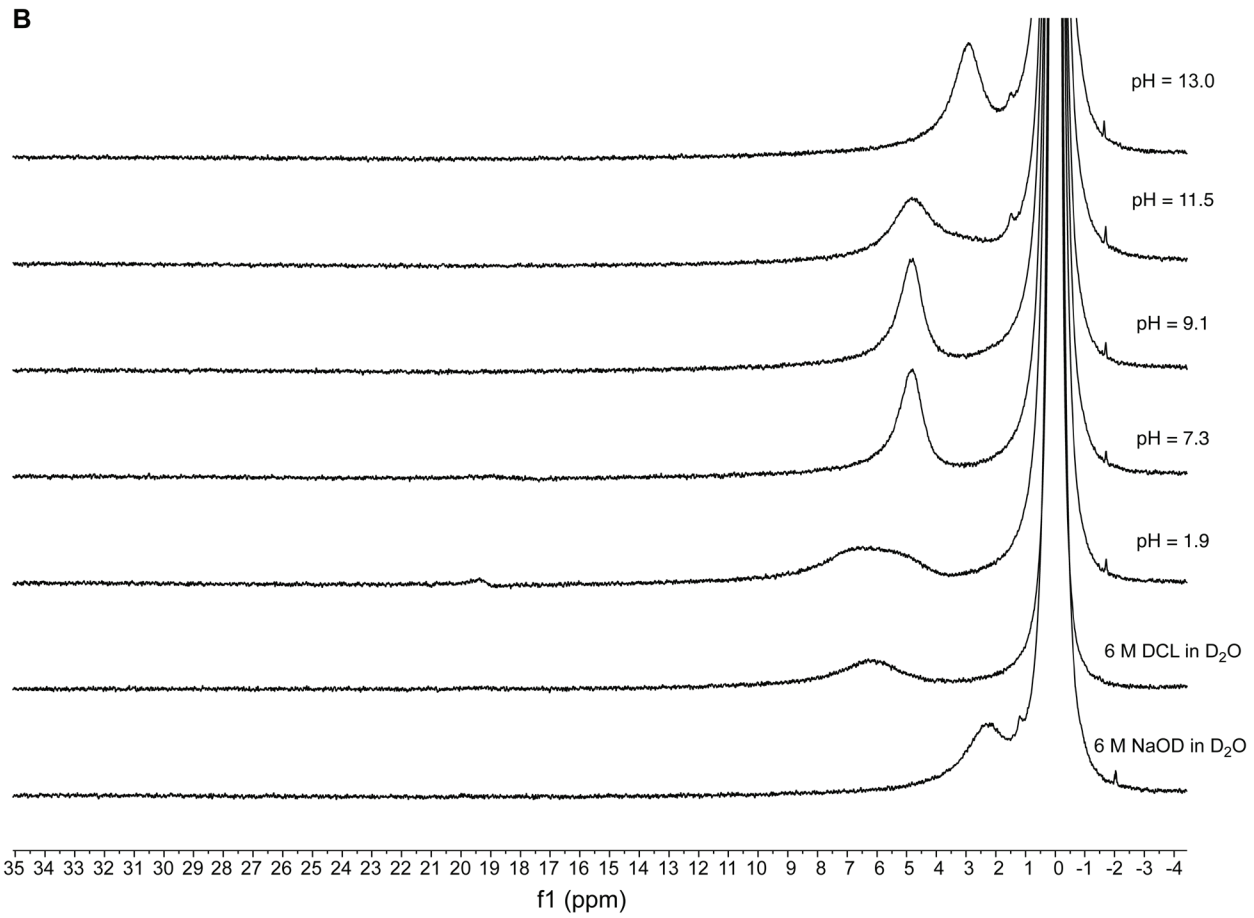
B
pH = 13.0
pH = 11.5
pH = 9.1
pH = 7.3
pH = 1.9
6 M DCL in D2O
6 M NaOD in D2O
35 34 33 32 31 30 29 28 27 26 25 24 23 22 21 20 19 18 17 16 15 14 13 12 11 10 9 8 7 6 5 4 3 2 1 0 -1 -2 -3 -4
f1 (ppm)

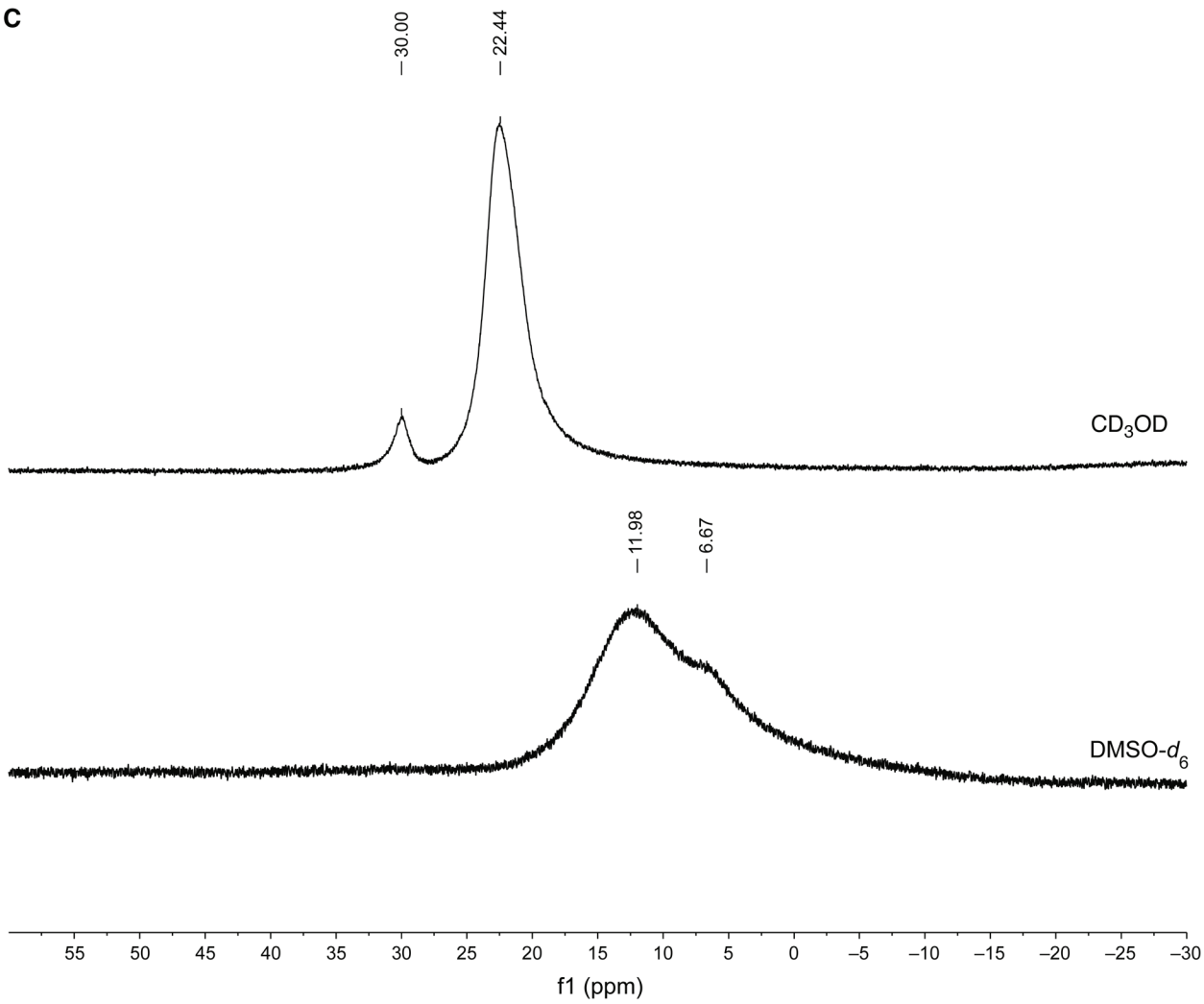

Fig. S1. (*A*) Representative ^{11}B-NMR spectra for the determination of the pK_a values of 2-CPBA. A solution of 2-CPBA (0.10 M) was prepared in 10 mL of 1 M aqueous NaOH containing D_2O (5% v/v). The solution pH was adjusted with 10 M NaOH or concentrated HCl, and 650 µL samples were removed at the designated pH values and analyzed by ^{11}B NMR spectroscopy, referencing to the solvent peak except in the case specified. The pK_a was calculated by fitting the fraction of dianion/monoanion to the expected speciation based on pH. The shift observed in the low pH samples is likely affected by a strong shift in the solvent reference peak, as the sample with external reference under extremely low pH conditions does not show the same shift. (*B*) Representative ^{11}B-NMR spectra of 2-CMPBA at various pH values, prepared at 0.050 M under the same conditions as in panel *A*. All samples contained a sealed capillary of $BF_3{\cdot}Et_2O$ as an internal standard. The observed chemical shifts are consistent with an anionic boronate at all pH values tested, and no clear transition indicative of a pK_a value was apparent. (*C*) Representative ^{11}B-NMR spectra of 2-CPBA in DMSO-d_6 and CD_3OD. In DMSO-d_6, 2-CPBA exhibits shifts similar to those in water, suggesting that the anionic cyclic structure is dominant. In CD_3OD, the major peak shifts downfield, indicative of a more neutral boron center though one more anionic than a standard phenylboronic acid (~30 ppm). The smaller peak at 30 ppm could result from a methanol adduct.

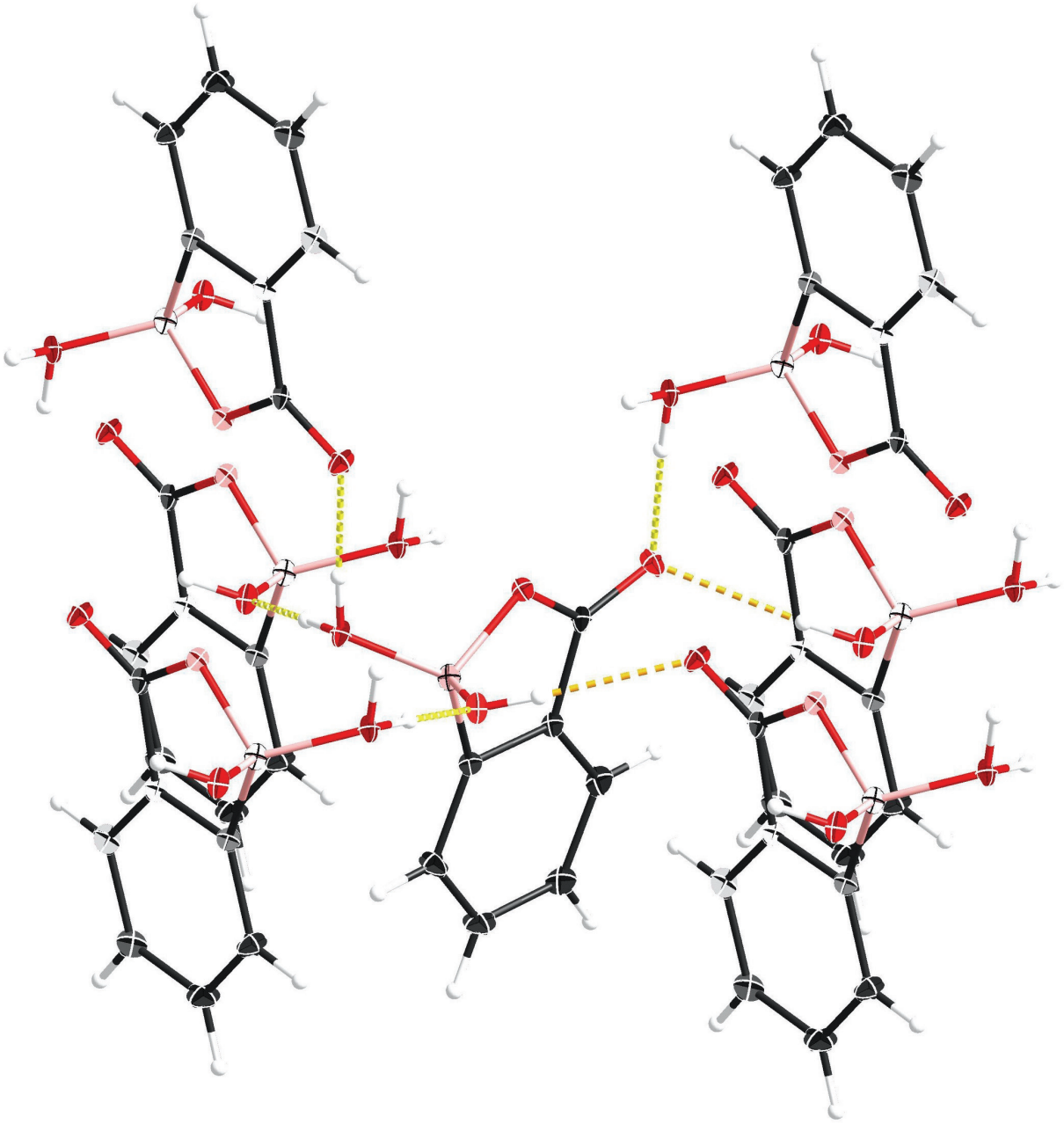

Fig. S2. Crystal-packing diagram of hydrated BOL.

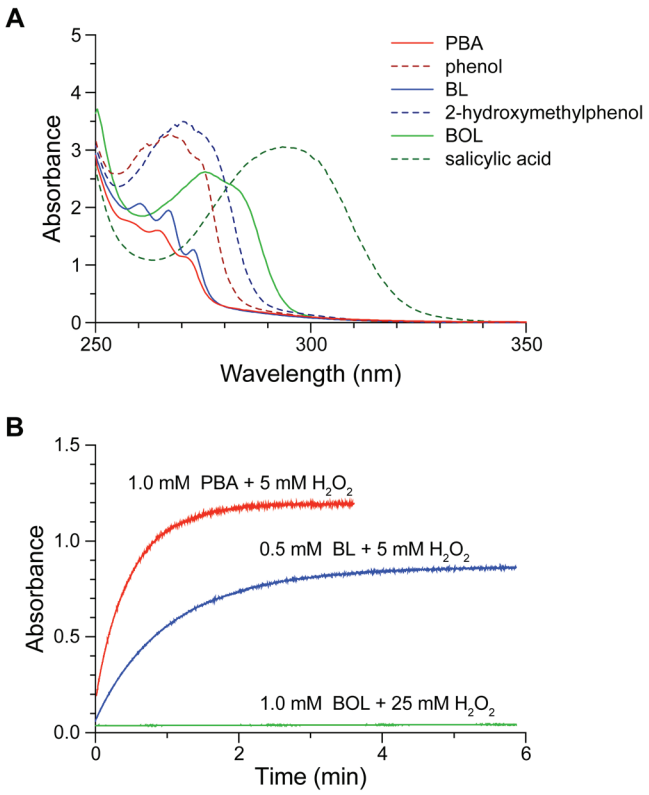

Fig. S3. UV-Spectroscopic basis for assays of the oxidation of boronic acids. (*A*) UV spectra of PBA, BL, BOL, and their phenolic oxidation products. (*B*) Representative raw data showing the change in absorbance upon oxidation in PBS.

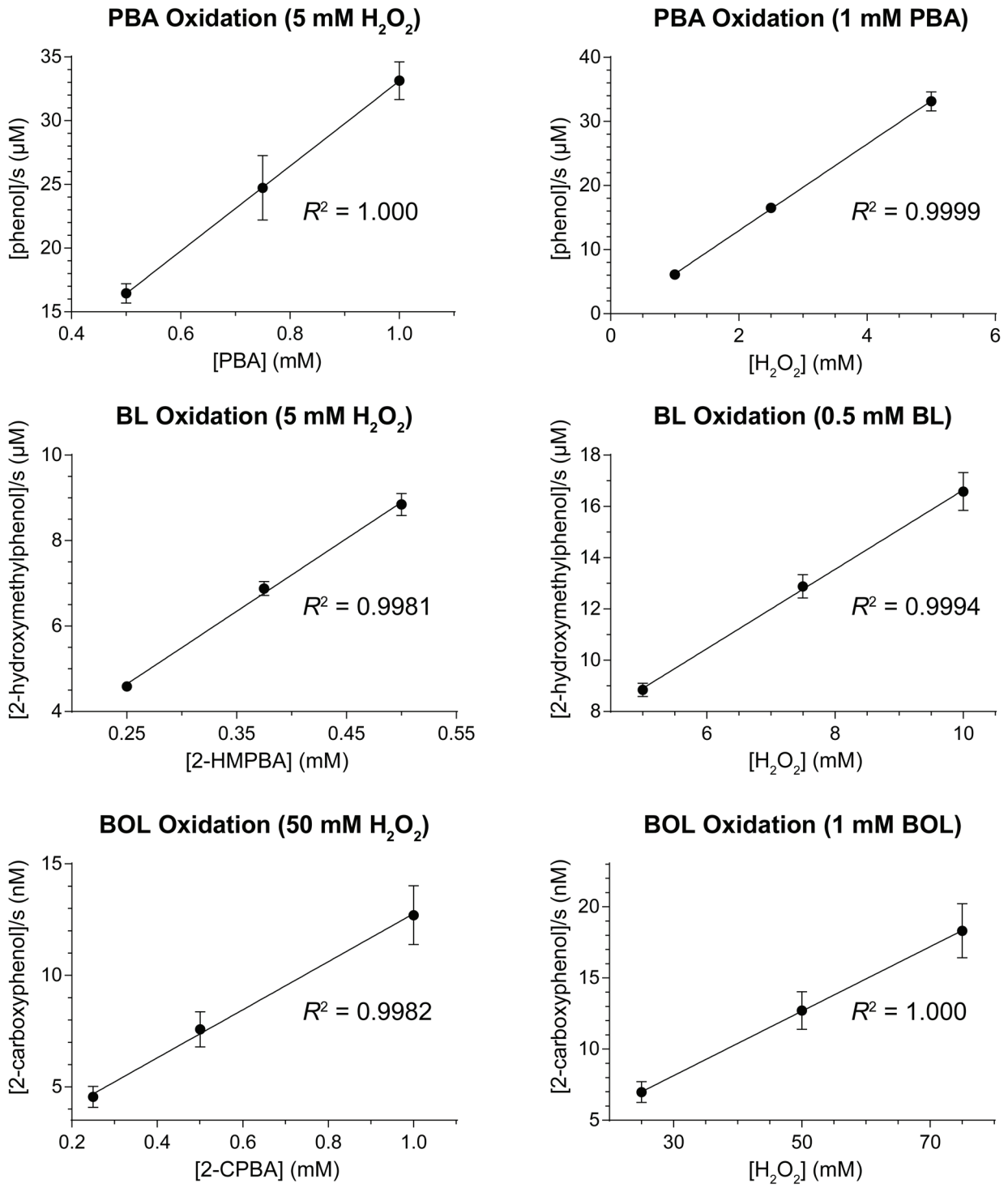

Fig. S4. Kinetic data for the oxidation of boronic acids by hydrogen peroxide at pH 7.4. Second-order rate constants derived from these data are listed in Table S1.

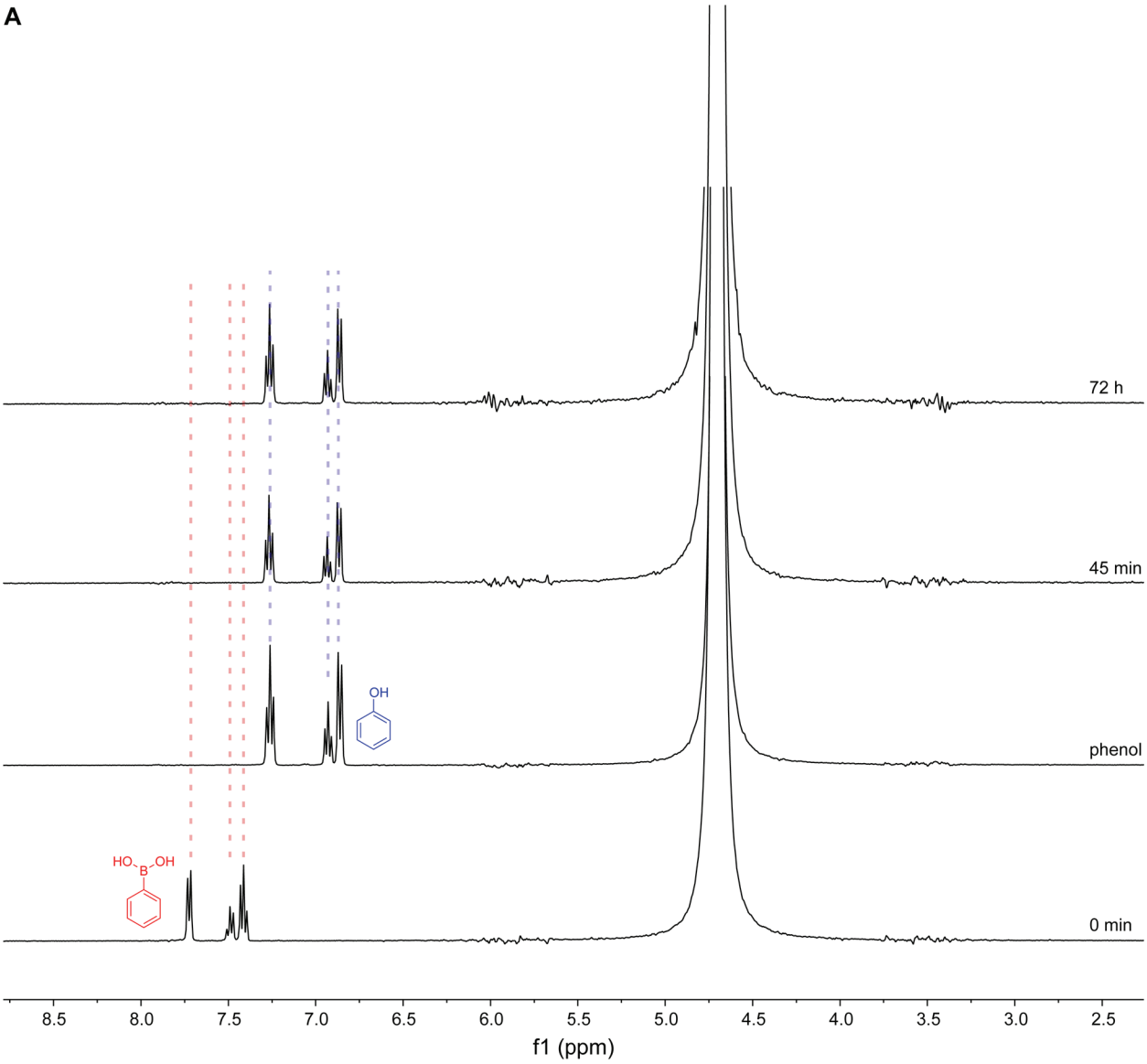
A
72 h
45 min
phenol
0 min
OH
HO
B
OH
8.5
8.0
7.5
7.0
6.5
6.0
5.5
5.0
4.5
4.0
3.5
3.0
2.5
f1 (ppm)

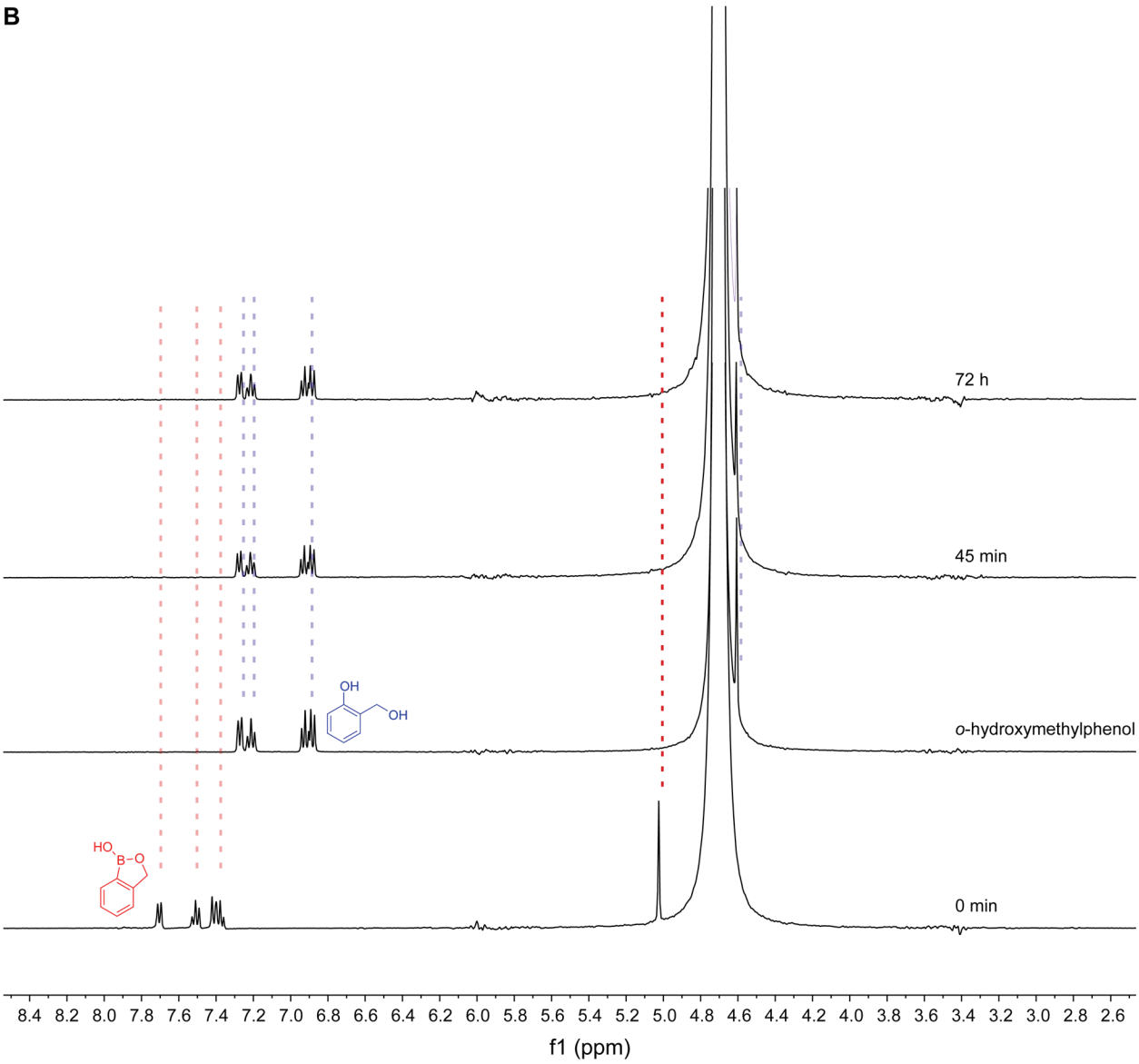
B
72 h
45 min
o-hydroxymethylphenol
0 min
OH
OH
HO
B
O
8.4 8.2 8.0 7.8 7.6 7.4 7.2 7.0 6.8 6.6 6.4 6.2 6.0 5.8 5.6 5.4 5.2 5.0 4.8 4.6 4.4 4.2 4.0 3.8 3.6 3.4 3.2 3.0 2.8 2.6
f1 (ppm)

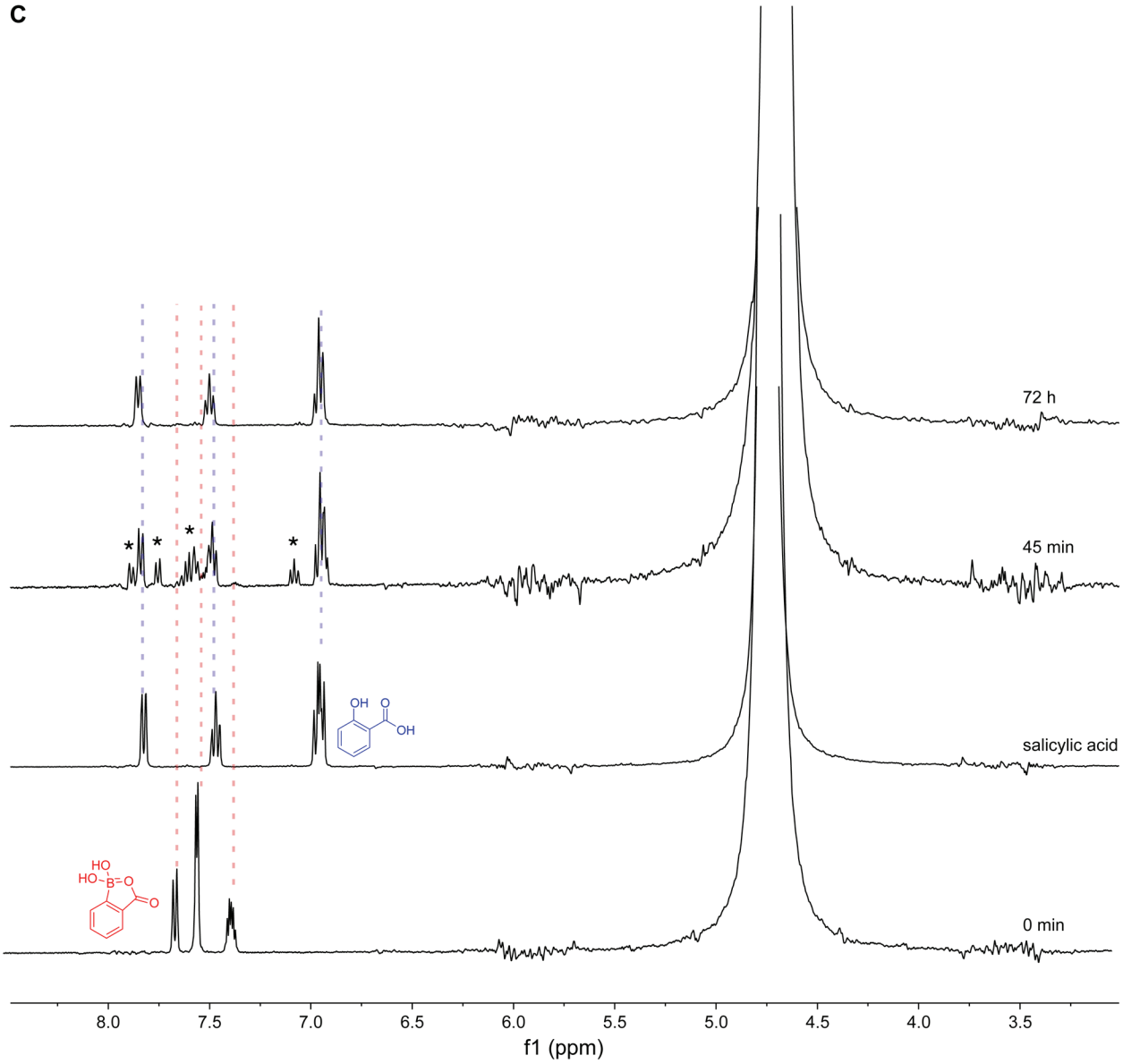
c
72 h
45 min
salicylic acid
0 min
OH
O
OH
HO
HO
B
O
O
8.0
7.5
7.0
6.5
6.0
5.5
5.0
4.5
4.0
3.5
f1 (ppm)

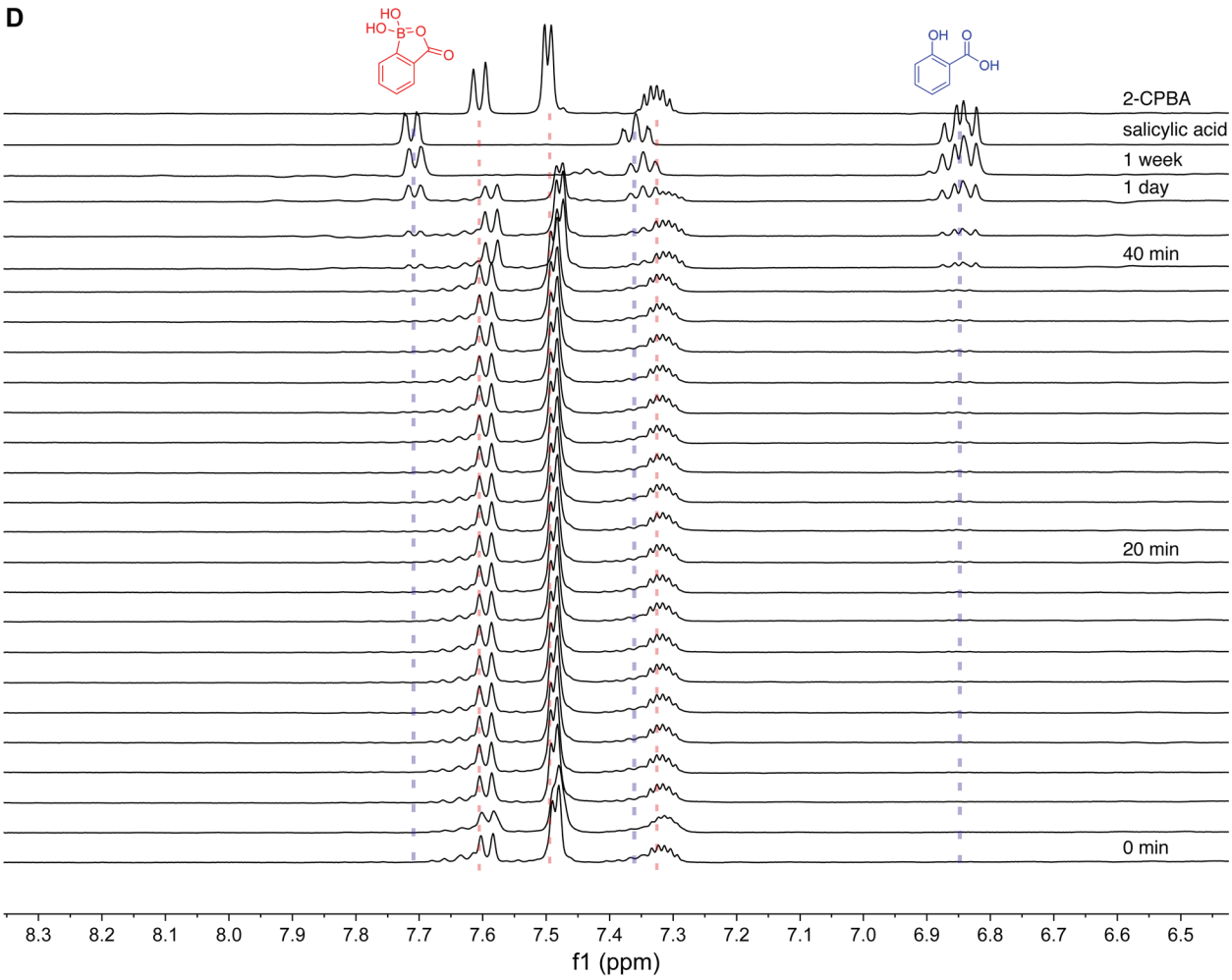

Fig. S5. ^{1}H-NMR spectra acquired during the oxidation of boronic acids: (*A*) PBA, *(B)* 2-HMPBA, and (*C*,*D*) 2-CPBA. **Procedure:** Solutions of boronic acids (50 mM) were prepared in PBS. A solution of sodium bisulfite (0.5 M) in D_2O was prepared to quench the oxidation reaction. A 2-mL aliquot of a boronic acid solution was placed in a 1-dram vial, and 100 µL was added to 600 µL of the quench solution to provide an initial sample. Hydrogen peroxide (50 µL of a 30% v/v aqueous solution) was added to each boronic acid solution, and the resulting solutions were stirred for 45 min. A 100-µL aliquot of the reaction mixture was added to 600 µL of the quench solution, and the samples were analyzed by ^{1}H-NMR spectroscopy. Solutions of phenol, 2-hydroxymethylphenol, and salicylic acid were subjected to the same quench and analysis. The reaction mixtures were incubated for 72 h and another aliquot was quenched and analyzed. No ^{1}H-NMR peaks corresponding to oxidation of the phenols were observed. In panel *C*, peaks not corresponding to the boronic acid or phenol product are marked with asterisks and are likely attributable to a boronic acid–peroxide complex. In panel *D*, 0.99 mL of 2-CPBA (40 mM) in 0.10 M sodium phosphate buffer, pH 7.3, containing D_2O (10% v/v) was added to an NMR tube, and the sample was locked and shimmed in an NMR spectrometer. Hydrogen peroxide (10 µL of a 30% v/v aqueous solution) was added to the tube, the contents were mixed thoroughly by shaking, and the tube was returned to the spectrometer and analyzed (16 scans, 5-s relaxation delay), obtaining a spectrum approximately every 2 min. Spectra of the starting material and product alone were obtained in the same buffer solution.

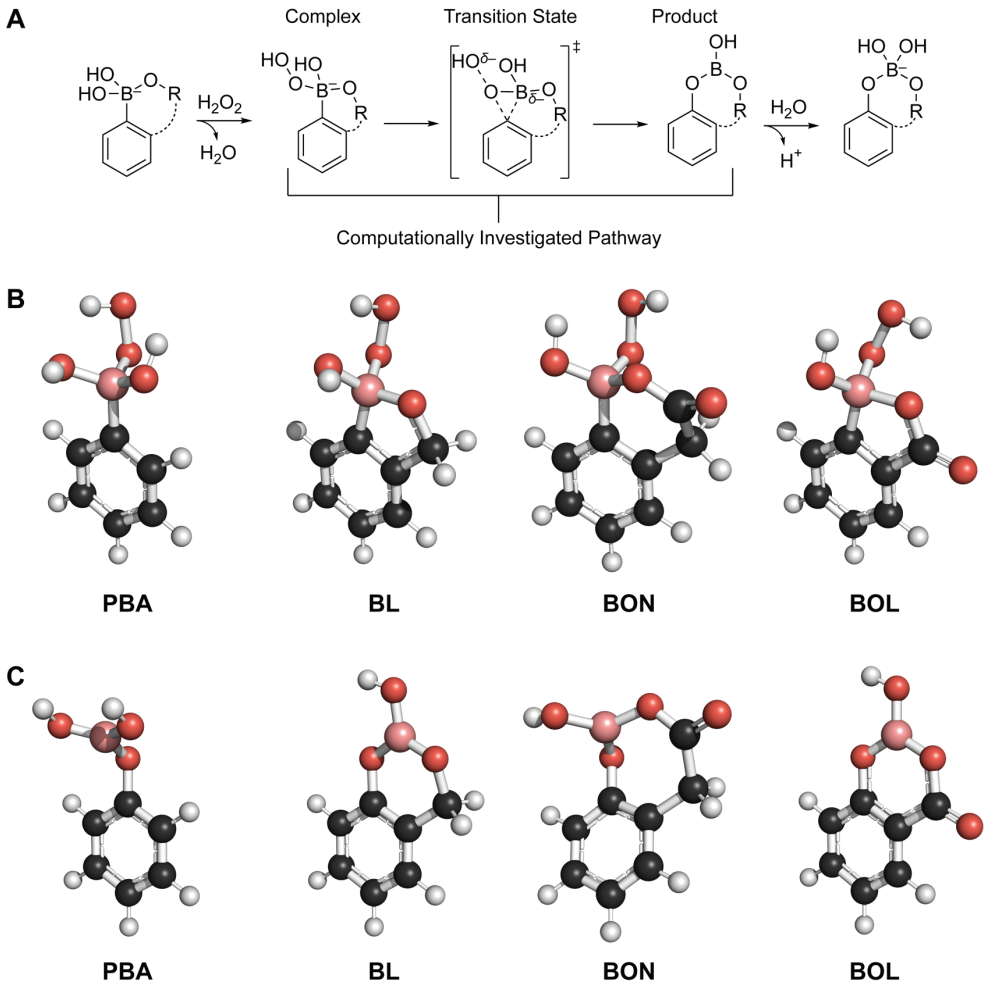

Fig. S6. (A) Putative mechanism of boronic acid oxidation by hydrogen peroxide. (B) Optimized structure of each complex with peroxide anion. (C) Optimized structure of each product. The optimized structure of each transition state is shown in Fig. 4.

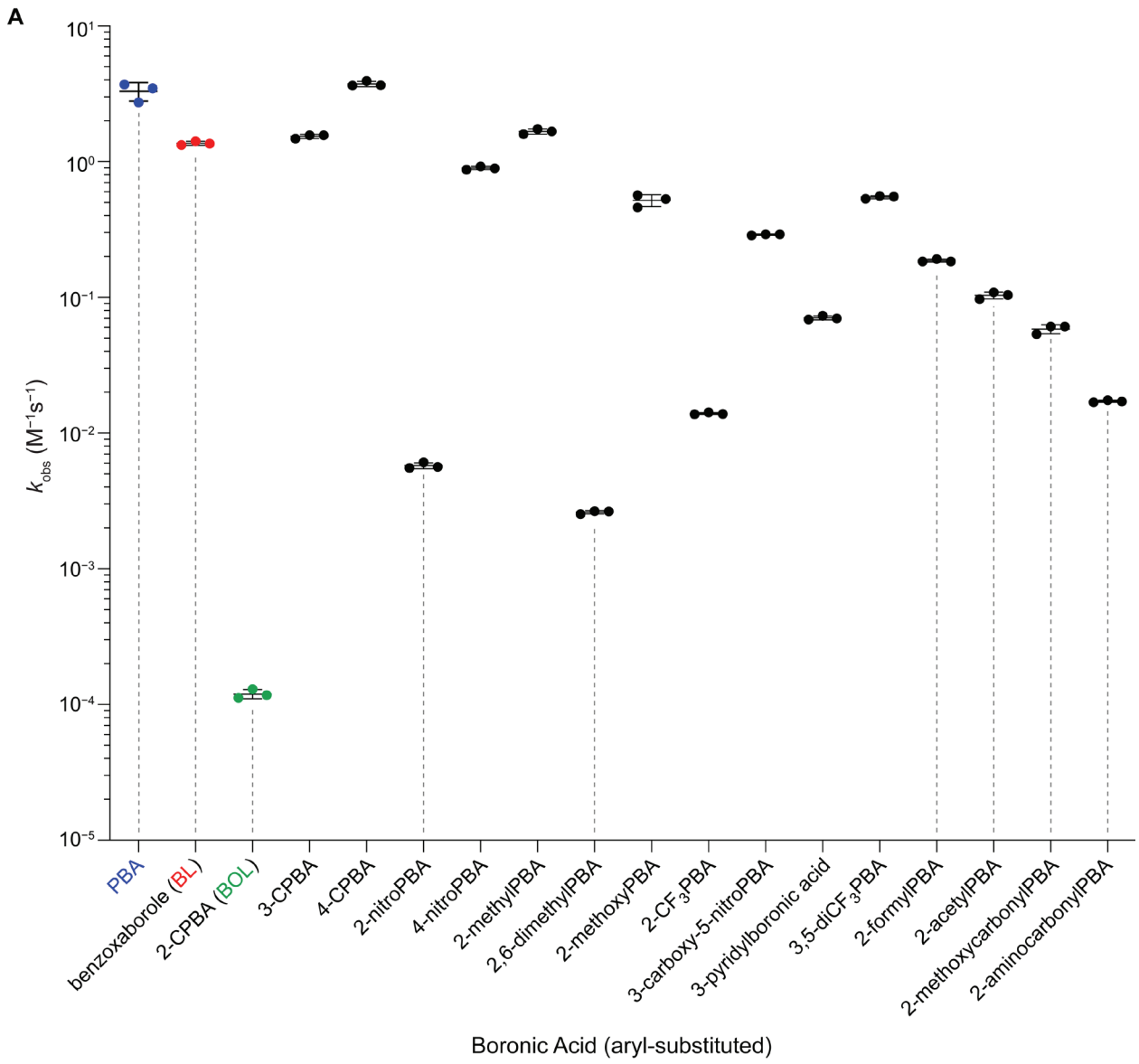
A
10^{1}
10^{0}
10^{-1}
10^{-2}
10^{-3}
10^{-4}
10^{-5}
k_{obs} ($M^{-1}s^{-1}$)
PBA
benzoxaborole (BL)
2-CPBA (BOL)
3-CPBA
4-CPBA
2-nitroPBA
4-nitroPBA
2-methylPBA
2,6-dimethylPBA
2-methoxyPBA
2-CF_3PBA
3-carboxy-5-nitroPBA
3-pyridylboronic acid
3,5-diCF_3PBA
2-formylPBA
2-acetylPBA
2-methoxycarbonylPBA
2-aminocarbonylPBA
Boronic Acid (aryl-substituted)

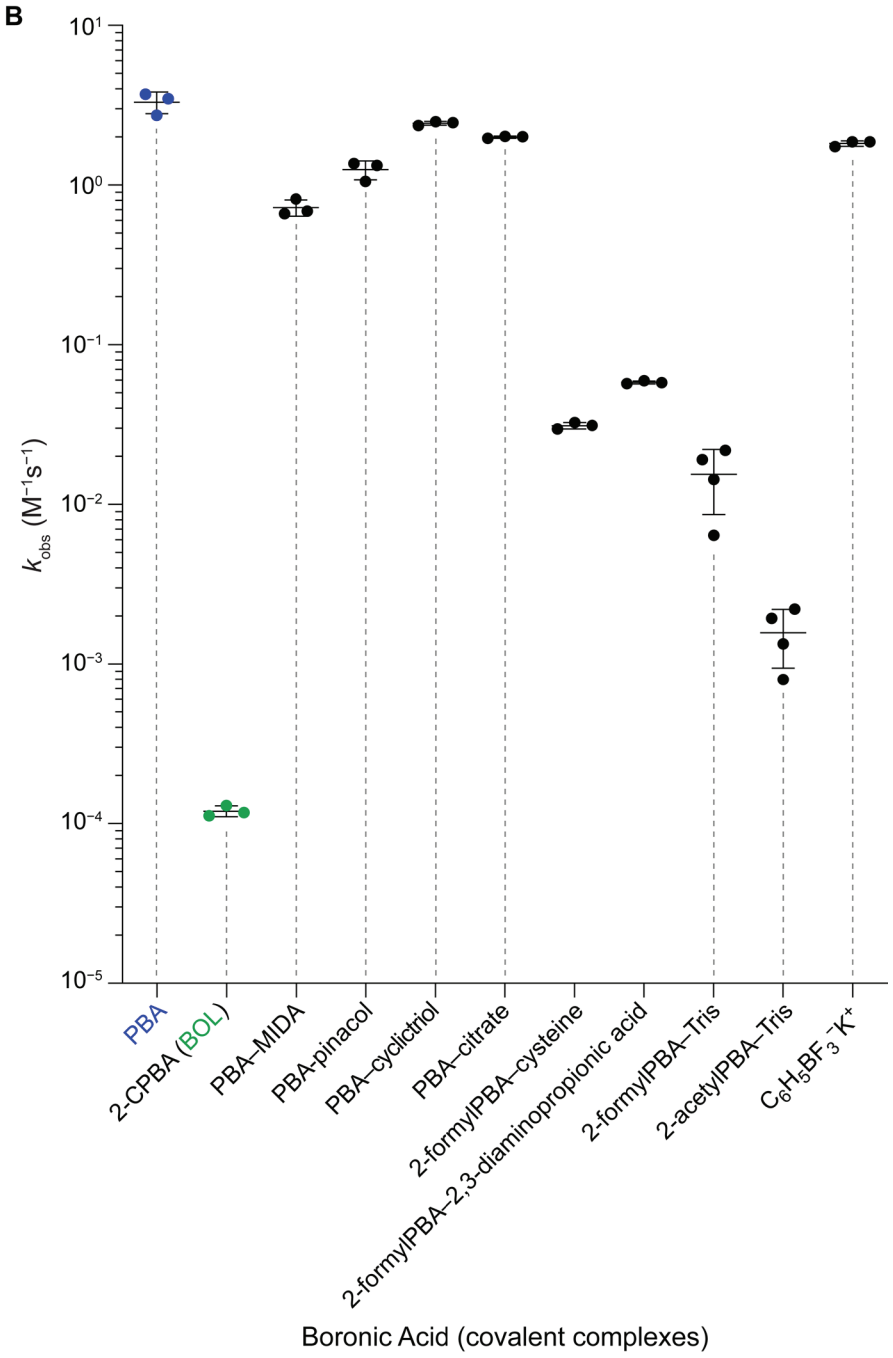

Fig. S7. Graph of k_{obs} values for the oxidation of PBA and representative derivatives and complexes. (A) PBA derivatives with aryl substitutions. (B) PBA covalent complexes. All reaction mixtures contained a boronic acid (1 mM) and hydrogen peroxide (5 mM) in 100 mM sodium phosphate buffer, pH 7.4. Reactions were monitored by UV spectroscopy using a wavelength and extinction coefficient appropriate for the phenol product. Values (bars) are the mean ± SD from ≥3 reactions (●). Boronic acids discussed explicitly in the main text are indicated with vertical dotted lines. MIDA, *N*-methyliminodiacetic acid; Tris, tris(hydroxymethyl)aminomethane.

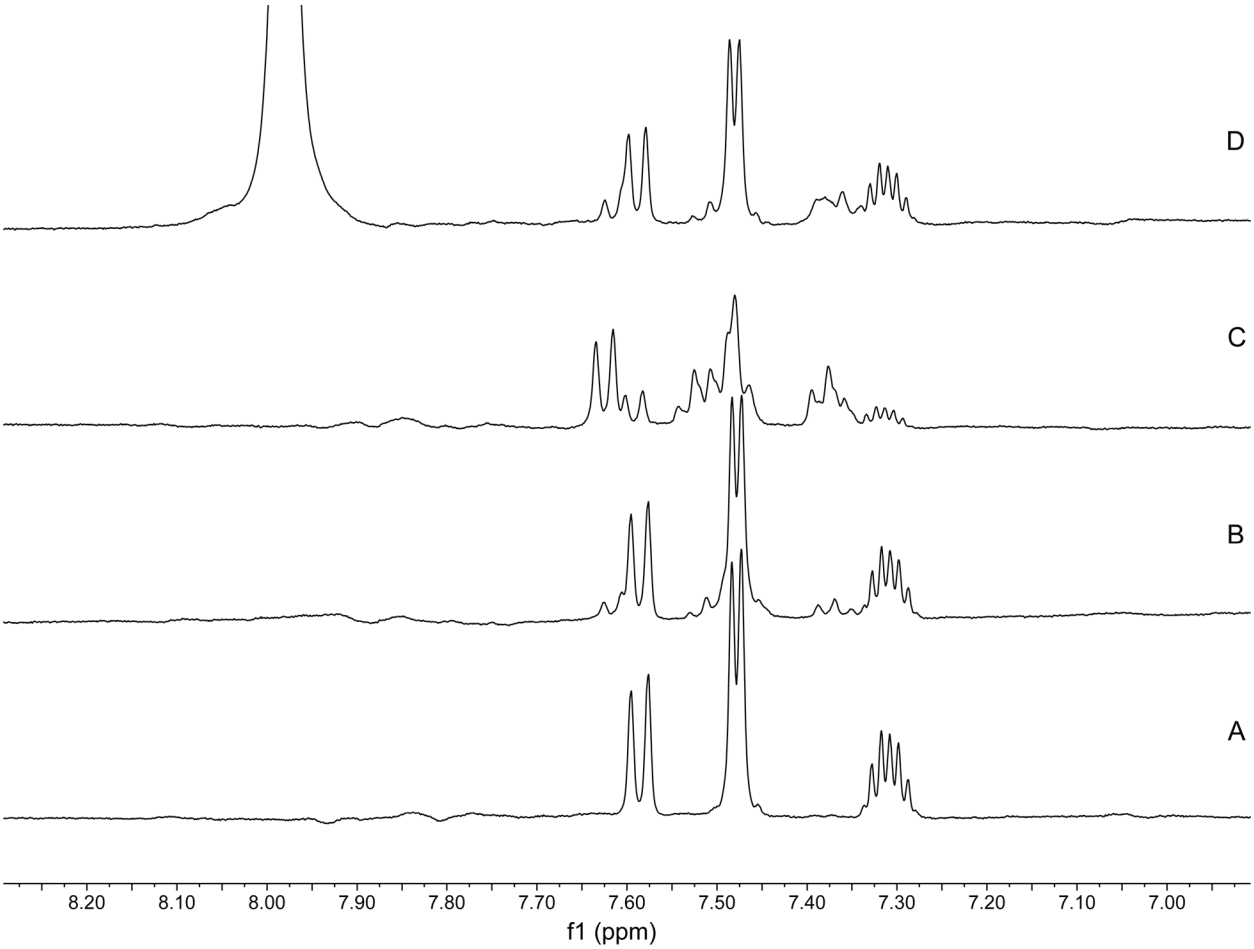

Fig. S8. Representative ^{1}H-NMR spectra for the determination of the affinity of BOL for saccharides. (A) 0.015 M BOL in 0.10 M phosphate buffer, pH 7.4. Equilibrated solutions of BOL (0.015 M) with 0.15 M saccharide solutions: (B) glucose, (C) fructose, and (D) *N*-acetylneuraminic acid.

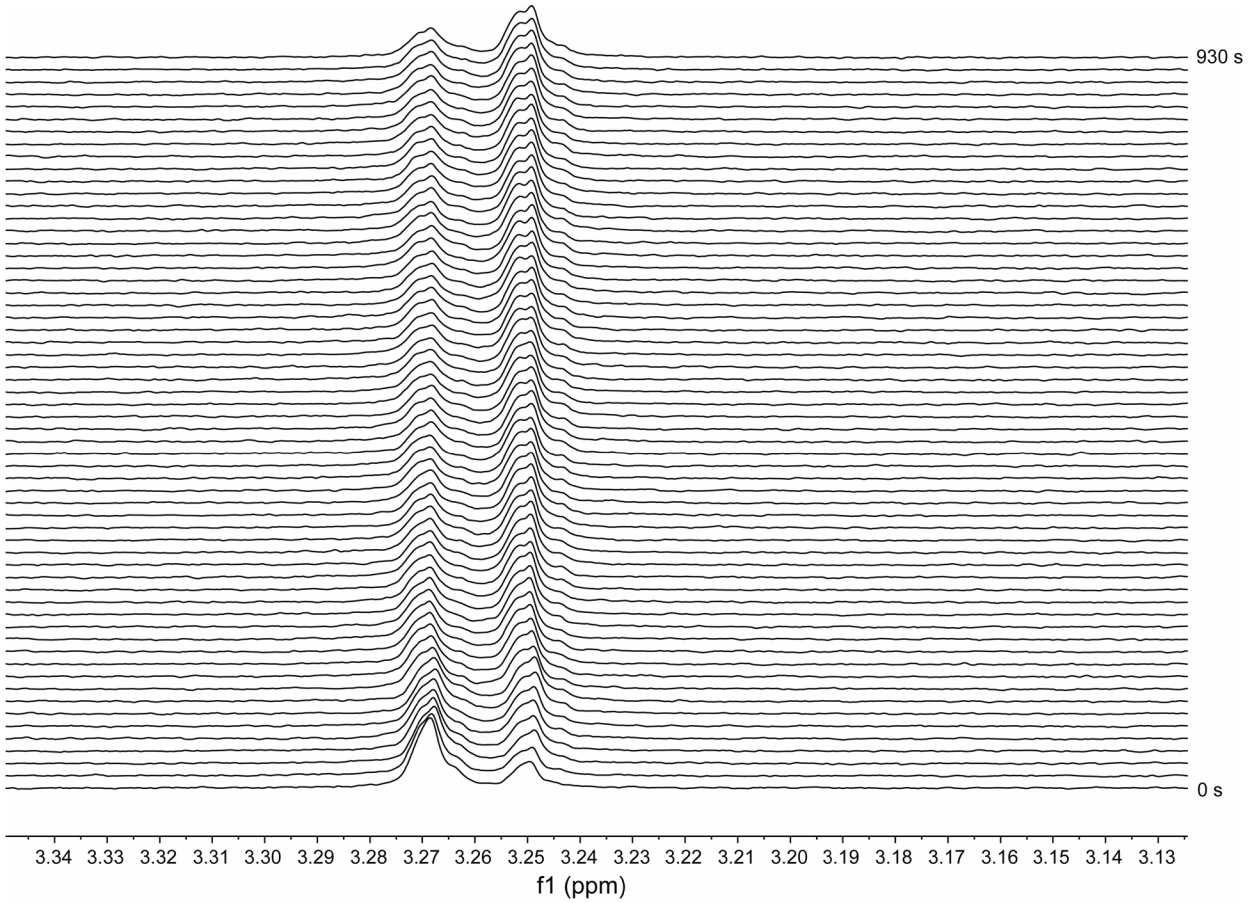

Fig. S9. Representative ^{1}H-NMR spectra for the determination of the k_{on} value for PBA + nopoldiol–PEG. **Procedure:** 0.050 M Sodium phosphate buffer, pD 7.4, was prepared in D_2O and mixed with CD_3CN (7:3 buffer/CD_3CN) as a stock buffer solution. Nopoldiol–PEG was dissolved in the stock buffer to a concentration of 1 mM. An internal standard solution of 9 mM DMSO in the stock buffer was prepared and used to prepare 12 mM solutions of PBA, 2-CPBA, and 2-HMPBA. A 600-µL aliquot of the diol stock was placed in an NMR tube, and the sample was locked to CD_3CN and shimmed. Then, a 50-µL aliquot of the boronic acid stock solution was added, the tube shaken to mix, and a ^{1}H spectrum obtained approximately every 15 s. This analysis was performed in triplicate for each boronic acid. The free-diol peak at 3.26 ppm and complex peak at 3.24 ppm (corresponding to the PEG methoxy group) were integrated, and the ratios were used to calculate relative concentrations of species from initial concentrations. The slope of a plot of 1/[diol] versus time was recorded as the second-order rate constant, k_{on}.

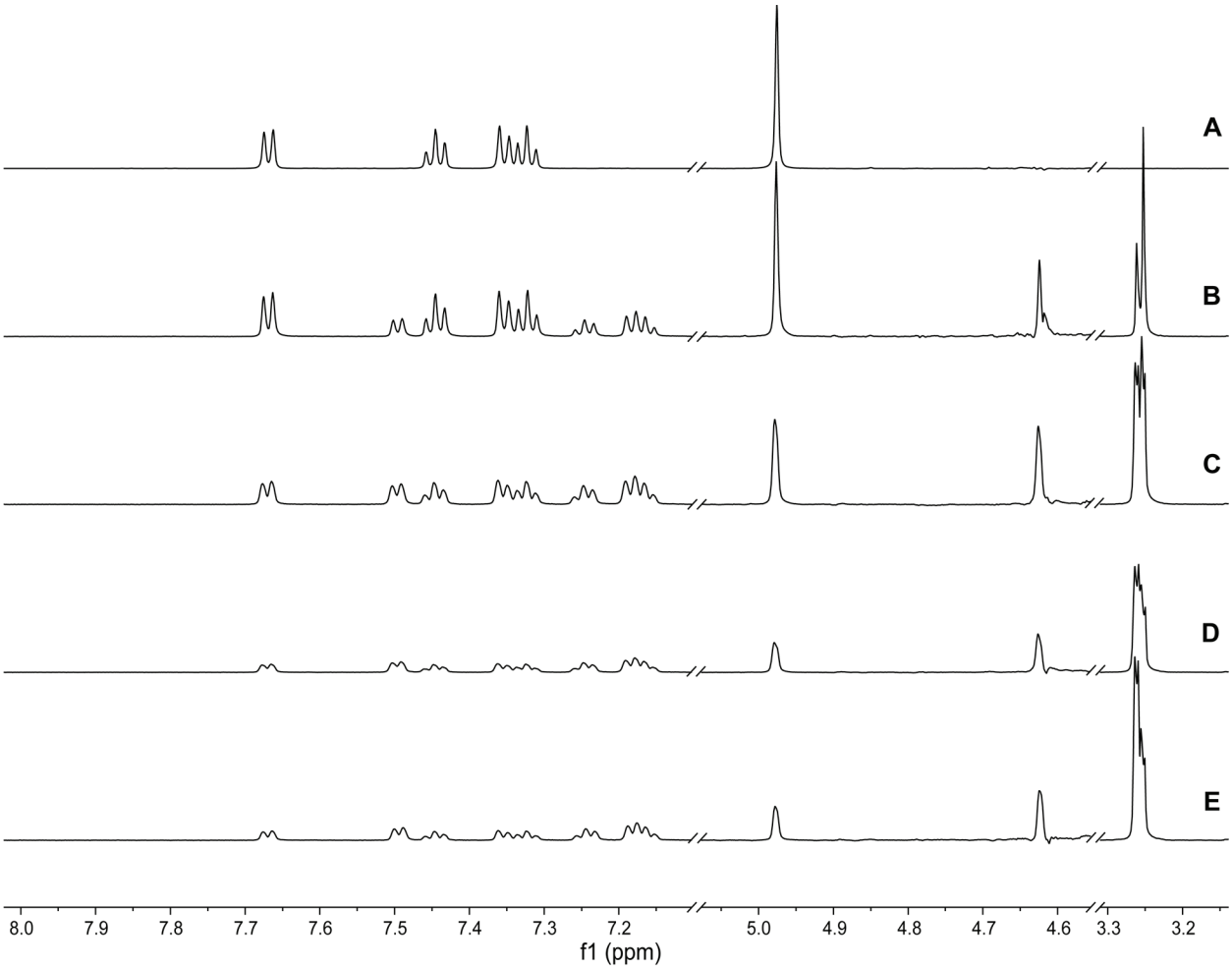

Fig. S10. Representative ^{1}H-NMR spectra for the determination of the affinity of BL for nopoldiol–PEG. (A) BL stock solution in 70:30 0.050 M sodium phosphate buffer in D_2O (pD 7.4)/CD_3CN. (B) 2.5 mM diol and 5 mM BL. (C) 3.3 mM diol and 3.3 mM BL. (D) 3.8 mM diol and 2.5 mM BL. (E) 3.3 mM diol and 1.7 mM BL. **Procedure:** A 5 mM stock solution of nonpoldiol–Peg was prepared in the same buffer used for the measurement of k_{on}. A 10 mM stock of boronic acid with 9 mM DMSO was prepared in the same buffer. The stock solutions were mixed to obtain 4 different concentrations and diol:boronic acid ratios. The samples were shaken to mix, allowed to equilibrate for at least 2 h at room temperature, then analyzed by ^{1}H-NMR spectroscopy. Results from locking and shimming on the D_2O peak were superior to those from the CD_3CN peak. The ratio of complex to free diol was calculated either by the ratio of the diol:complex peak as described in the kinetics or by integration of the boronic acid peaks, which showed distinct shifts for the complex and free boronic acid and often gave greater precision than the use of the PEG methoxy peak due to overlap of the complex and free-diol methoxy peaks. Equilibrium concentrations of the species were calculated from their initial concentrations, and the value of K_{eq} was calculated according to the equation: K_{eq} = [complex]/(boronic acid][diol]).

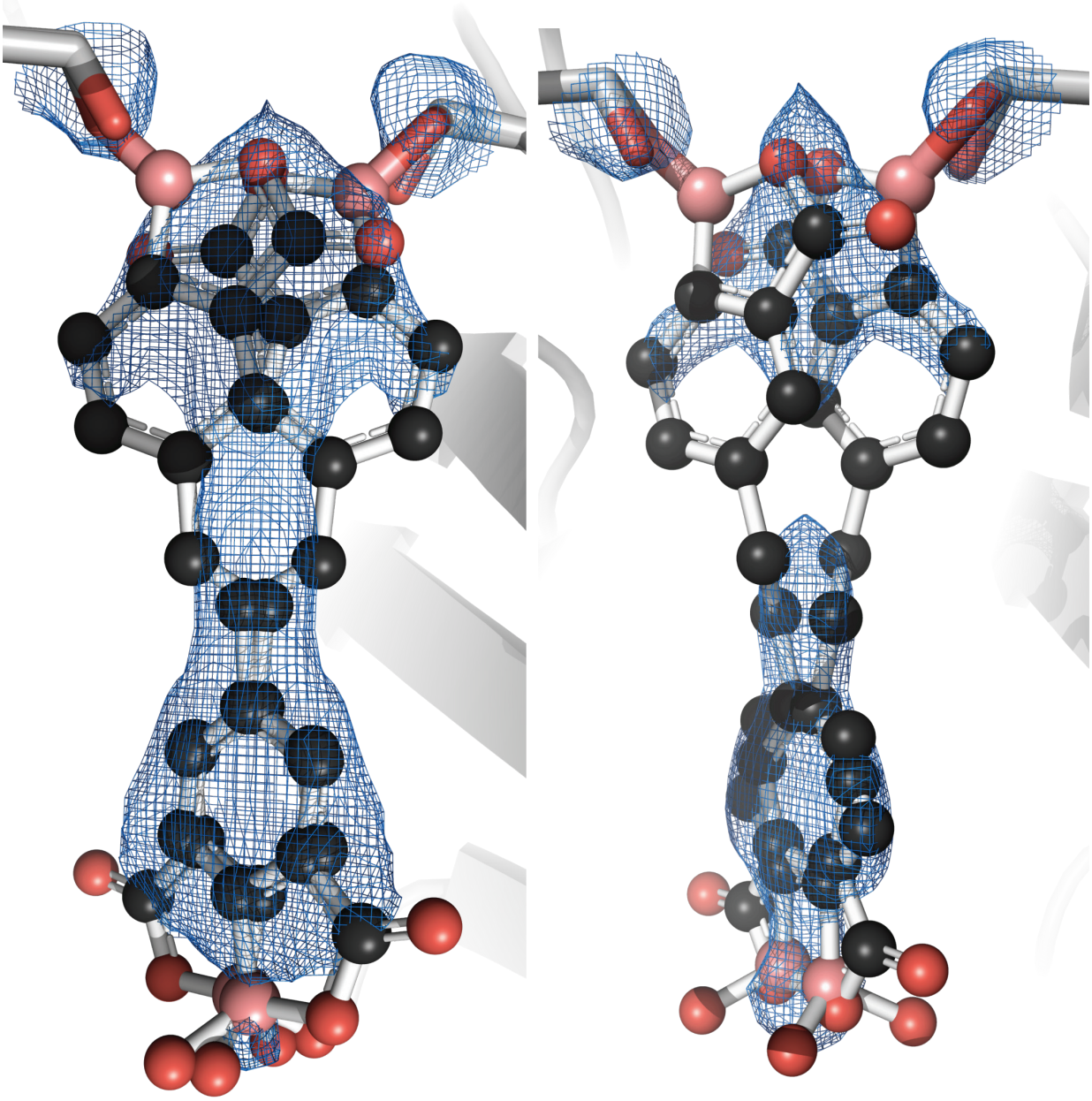

Fig. S11. Electron densities of stilbene **1** bound to transthyretin. Both non-crystallographic symmetry-related binding sites were occupied by ligand. The ligand binding site lies on a two-fold axis. The model and its crystallographic symmetry mate are shown, along with a $2F_o - F_c$ map contoured at 1σ (blue mesh) for chain A (left) and chain B (right).

Atomic Coordinates of Optimized Structures

PBA_Complex

C	2.61827900	1.12521200	-0.19495500
C	1.23227000	1.19868800	-0.05840900
C	0.44567400	0.05242800	0.09478700
C	1.11039300	-1.17977300	0.10838800
C	2.49341900	-1.27019400	-0.03071300
C	3.25563200	-0.11300800	-0.18366700
H	3.20433000	2.03264900	-0.30985700
H	0.73206100	2.16218300	-0.05960600
H	0.51653000	-2.07939900	0.24074700
H	2.98178700	-2.24040600	-0.01828700
H	4.33412300	-0.17649900	-0.29045500
O	-1.70824700	-0.91796700	1.16823200
H	-1.80290300	-0.50654400	2.02803100
O	-1.58202600	1.46575300	0.69708600
H	-2.44895400	1.62446400	0.31474600
O	-1.72543100	-0.20430700	-1.09532100
O	-3.15761200	-0.28048700	-0.94207200
H	-3.20705000	-0.85707400	-0.16201400
B	-1.17147900	0.13131400	0.24414200

PBA_TS

C	2.49121700	1.20031600	0.10719200
C	1.09967700	1.20925000	0.04165700
C	0.38654400	0.01131700	0.00406800
C	1.07729300	-1.19829000	0.08020200
C	2.46838500	-1.21213800	0.14777700
C	3.17775000	-0.01176700	0.15992400
H	3.03998500	2.13549300	0.12162200
H	0.57097000	2.15698900	0.00923200
H	0.52012800	-2.12904900	0.06568400
H	3.00043200	-2.15603800	0.19375500
H	4.26020500	-0.02070800	0.21479500
O	-1.67877900	-1.25390300	-1.12350200
H	-1.99296900	-1.10141400	-2.01739700
O	-1.73479800	1.10398800	-1.29646400
H	-1.69954100	1.90932900	-0.77570800
O	-1.30653200	0.05944500	0.87929500
O	-3.04840300	0.10635700	1.51030400
H	-3.07996000	-0.82699600	1.73848500
B	-1.33526700	-0.01736500	-0.51049100

PBA_Product

C	-2.22122800	1.20337100	-0.19541500
C	-0.90317800	1.20945000	0.24789000
C	-0.25258900	-0.00000300	0.46768800
C	-0.90317400	-1.20945600	0.24787500
C	-2.22122400	-1.20337500	-0.19543000
C	-2.88371500	-0.00000200	-0.41849200
H	-2.73216800	2.14381700	-0.36487400
H	-0.36702000	2.13258900	0.43154100
H	-0.36701400	-2.13259600	0.43151400
H	-2.73216200	-2.14382100	-0.36490100
H	-3.91111800	-0.00000100	-0.76124800
O	2.56740400	-1.21056000	-0.37254100
H	3.29641300	-1.18775000	-0.99412300
O	2.56736900	1.21057300	-0.37256200
H	3.29637700	1.18777300	-0.99414700
O	1.04154500	-0.00000400	0.93510400
B	2.08335800	0.00000300	0.03430700

BOL_Complex

C	0.41434200	-0.37053600	0.11937500
C	1.04169400	0.86602700	-0.04542400
C	2.42042500	0.98129800	-0.19748200
C	3.19465600	-0.17857500	-0.18016600
C	2.58908500	-1.42620900	-0.01565400
C	1.20401700	-1.52100900	0.12998700
H	2.89200400	1.95151400	-0.32313500
H	4.27135300	-0.11212000	-0.29106000
H	3.20184800	-2.32115000	-0.00157700
H	0.74758100	-2.49947000	0.25482000
B	-1.17588200	-0.08785700	0.25203200
C	0.01643200	1.97900200	-0.03121800
H	-0.05817500	2.44215100	-1.02562100
H	0.28932000	2.77229100	0.67474600
O	-1.21183800	1.39468800	0.34513100
O	-1.80319300	-0.63774800	-0.98448600
O	-1.93483900	-0.66346200	1.37108700
H	-1.91029400	-0.05883500	2.11518100
O	-3.23159400	-0.47335800	-0.90353800
H	-3.38642600	-0.67604800	0.03442300

BOL_TS

C	0.38149400	-0.39892900	0.08455300
C	0.92588600	0.86752600	-0.12218500
C	2.29987100	1.02811000	-0.25411100
C	3.12209500	-0.09856700	-0.18823700
C	2.57446800	-1.36686900	0.01097400
C	1.19349600	-1.52371800	0.13747600
H	2.73241500	2.01395100	-0.39344700
H	4.19592200	0.01360700	-0.28426100
H	3.22592700	-2.23189900	0.06349000
H	0.76283200	-2.51075800	0.27272800
B	-1.30986200	-0.00773600	0.52607600
C	-0.13613600	1.94260200	-0.10908600
H	-0.43168200	2.18900700	-1.13779200
H	0.21352400	2.86088400	0.36923400
O	-1.23675000	1.42299300	0.61291800
O	-1.33459300	-0.64591800	-0.71374900
O	-1.97462900	-0.57191900	1.63449500
H	-2.28724000	-1.44928100	1.40052800
O	-3.09004200	-0.65071900	-1.31895600
H	-2.94131500	0.01673600	-1.99482600

BOL_Product

C	-0.29330200	-0.60220800	0.10280000
C	-0.52874300	0.76917600	0.05950300
C	-1.84036900	1.21960000	-0.05803200
C	-2.89871000	0.32098800	-0.11572500
C	-2.64392300	-1.04717300	-0.06467300
C	-1.34005700	-1.51335300	0.03875000
H	-2.03018100	2.28734300	-0.10224200
H	-3.91480500	0.68413200	-0.20477300
H	-3.46267100	-1.75477000	-0.11273800
H	-1.11251500	-2.57162300	0.07101200
B	2.04705400	-0.22325500	-0.03707000
C	0.63547600	1.71795800	0.18050500
H	0.71313500	2.09172100	1.20750400
H	0.49436300	2.57706000	-0.47749100
O	1.87347000	1.11547100	-0.16693600
O	0.98709900	-1.08468100	0.19912500
O	3.29467300	-0.74172200	-0.15154100
H	3.29324300	-1.70007100	-0.09987100

BL_Complex

C	0.43032800	-0.65426600	0.10103600
C	0.96250100	0.62903900	0.01405900
C	2.31914100	0.88150800	-0.14134900
C	3.18193700	-0.20812000	-0.21309300
C	2.67433000	-1.50807200	-0.12696100
C	1.30709300	-1.73456000	0.02932100
H	2.67766600	1.90365000	-0.20194000
H	4.24907700	-0.05348000	-0.33335900
H	3.35861700	-2.34932100	-0.18207200
H	0.93063000	-2.75029000	0.09748600
B	-1.16769100	-0.50145000	0.27329600
O	-1.28424600	1.06743900	0.29394700
O	-1.84652700	-0.91129700	-0.96697900
O	-1.72503900	-1.06354700	1.46168100
H	-2.67912400	-1.08773800	1.35036800
O	-3.20738200	-0.46044100	-0.84432200
H	-3.07902700	0.49909600	-0.81299000
C	-0.12504800	1.66108900	0.12093600
O	0.04805800	2.86105000	0.05721500

BL_TS

C	0.33428700	-0.63323100	0.08100900
C	0.94073000	0.60943300	-0.07942200
C	2.32028200	0.73247900	-0.19326300
C	3.09347700	-0.42430100	-0.14757800
C	2.48660700	-1.67319400	0.01298900
C	1.10088000	-1.78881000	0.11644900
H	2.77370000	1.71175300	-0.29874900
H	4.17135400	-0.35815700	-0.23101700
H	3.10292600	-2.56413800	0.04985100
H	0.63262700	-2.76175300	0.21252000
B	-1.35158200	-0.14543100	0.49782900
O	-1.22477200	1.31811700	0.37094100
O	-1.36384500	-0.90695700	-0.64321500
O	-1.99240700	-0.49048700	1.68258000
H	-2.27069500	-1.40981800	1.65485100
O	-3.16610300	-0.92140200	-1.22776600
H	-2.97411700	-0.49538900	-2.06806000
C	-0.02563400	1.74270500	-0.01058100
O	0.22442000	2.90250100	-0.24331100

BL_Product

C	-0.29330200	-0.60220800	0.10280000
C	-0.52874300	0.76917600	0.05950300
C	-1.84036900	1.21960000	-0.05803200
C	-2.89871000	0.32098800	-0.11572500
C	-2.64392300	-1.04717300	-0.06467300
C	-1.34005700	-1.51335300	0.03875000
H	-2.03018100	2.28734300	-0.10224200
H	-3.91480500	0.68413200	-0.20477300
H	-3.46267100	-1.75477000	-0.11273800
H	-1.11251500	-2.57162300	0.07101200
B	2.04705400	-0.22325500	-0.03707000
C	0.63547600	1.71795800	0.18050500
H	0.71313500	2.09172100	1.20750400
H	0.49436300	2.57706000	-0.47749100
O	1.87347000	1.11547100	-0.16693600
O	0.98709900	-1.08468100	0.19912500
O	3.29467300	-0.74172200	-0.15154100
H	3.29324300	-1.70007100	-0.09987100

BON_SM

C	-3.41046500	0.22520500	0.15517100
C	-2.40329100	1.15443800	0.40712300
C	-1.06501000	0.78115900	0.28909900
C	-0.71414200	-0.51966600	-0.09300300
C	-1.73681200	-1.43525500	-0.34747600
C	-3.07780400	-1.07353700	-0.22302500
H	-4.45061500	0.51684700	0.24735100
H	-2.66045600	2.16962300	0.69322300
H	-1.47771000	-2.44428100	-0.65323200
H	-3.86059400	-1.79653200	-0.42407000
C	0.04795400	1.76181800	0.57272500
H	0.44241800	1.58025200	1.58036600
H	-0.29540700	2.79486800	0.53638400
C	1.23763000	1.62257900	-0.36560500
O	1.85299200	2.60573100	-0.74489800
O	1.58586500	0.41502400	-0.72600800
O	1.14655800	-1.91937800	-1.13489100
O	1.35472900	-1.09316200	1.15122700
H	2.05115800	-2.20999600	-0.98392800
B	0.84731100	-0.85410900	-0.22383600
O	2.76039000	-1.37544600	1.06207000
H	3.14200400	-0.50282500	0.89304700

BON_TS

C	-3.31393400	0.40291200	0.08657300
C	-2.26607700	1.28150700	0.35534800
C	-0.95093300	0.82210600	0.33537300
C	-0.69933500	-0.50961400	0.00378100
C	-1.74411300	-1.39601600	-0.24464900
C	-3.05665600	-0.93580400	-0.21006900
H	-4.33568200	0.76309100	0.11254900
H	-2.47306400	2.32044100	0.58948500
H	-1.53268800	-2.43463500	-0.47716300
H	-3.87720100	-1.61386100	-0.41347000
C	0.21980200	1.70740500	0.66156900
H	0.63224700	1.40716700	1.63243700
H	-0.06386500	2.75627000	0.72738000
C	1.37075300	1.59500400	-0.32603300
O	2.05704100	2.55566000	-0.60234500
O	1.60753000	0.41802900	-0.87149800
O	1.21207000	-1.79410500	-1.46781900
O	0.82629800	-1.15129800	0.86151900
H	1.03539000	-2.67589900	-1.13152300
B	0.95503900	-0.83485900	-0.47393200
O	2.53214600	-1.67875200	1.48630100
H	2.60194300	-0.94954800	2.10934200

BON_Prod

C	-3.32789034	0.36599511	0.06764961
C	-2.24457673	1.22390722	0.29361620
C	-0.93727065	0.72349303	0.42570458
C	-0.75172497	-0.68307464	0.38870266
C	-1.83710871	-1.53336869	0.13202071
C	-3.12239040	-1.01096700	-0.02844290
H	-4.31469905	0.76706416	-0.03360341
H	-2.41385710	2.27817673	0.36260869
H	-1.68019469	-2.58954374	0.06293916
H	-3.94713307	-1.66454961	-0.22216767
C	0.18605021	1.80790657	0.61154775
H	0.39187672	1.87631960	1.65933356
H	-0.20450430	2.73416294	0.24491945
C	1.55206863	1.57318784	-0.14643842
O	2.20113491	2.60307574	-0.46520863
O	2.08889288	0.42445182	-0.46232861
O	1.16867011	-1.59180580	-1.95159129
O	0.51490890	-1.26757981	0.60294380
H	1.01938843	-2.52408099	-1.77787322
B	1.26098124	-0.82926948	-0.61681902

^{1}H-NMR Spectrum of 2-CPBA (D_2O)

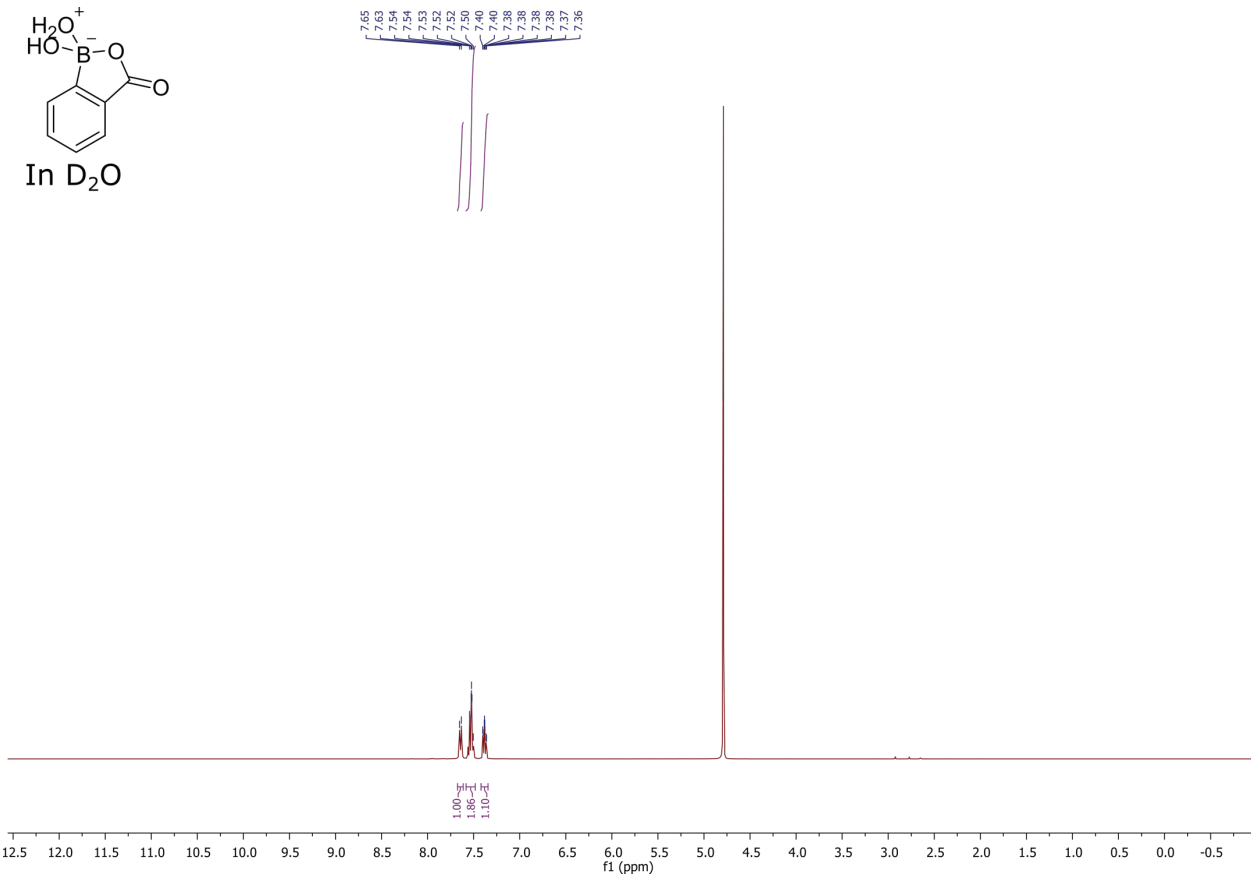

^{1}H-NMR Spectrum of 2-CPBA (DMSO-d_6)

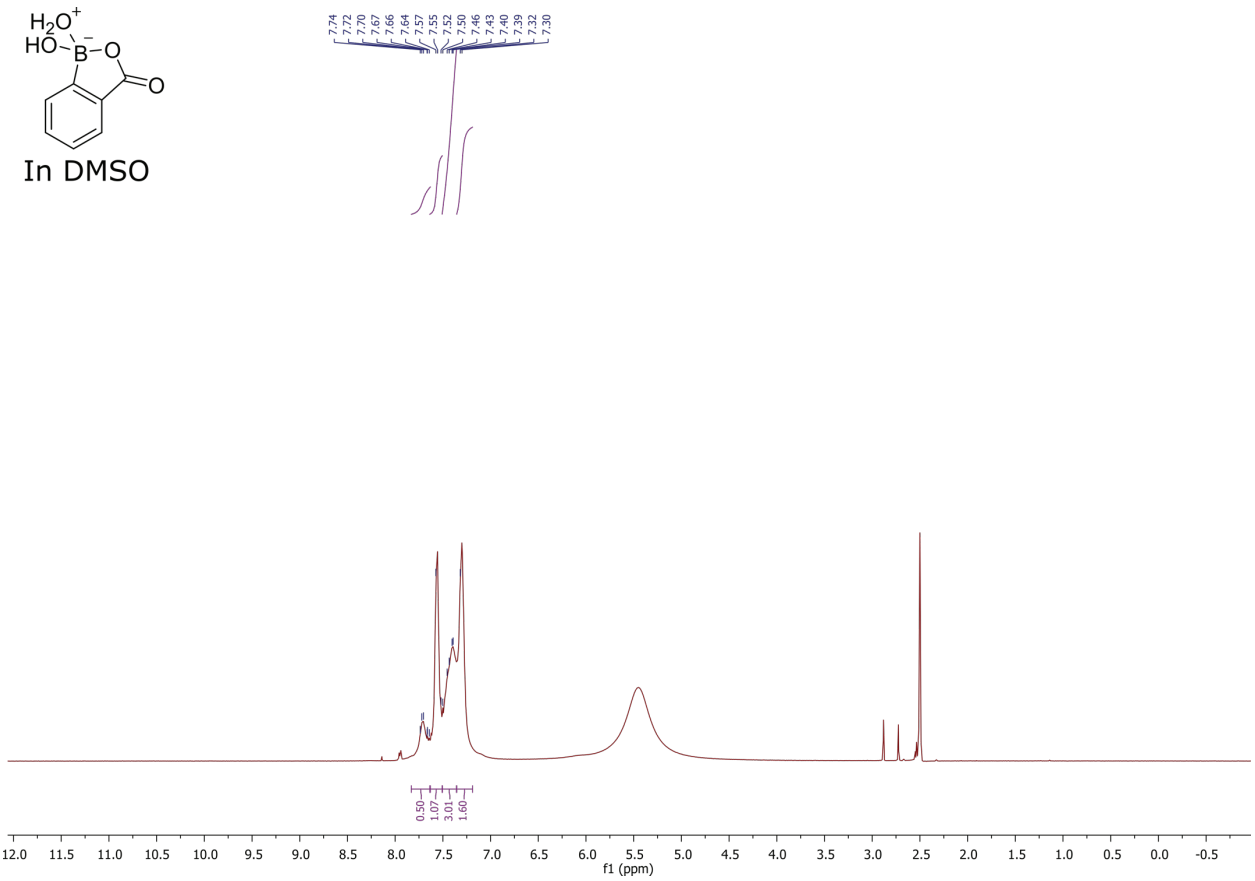

^{13}C-NMR Spectrum of 2-CPBA (D_2O)

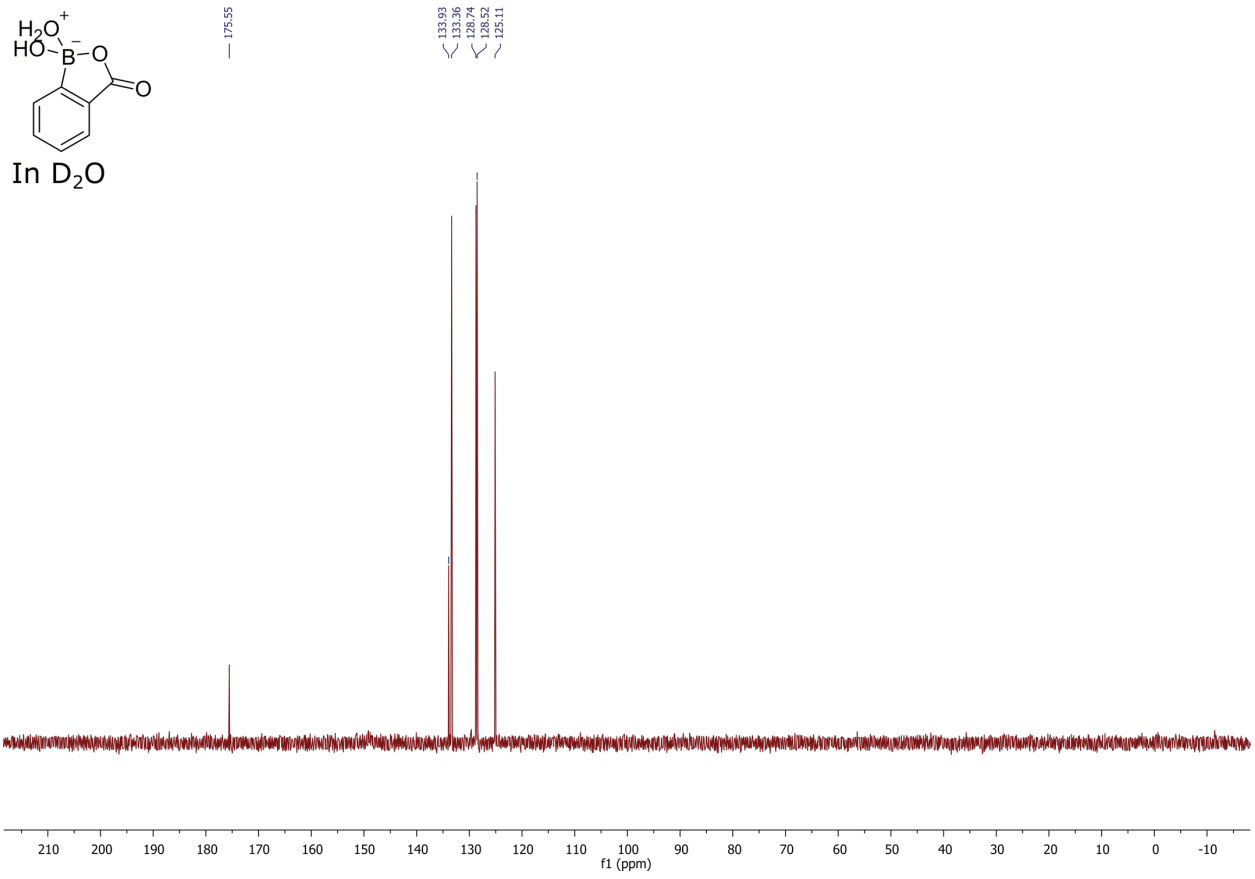

^{13}C-NMR Spectrum of 2-CPBA (DMSO-d_6)

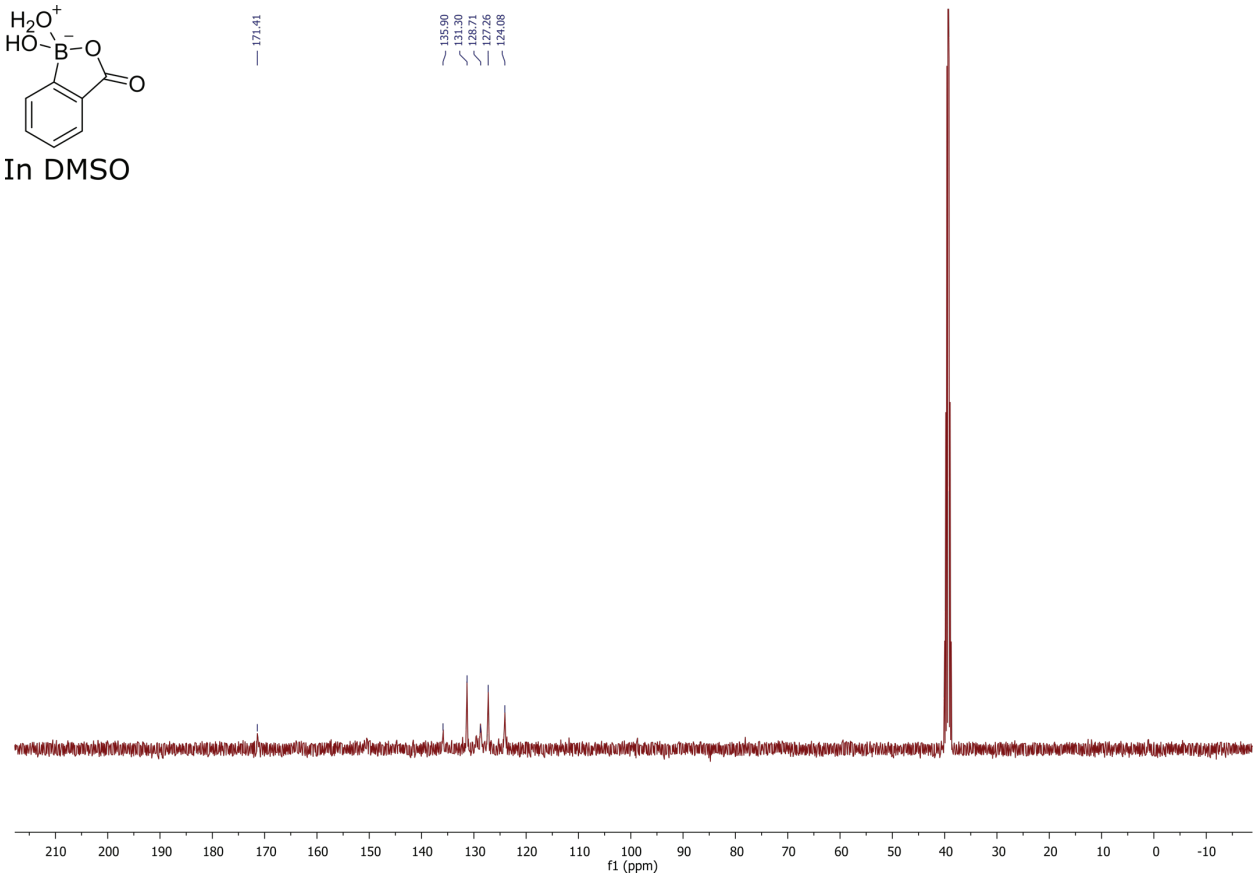

^{11}B-NMR Spectrum of 2-CPBA (D_2O)

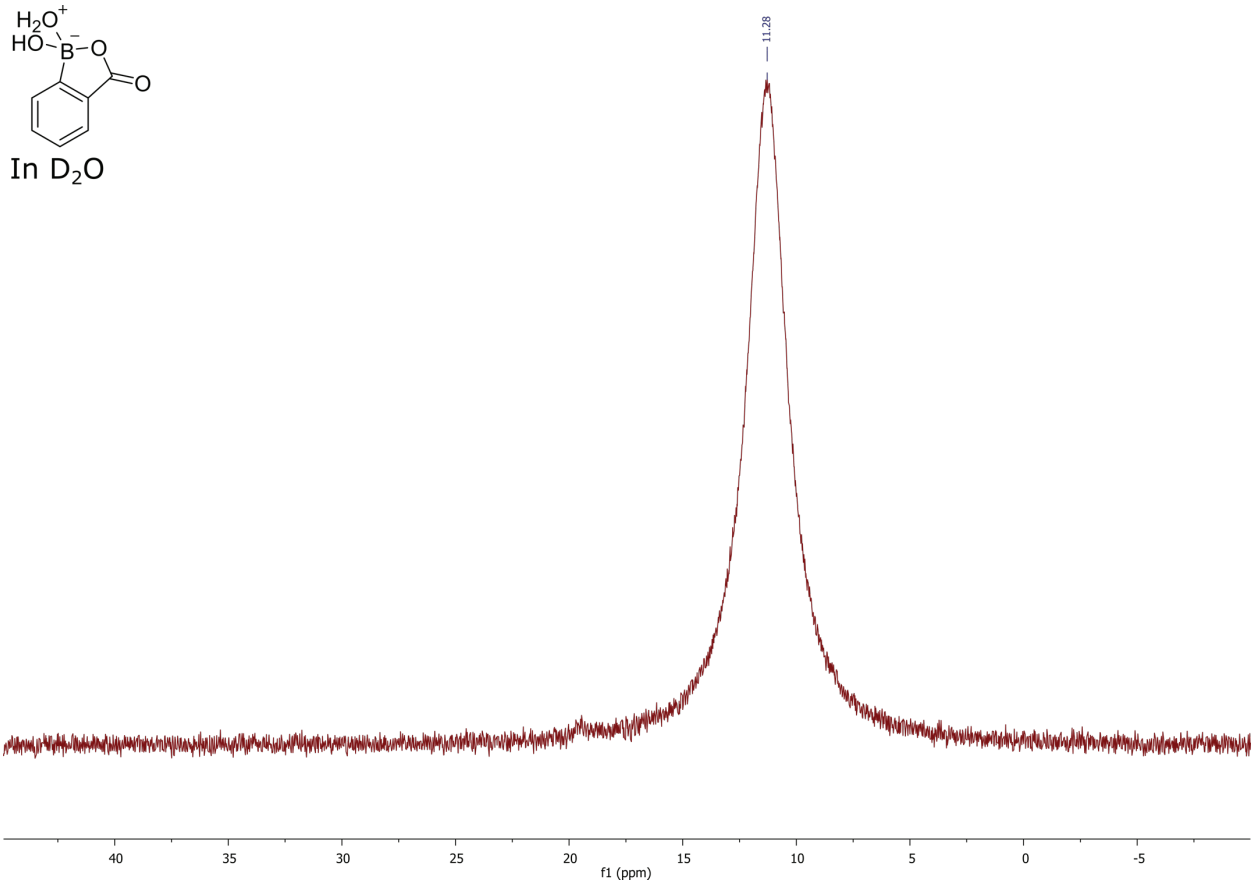

^{11}B-NMR Spectrum of 2-CPBA (DMSO-d_6)

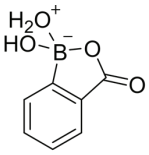

In DMSO

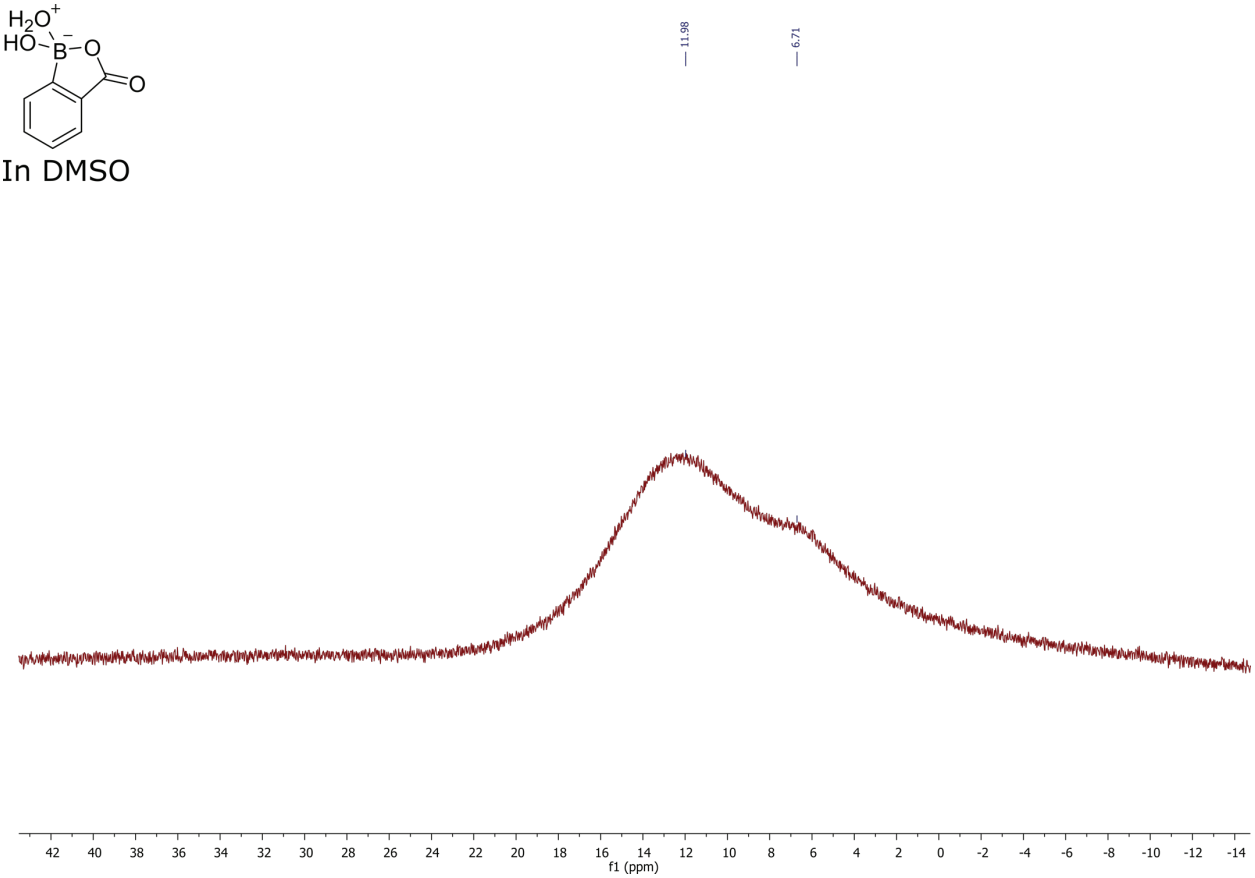

^{1}H-NMR Spectrum of 2-CMPBA (D_2O)

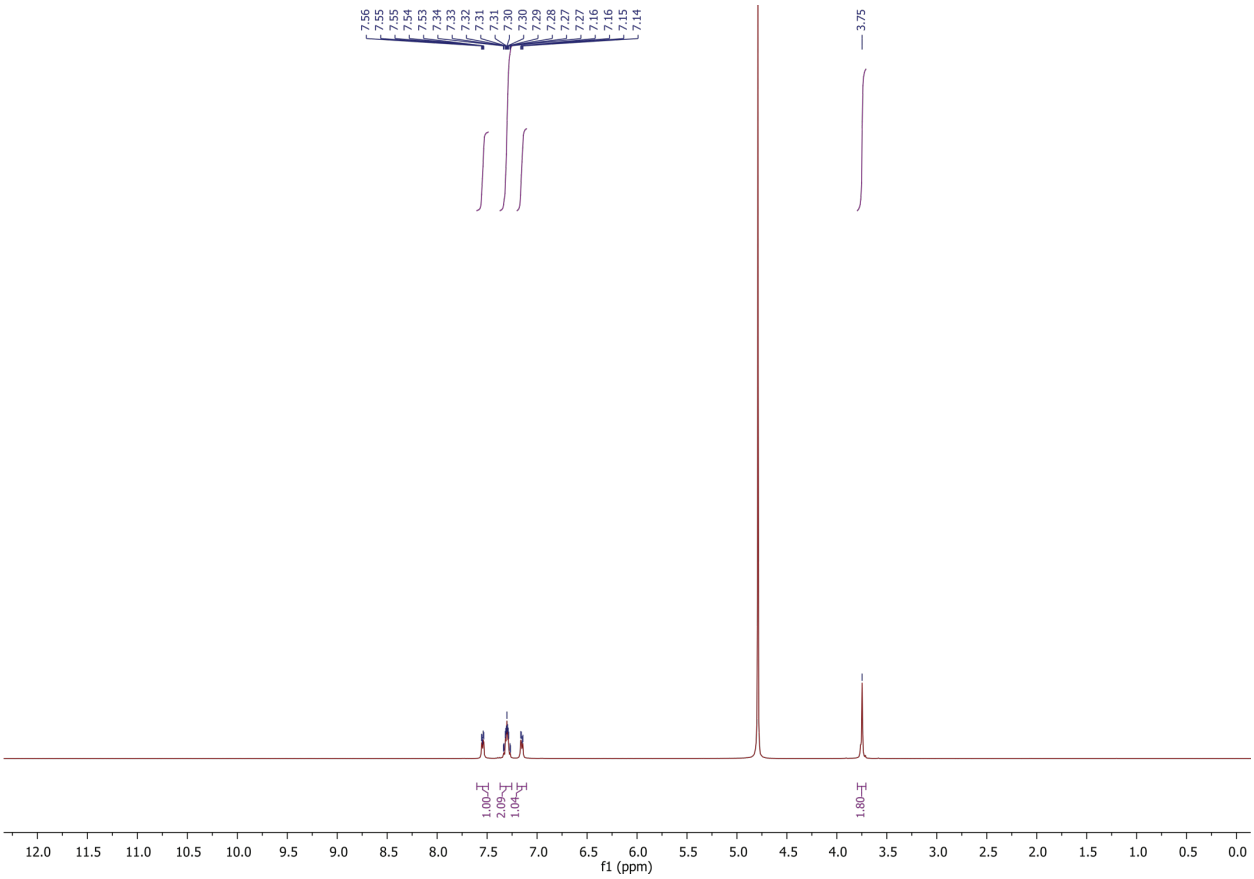

^{13}C-NMR Spectrum of 2-CMPBA (D_2O)

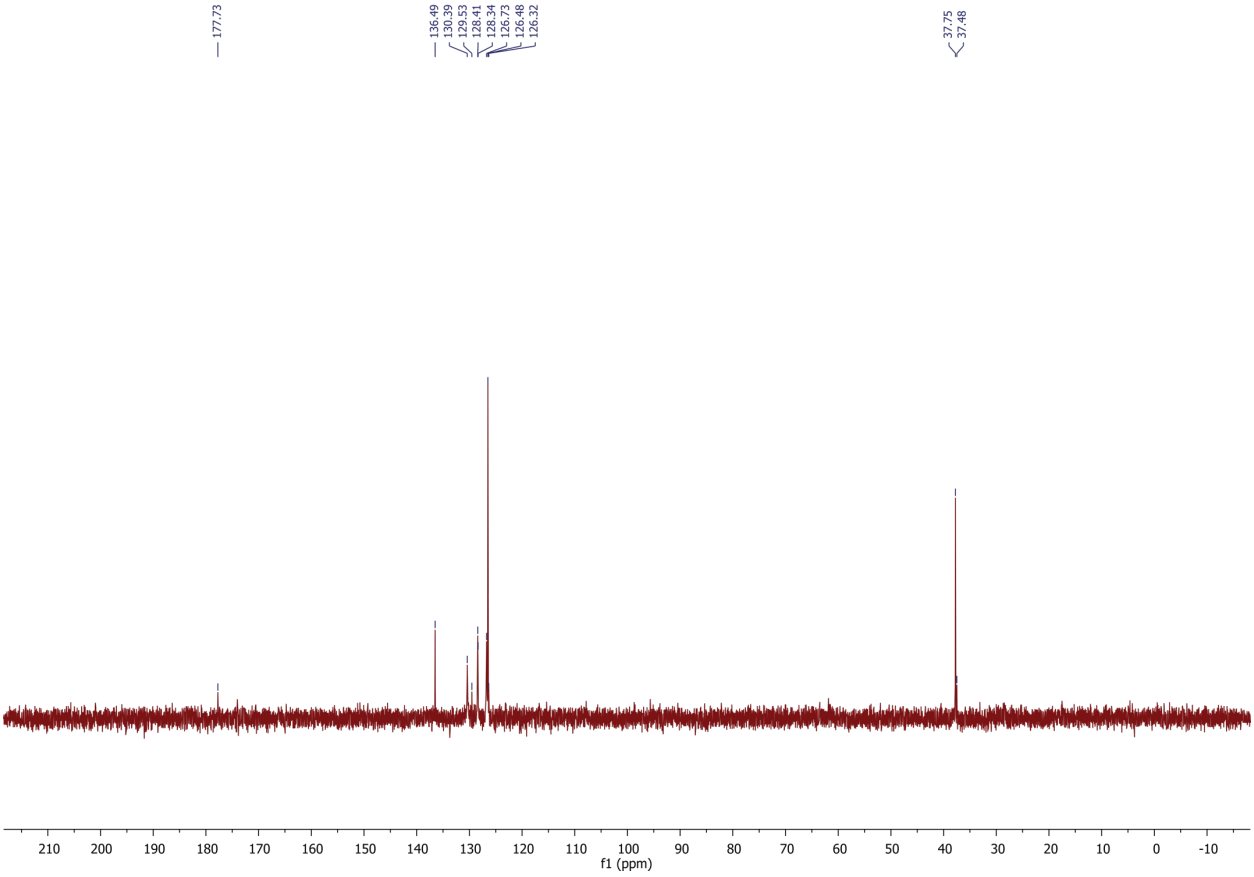

^{11}B-NMR Spectrum of 2-CMPBA (D_2O)

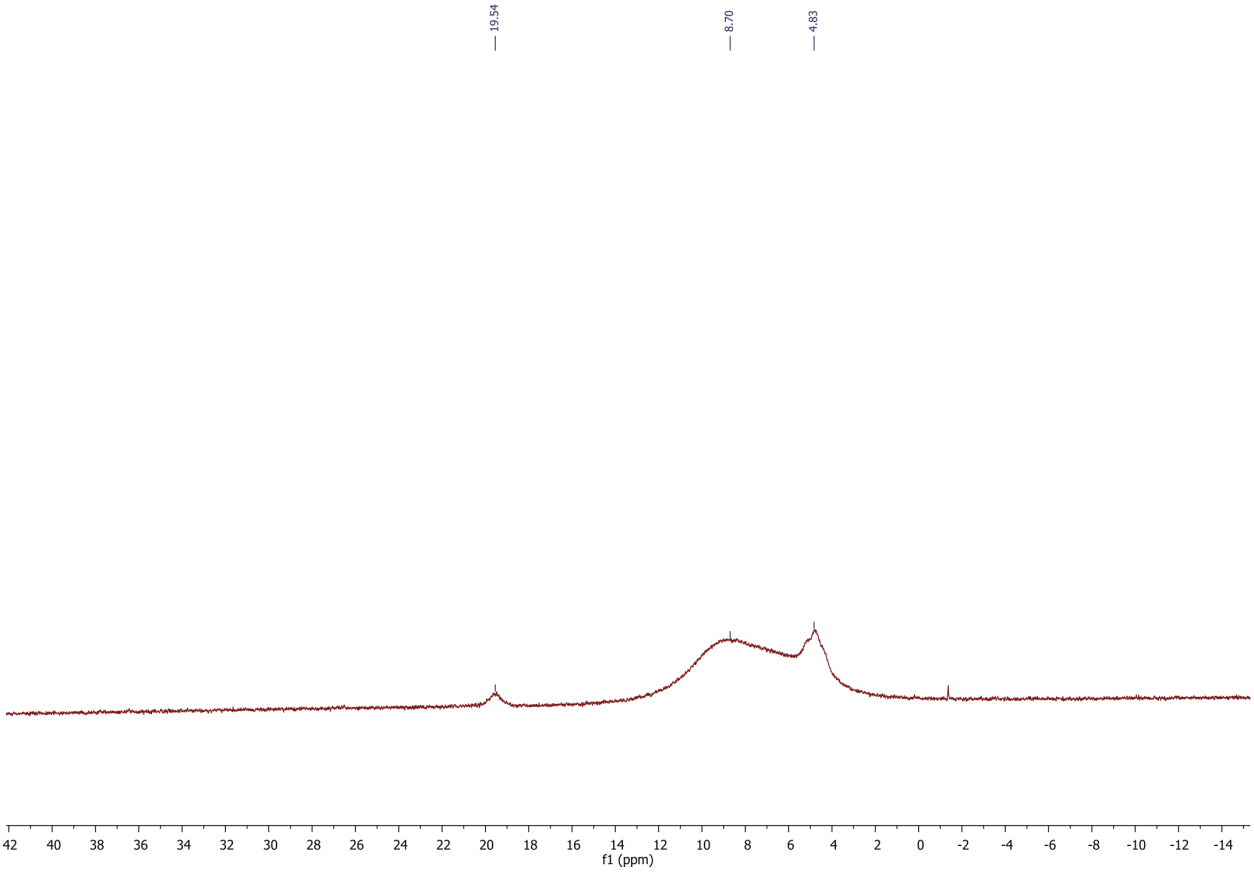

^{1}H-NMR Spectrum of Potassium Phenyltrifluoroborate

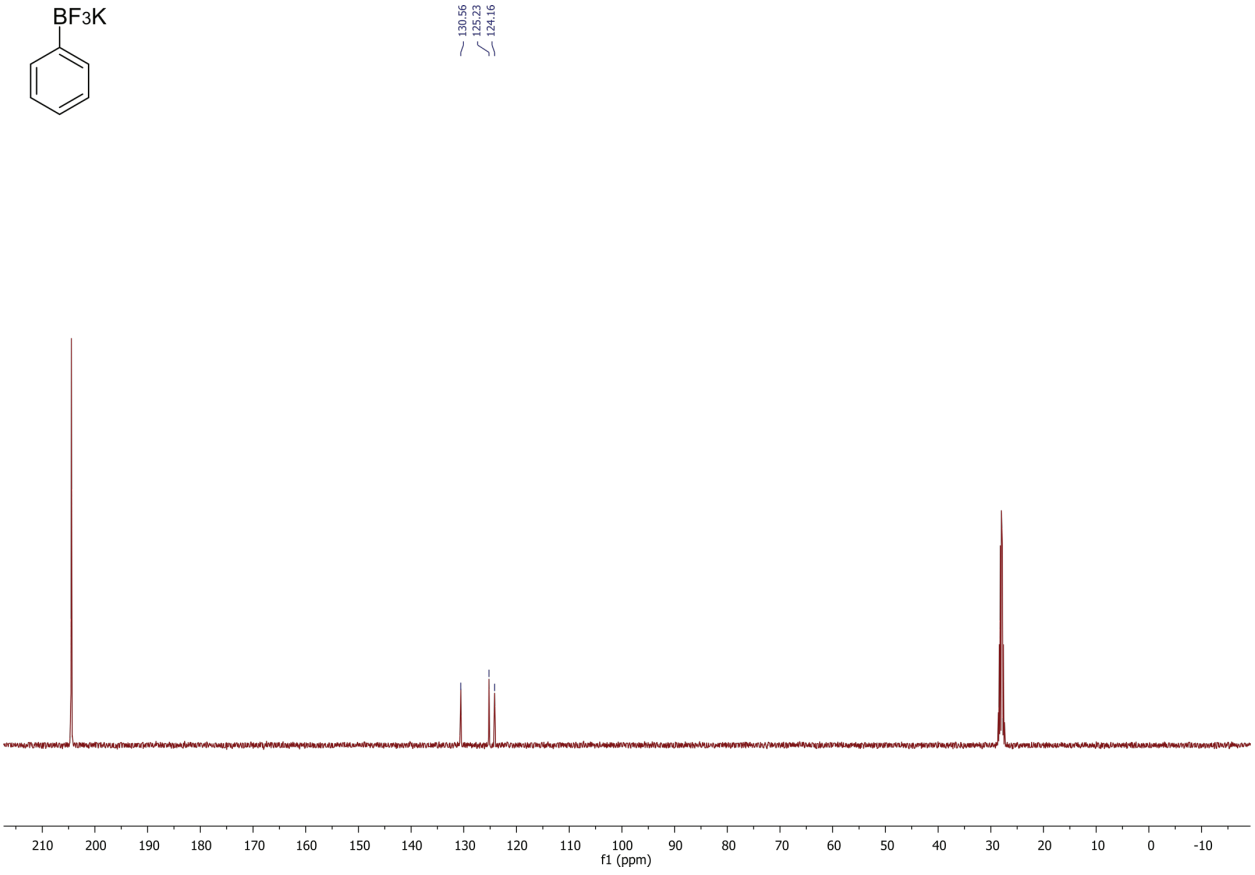

^{13}C-NMR Spectrum of Potassium Phenyltrifluoroborate

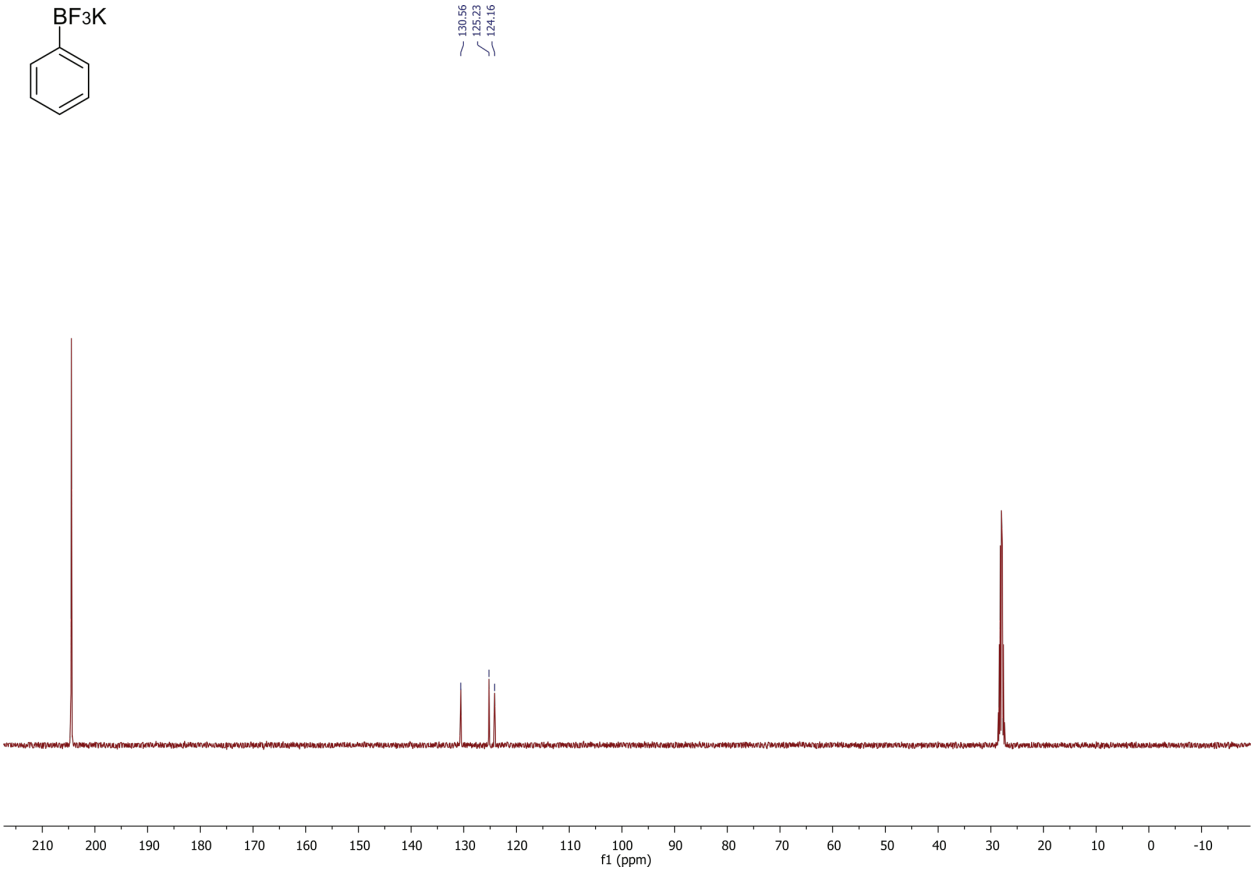

^{11}B-NMR Spectrum of Potassium Phenyltrifluoroborate

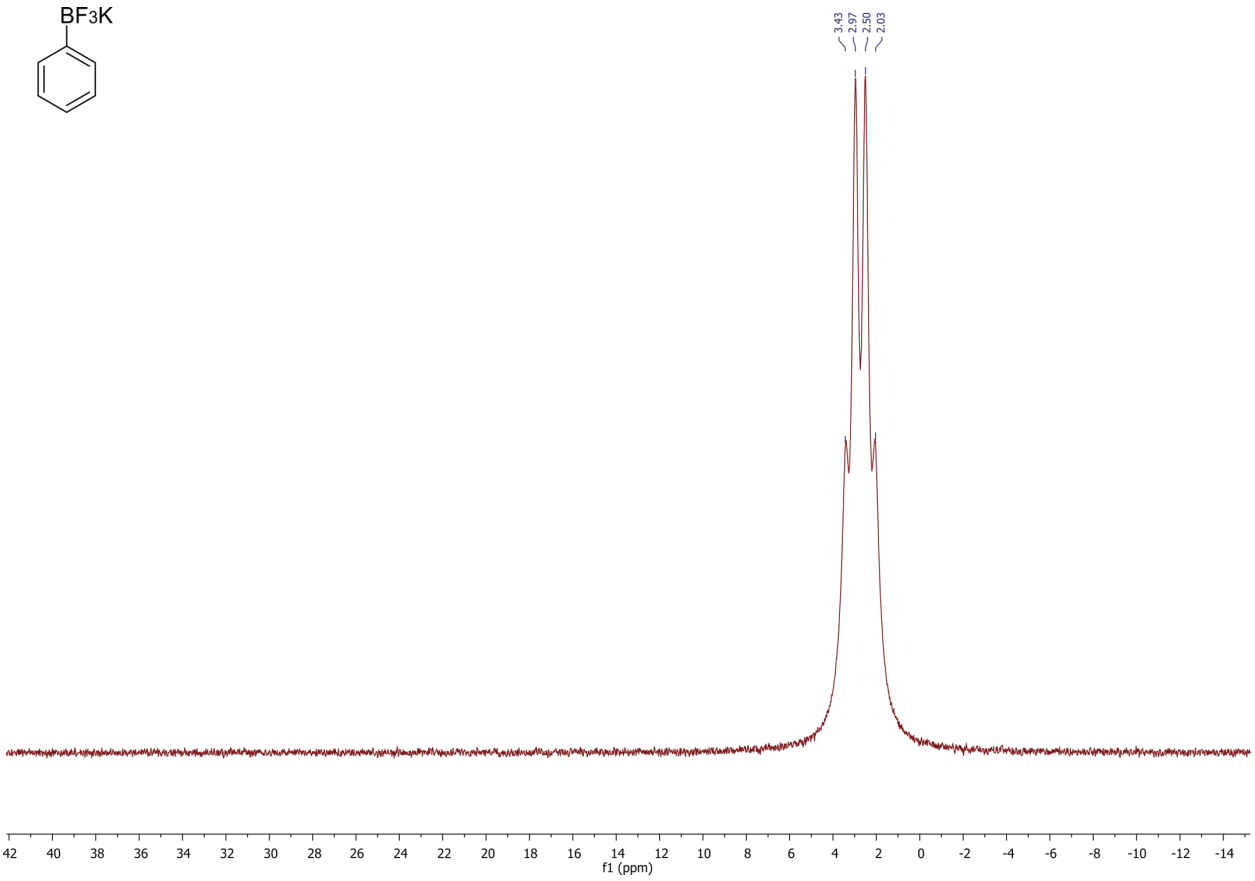

^{19}F-NMR Spectrum of Potassium Phenyltrifluoroborate

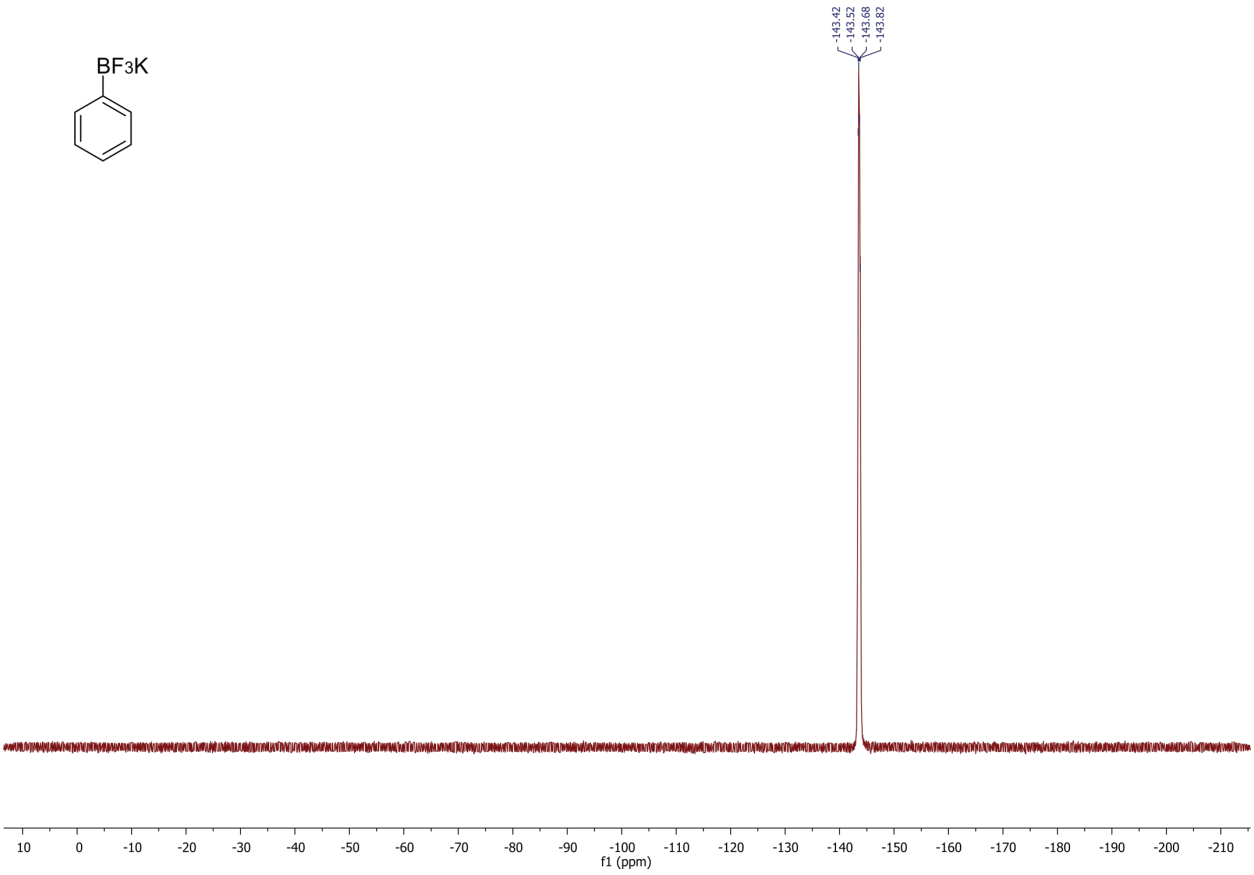

^{1}H-NMR Spectrum of Phenylboronic Acid–Cyclictriol Complex

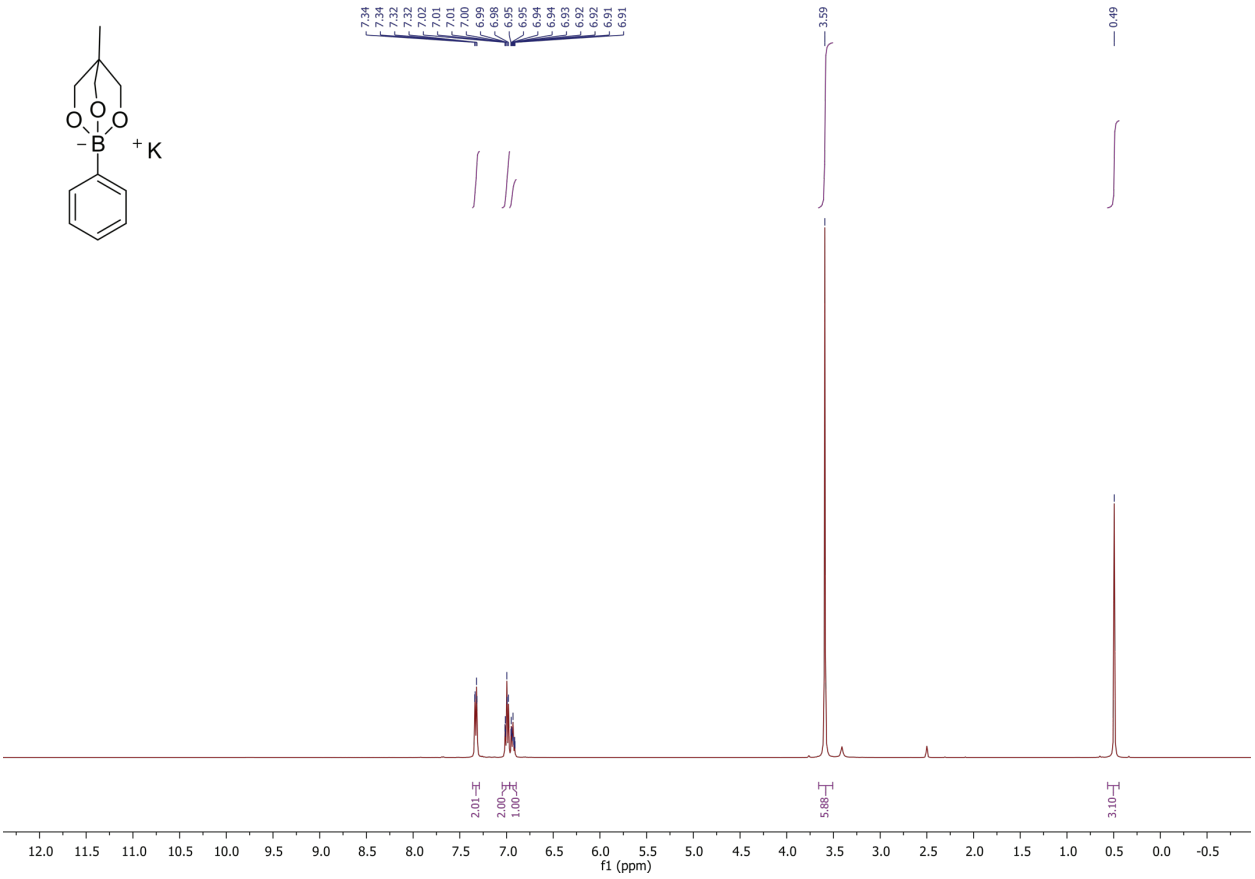

^{13}C-NMR Spectrum of Phenylboronic Acid–Cyclictriol Complex

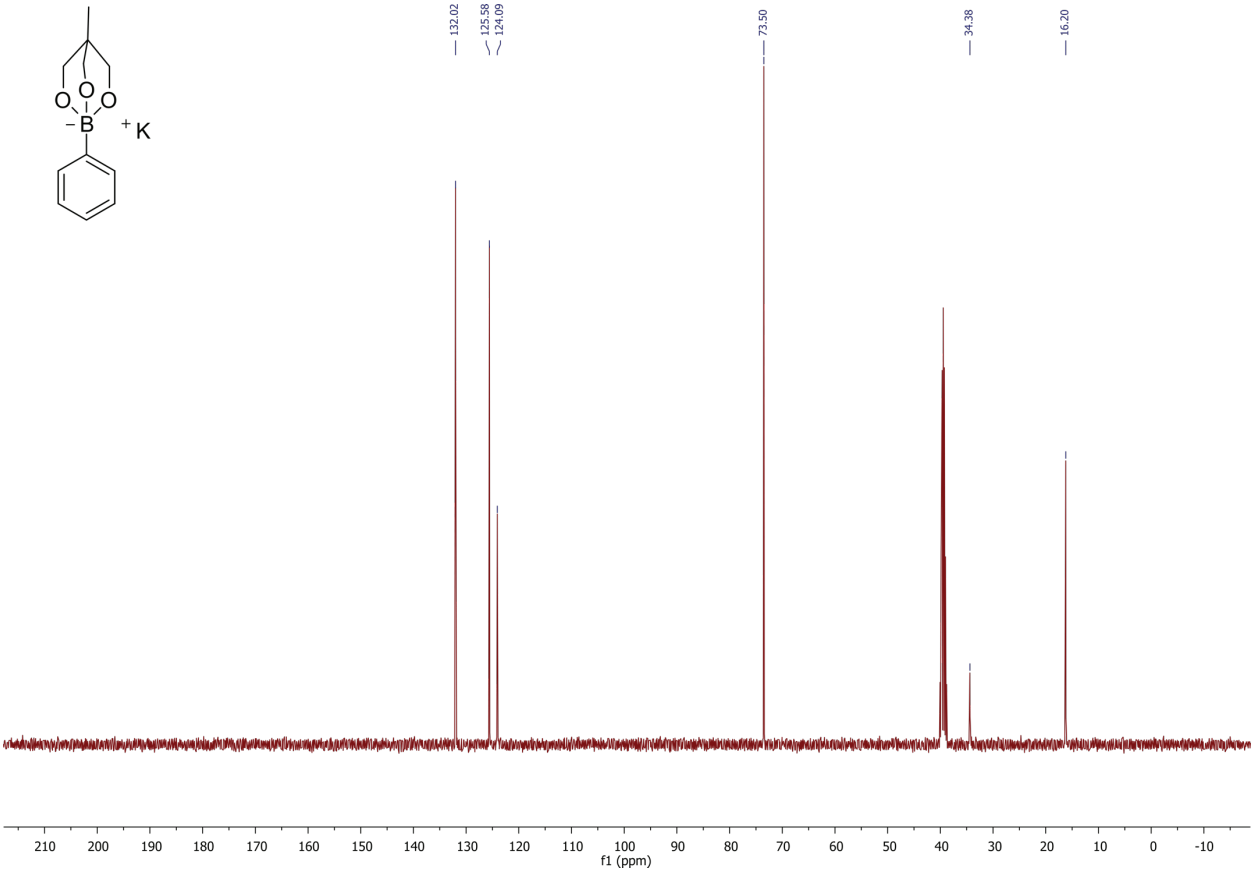

^{11}B-NMR Spectrum of Phenylboronic Acid–Cyclictriol Complex

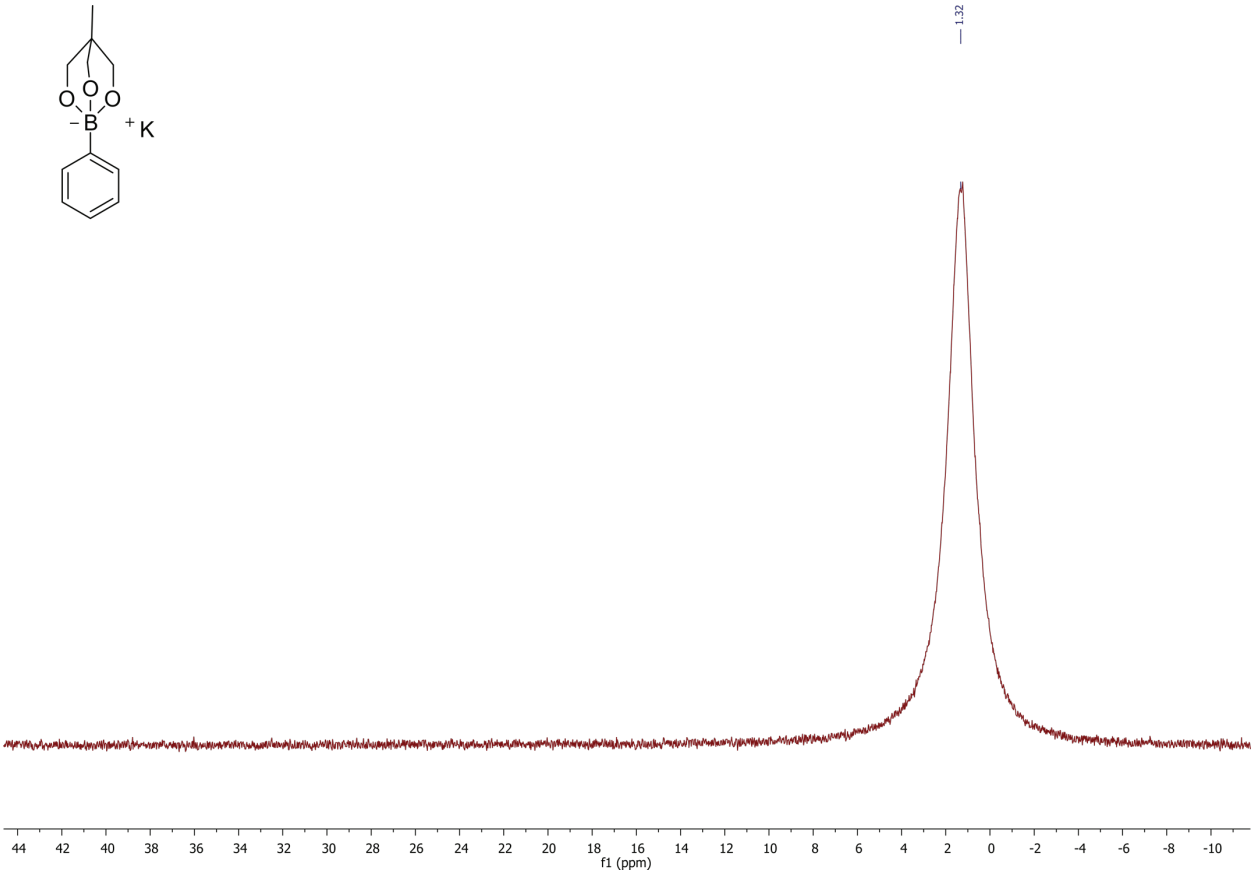

^{1}H-NMR Spectrum of Phenylboronic Acid–Citrate Complex

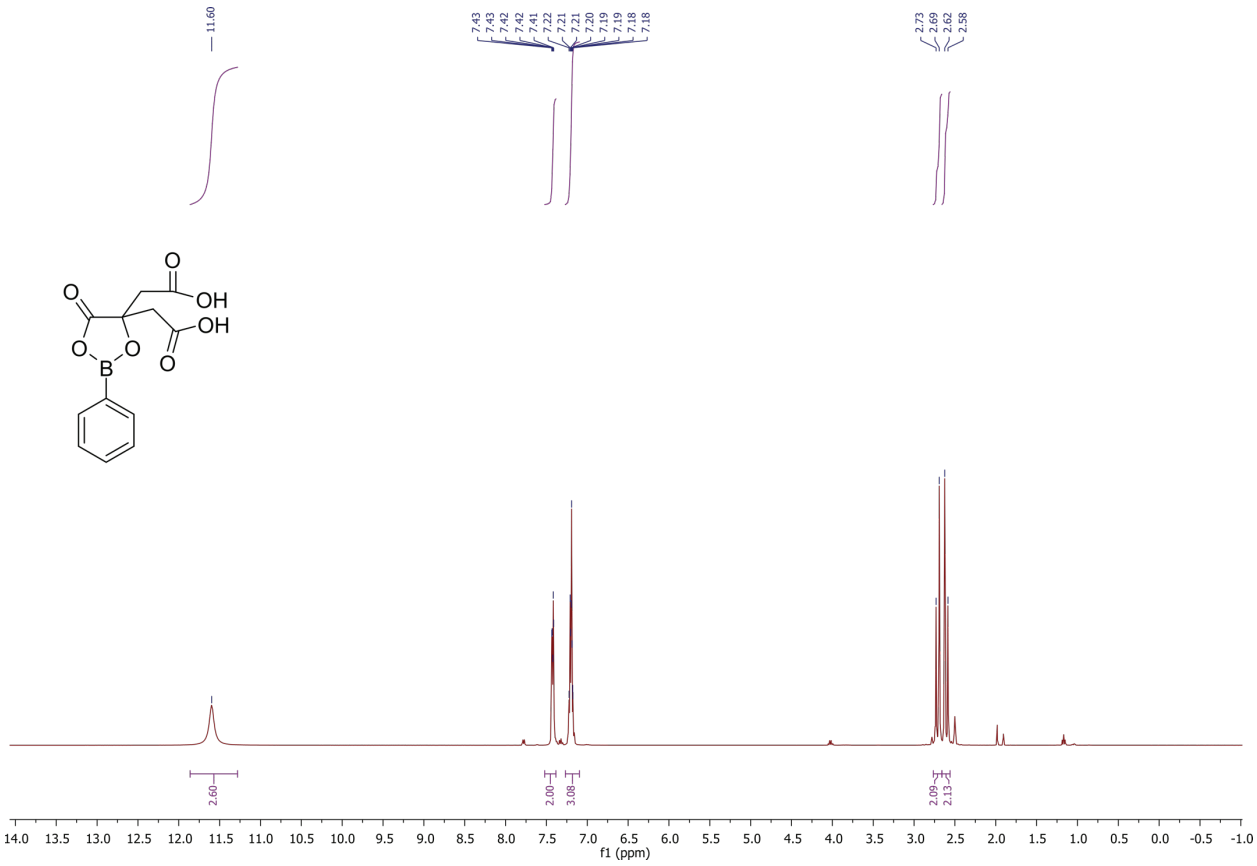

^{13}C-NMR Spectrum of Phenylboronic Acid–Citrate Complex

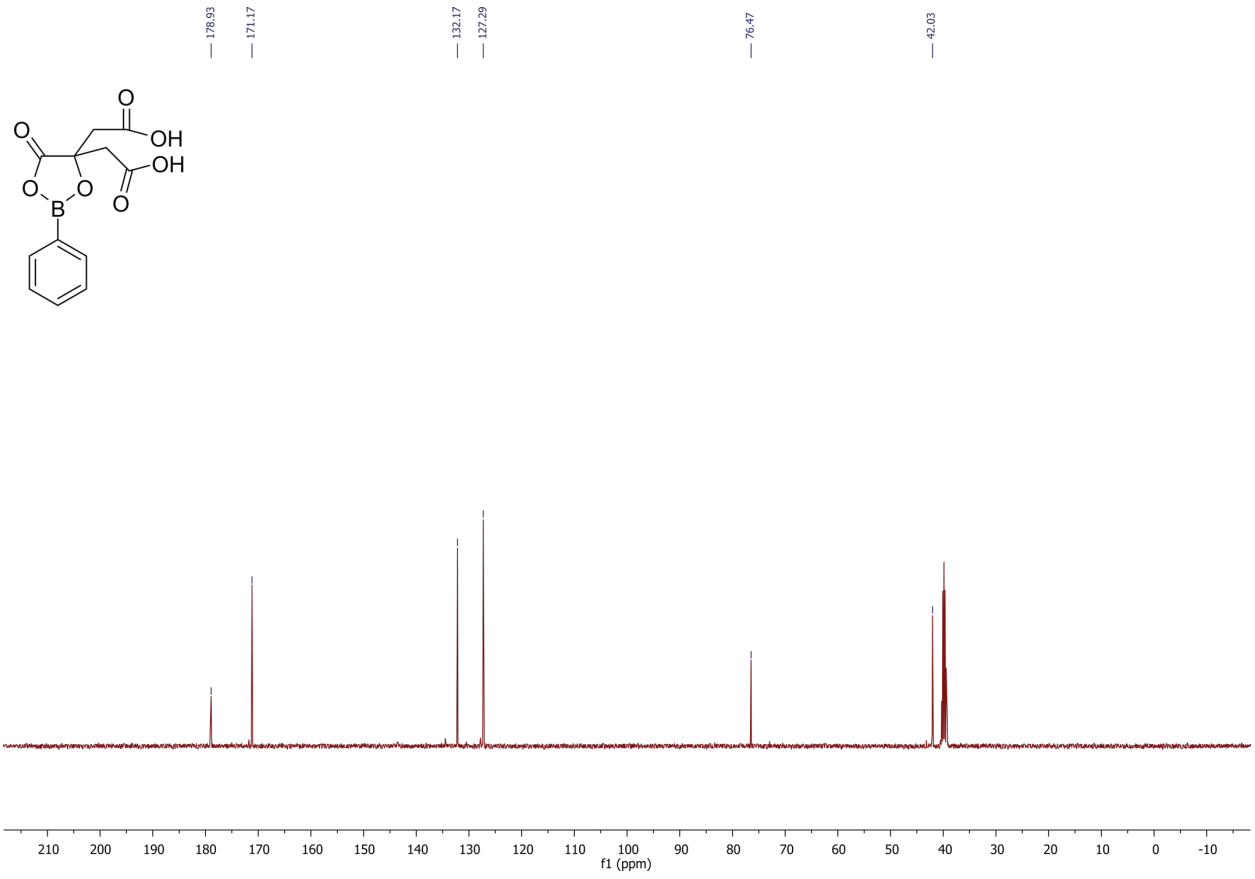

^{11}B-NMR Spectrum of Phenylboronic Acid–Citrate Complex

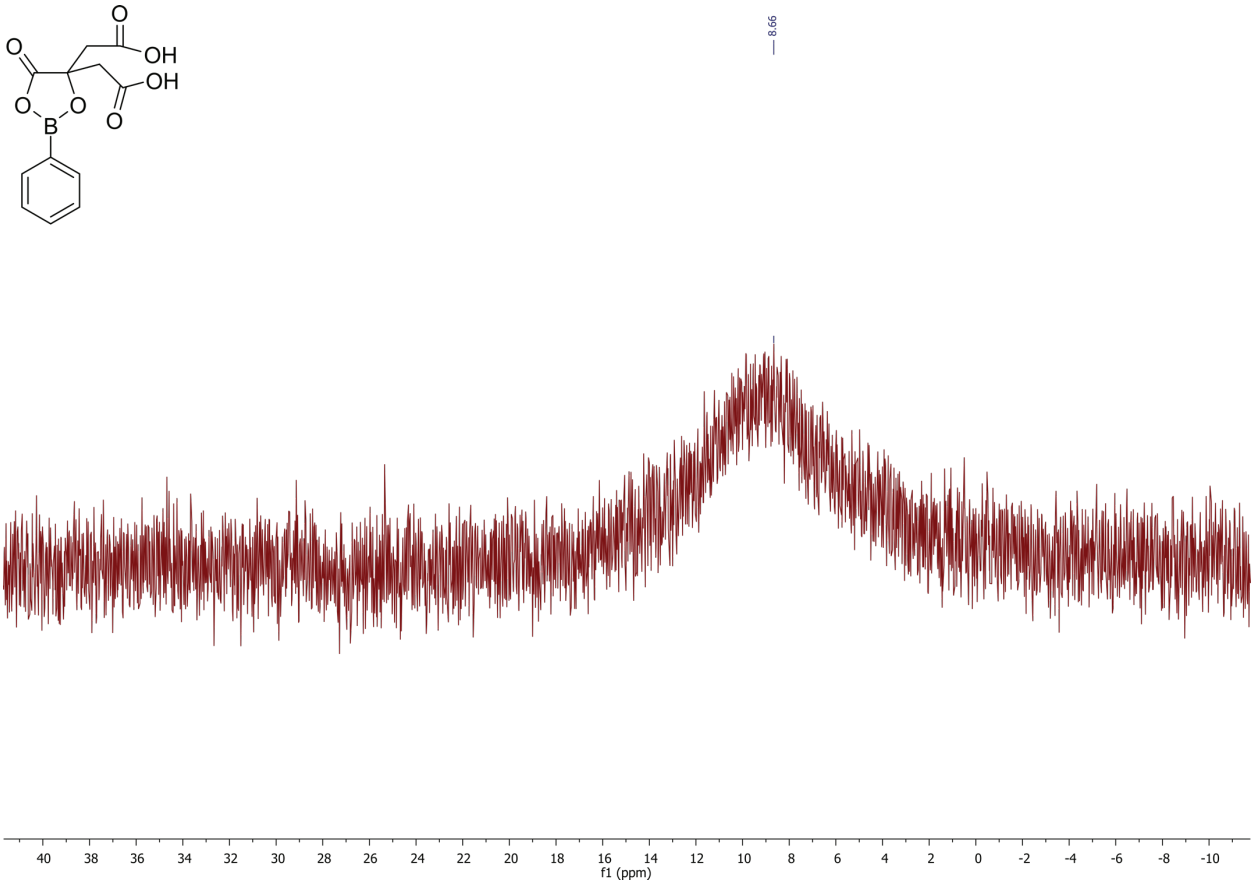

^{1}H-NMR Spectrum of 2-Formylphenylboronic Acid–Cysteine Complex

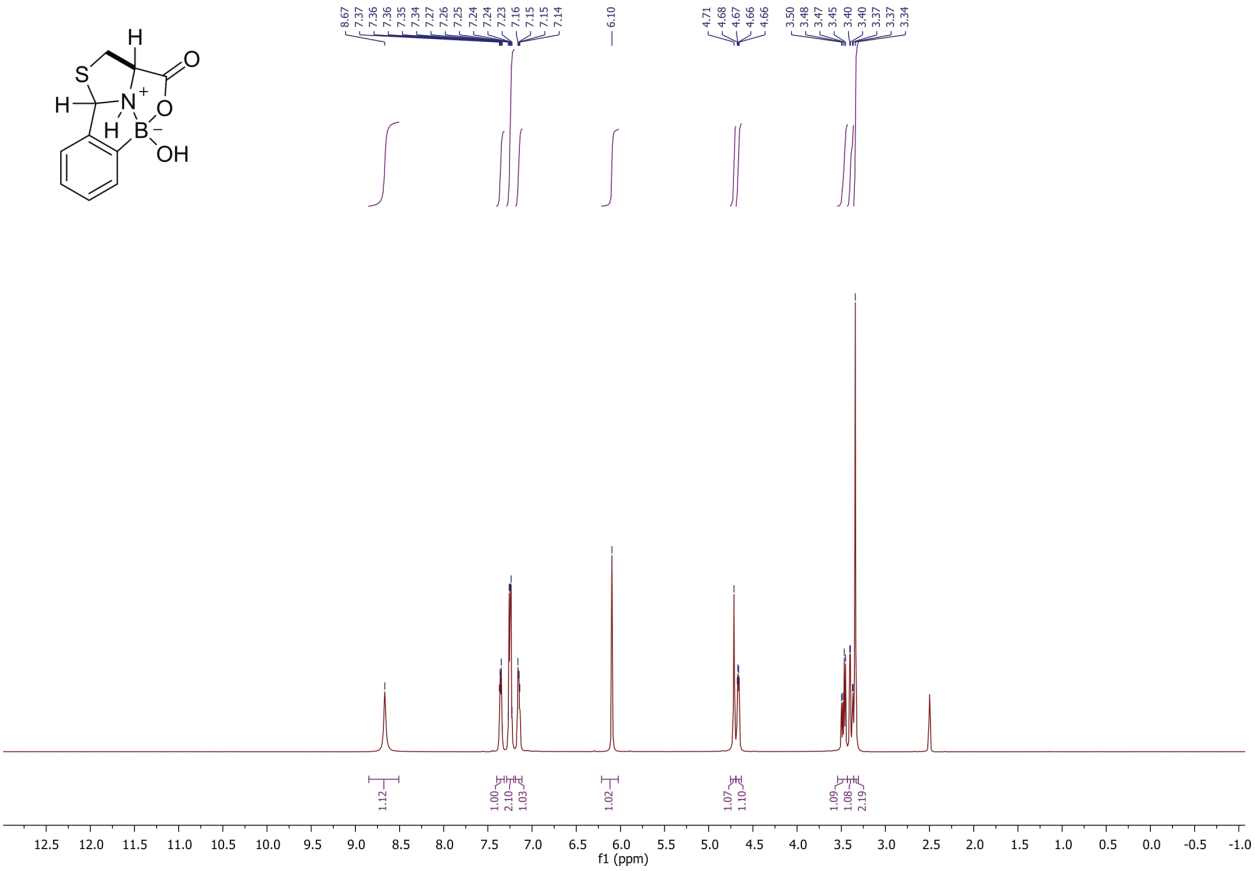

^{13}C-NMR Spectrum of 2-Formylphenylboronic Acid–Cysteine Complex

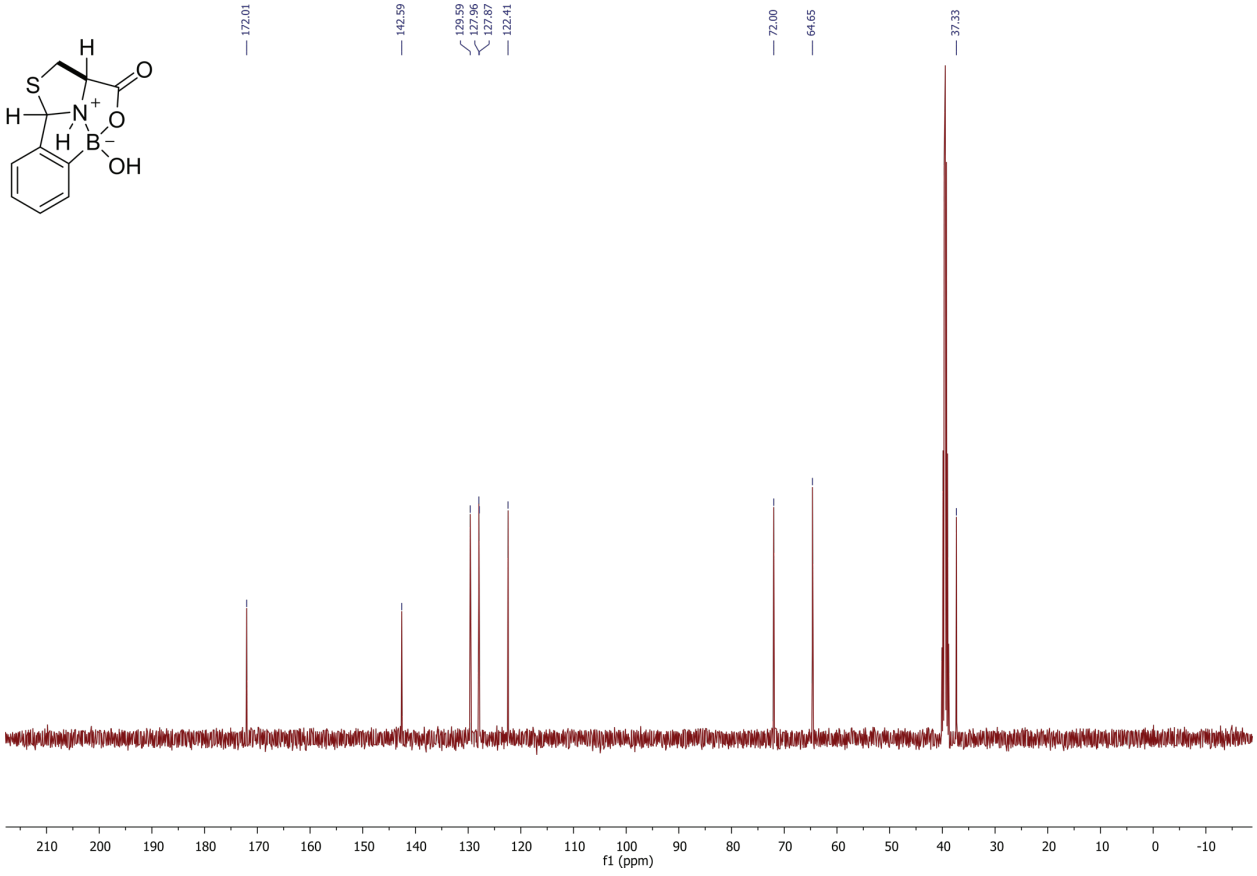

^{11}B-NMR Spectrum of 2-Formylphenylboronic Acid–Cysteine Complex

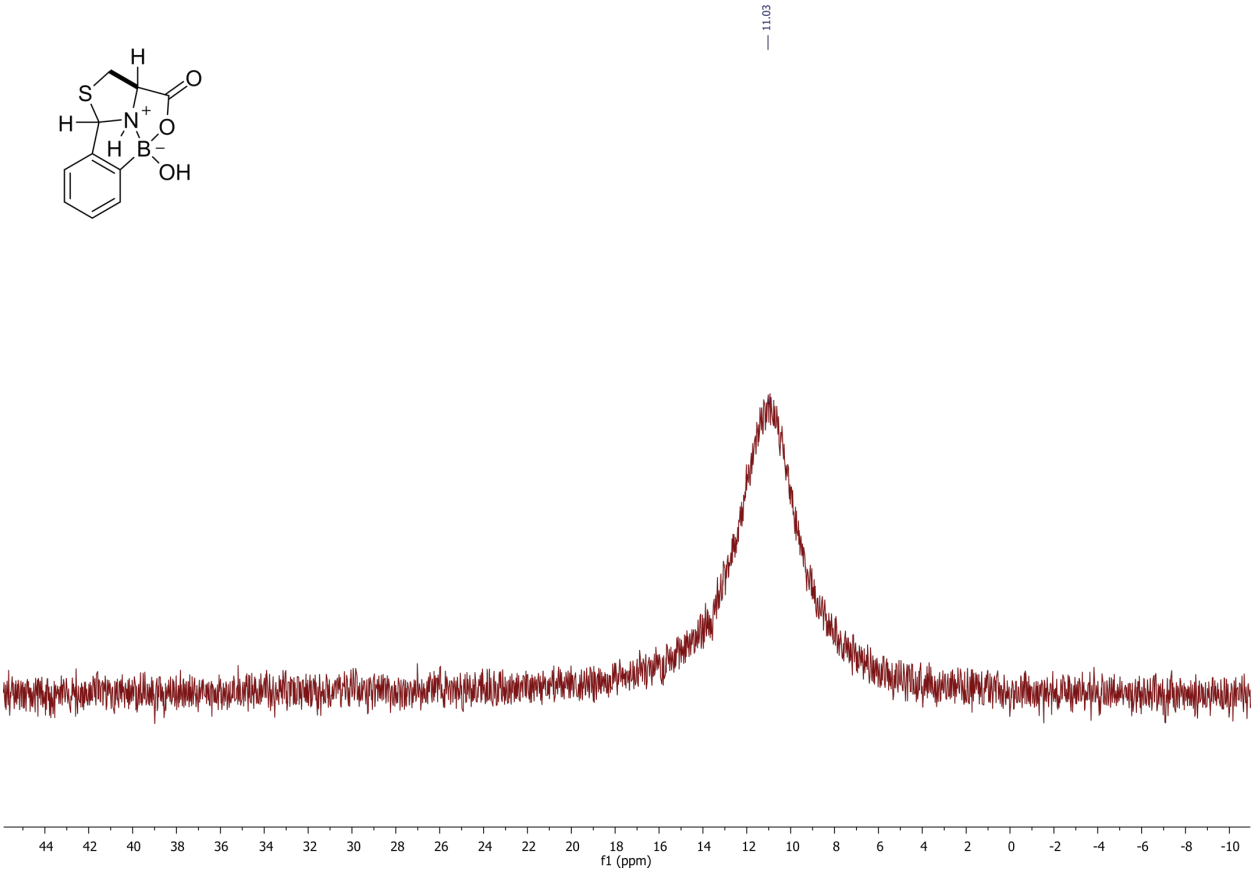

^{1}H-NMR Spectrum of 2-Formylphenylboronic Acid–Diaminopropionic Acid Complex

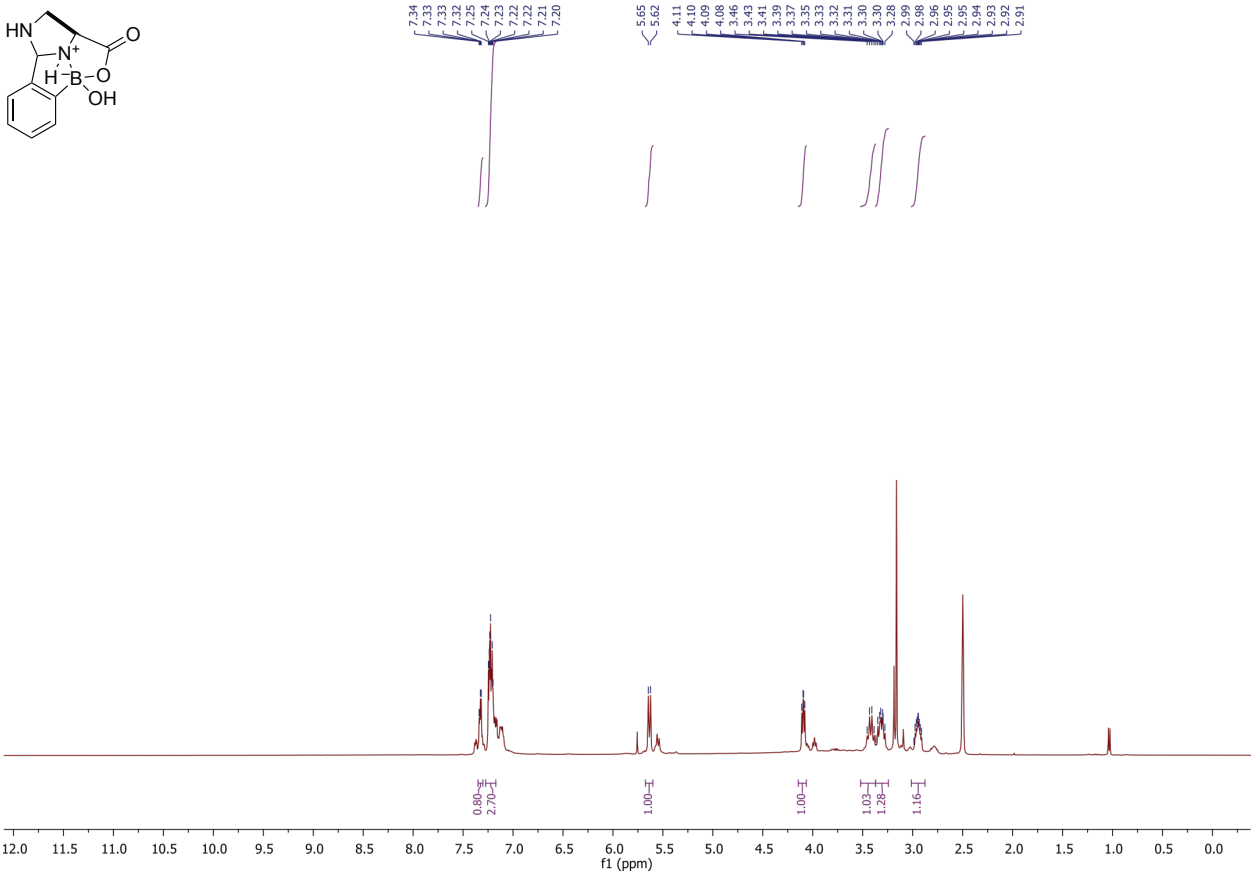

^{13}C-NMR Spectrum of 2-Formylphenylboronic Acid–Diaminopropionic Acid Complex

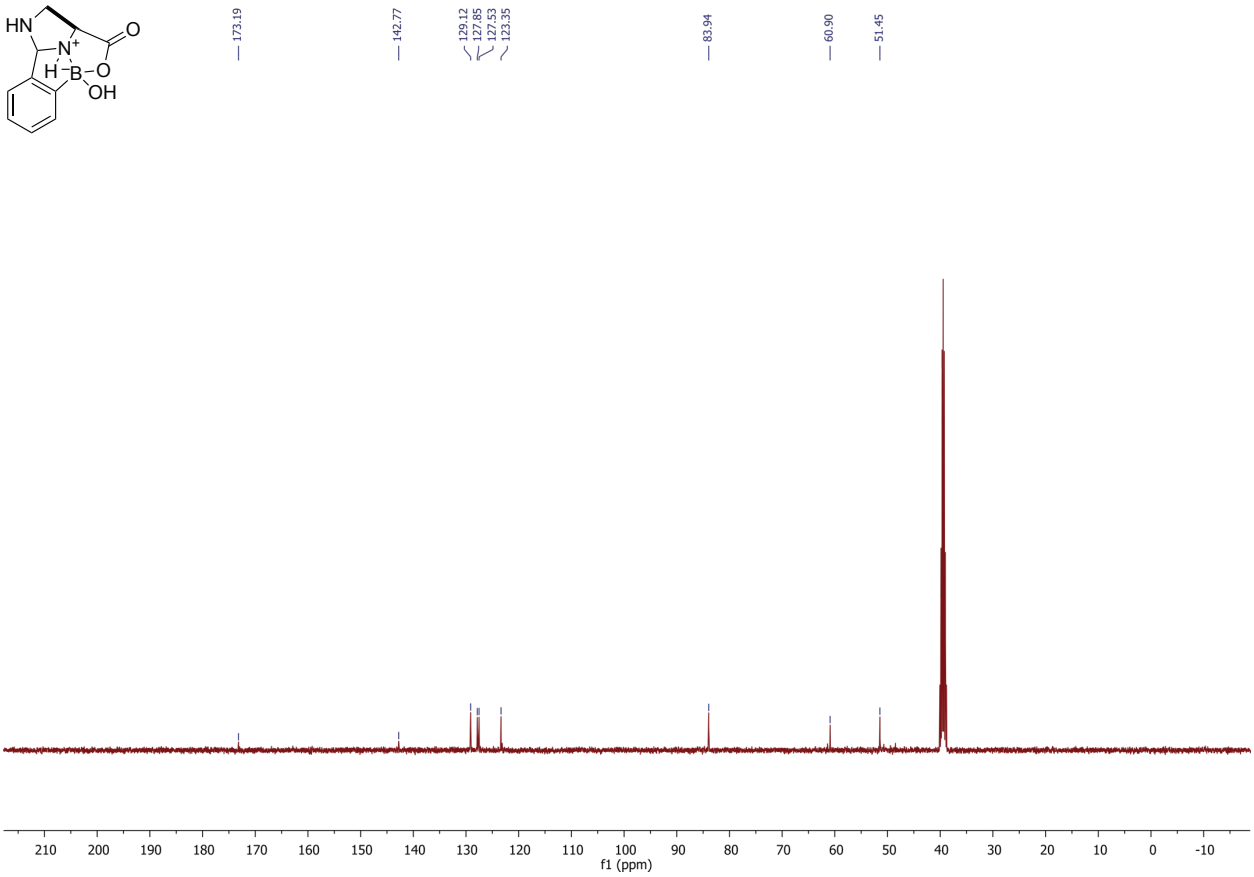

^{11}B-NMR Spectrum of 2-Formylphenylboronic Acid–Diaminopropionic Acid Complex

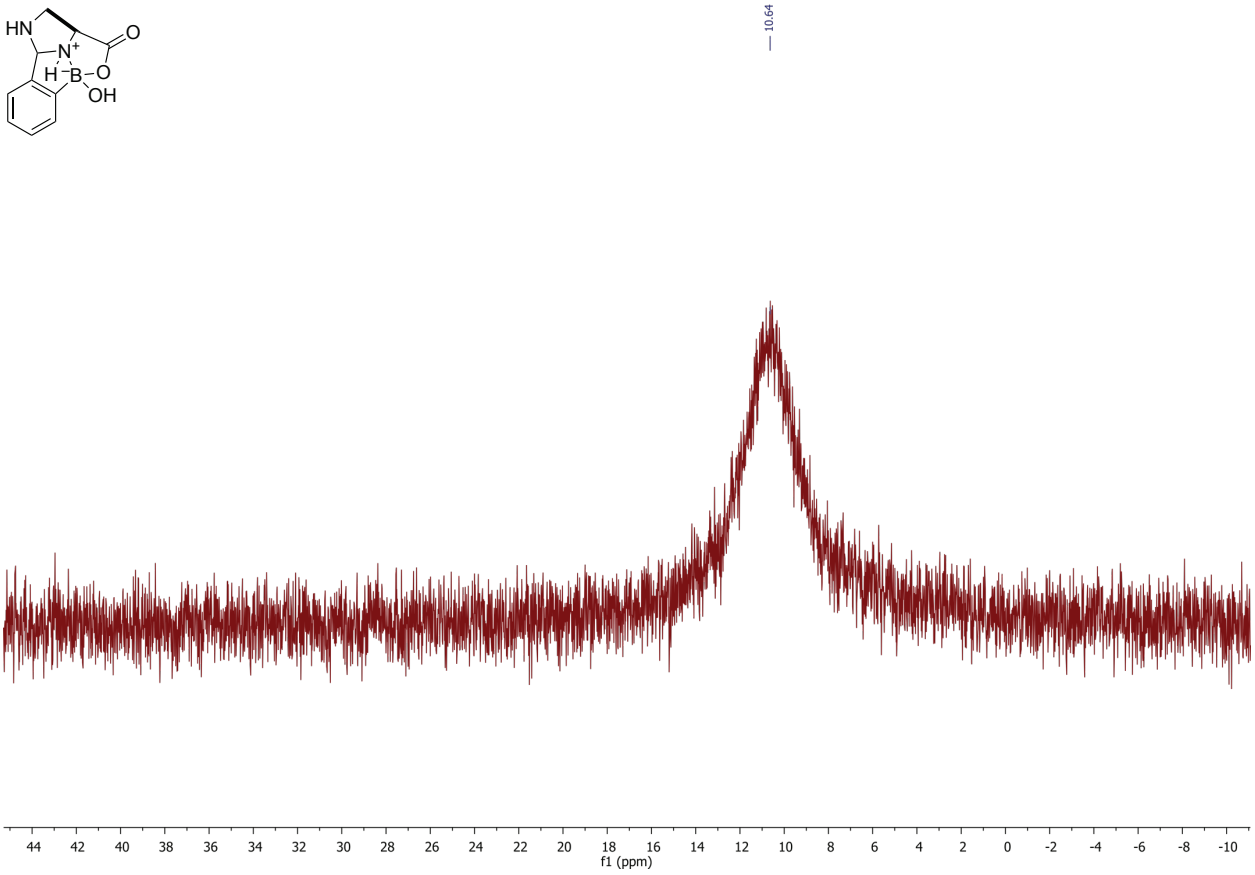

^{1}H-NMR Spectrum of 2-Formylphenylboronic Acid–Tris Base Complex

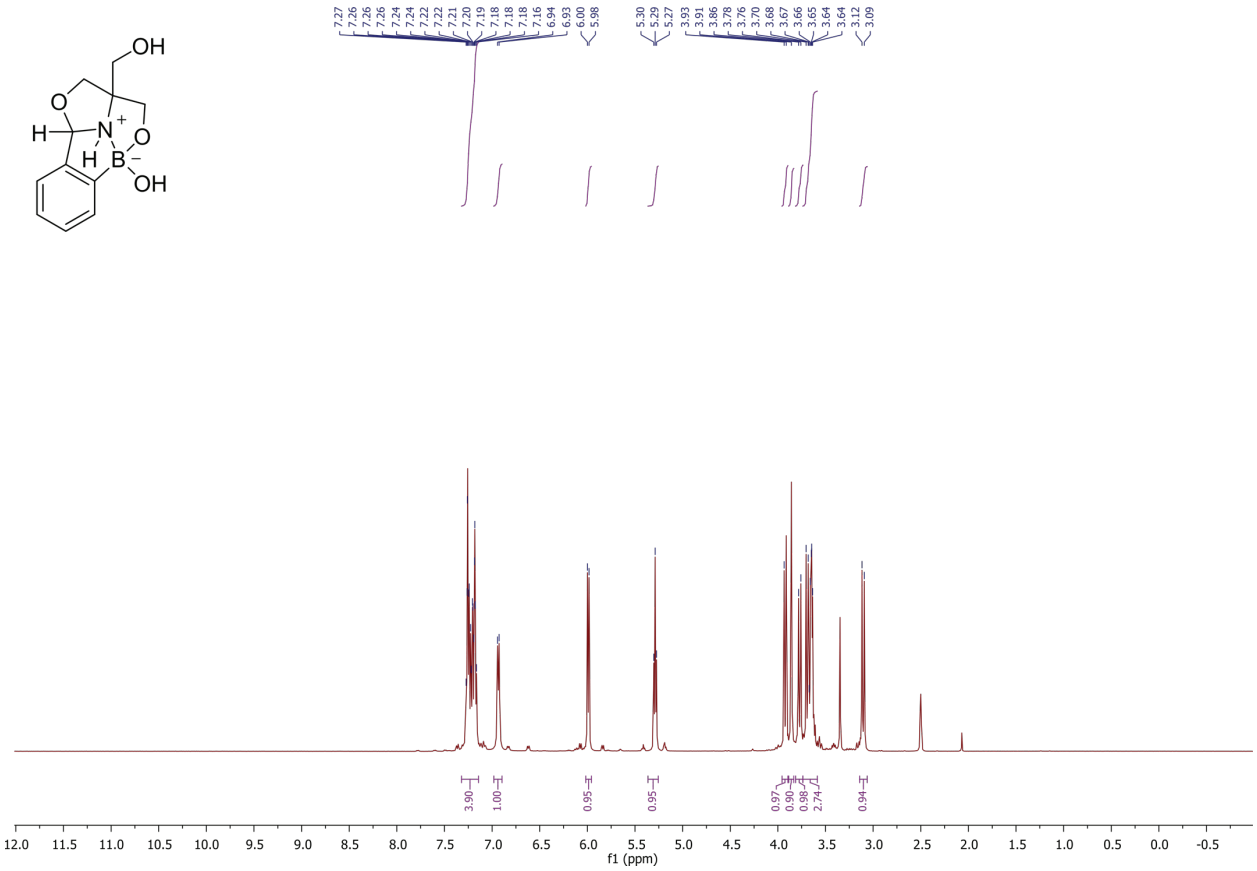

^{13}C-NMR Spectrum of 2-Formylphenylboronic Acid–Tris Base Complex

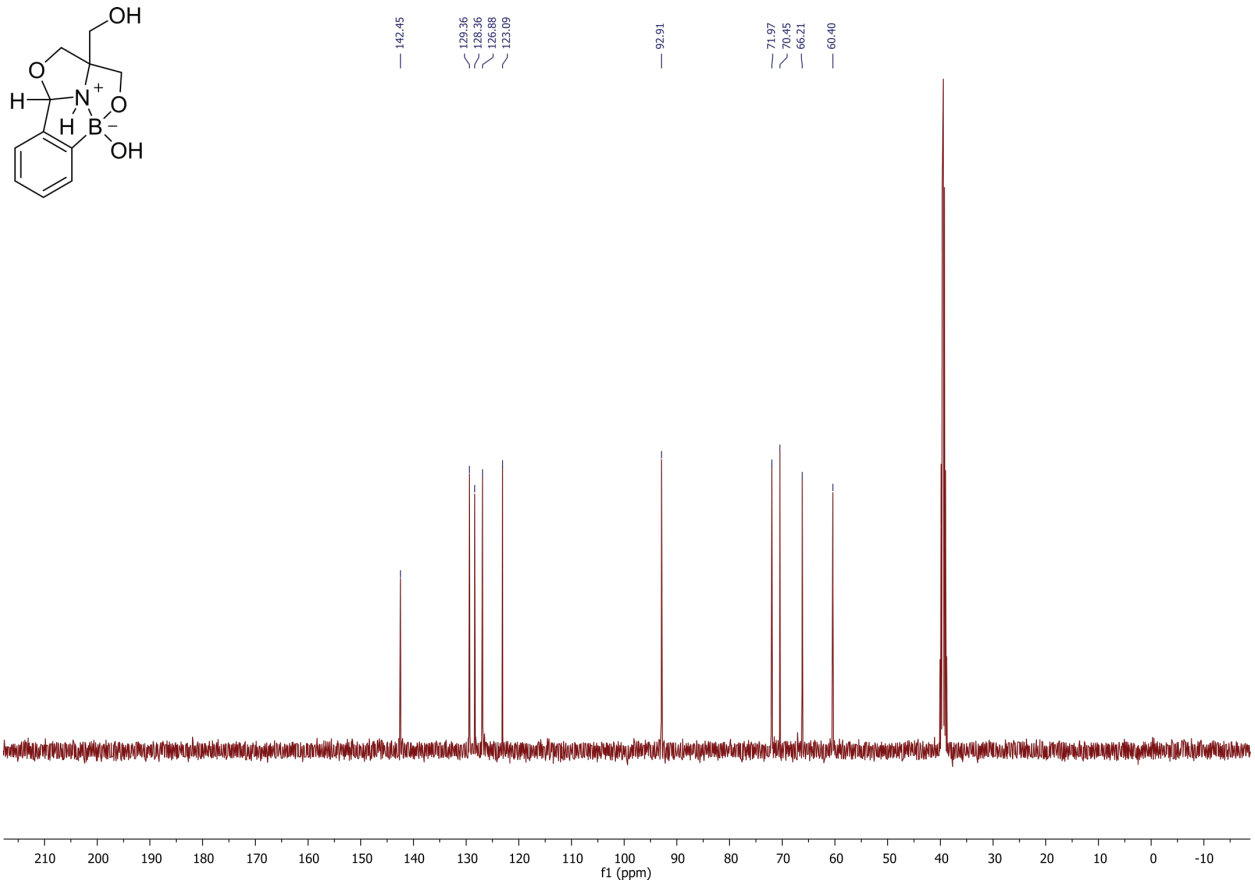

^{11}B-NMR Spectrum of 2-Formylphenylboronic Acid–Tris Base Complex

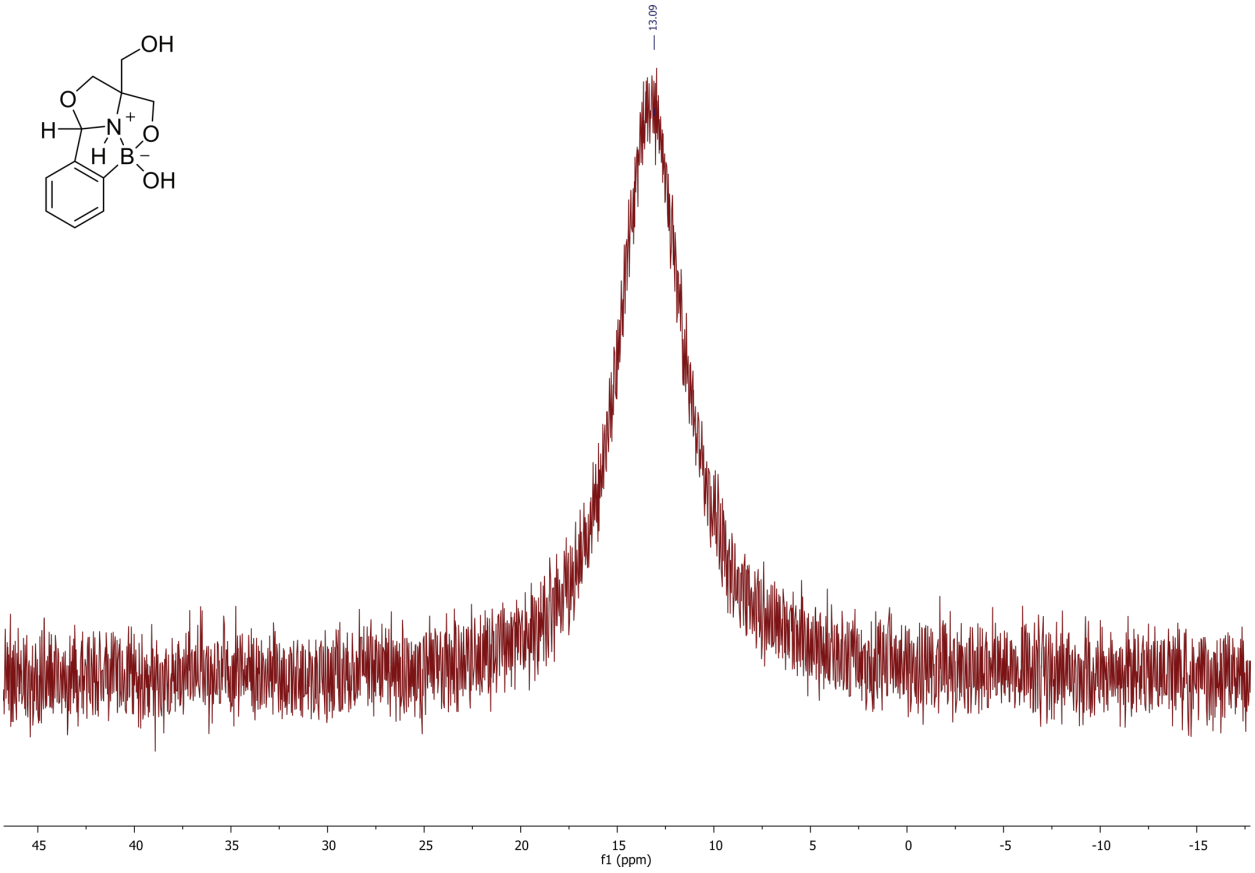

^{1}H-NMR Spectrum of 2-Acetylphenylboronic Acid–Tris Base Complex

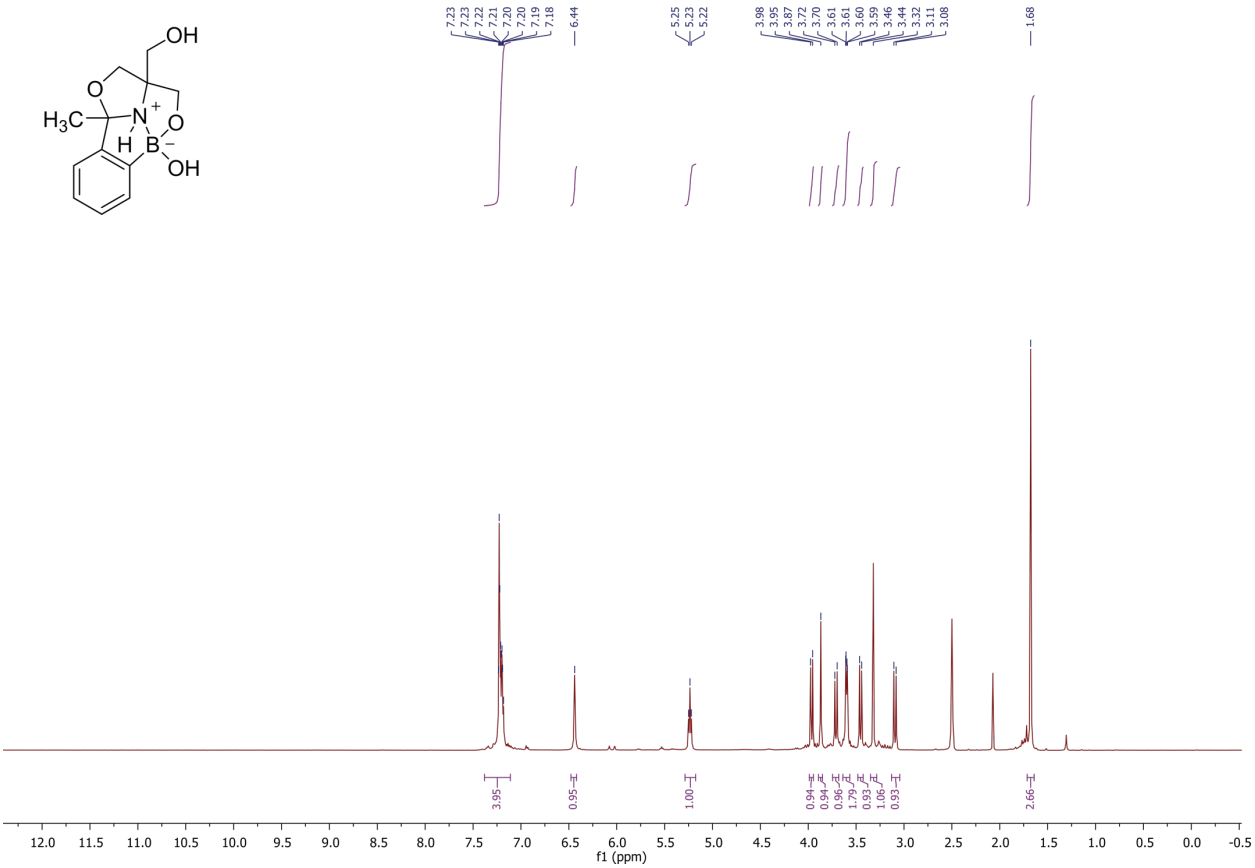

^{13}C-NMR Spectrum of 2-Acetylphenylboronic Acid–Tris Base Complex

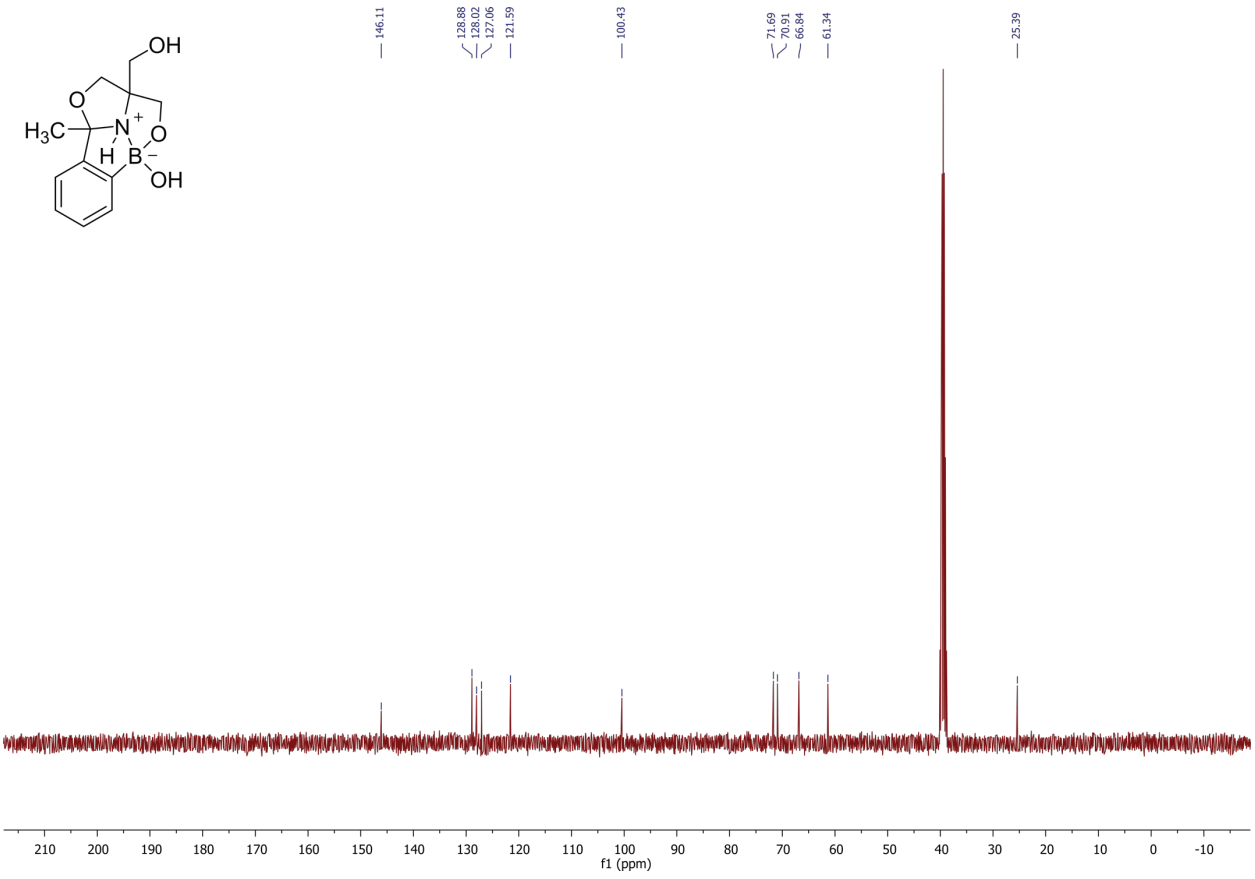

^{11}B-NMR Spectrum of 2-Acetylphenylboronic Acid–Tris Base Complex

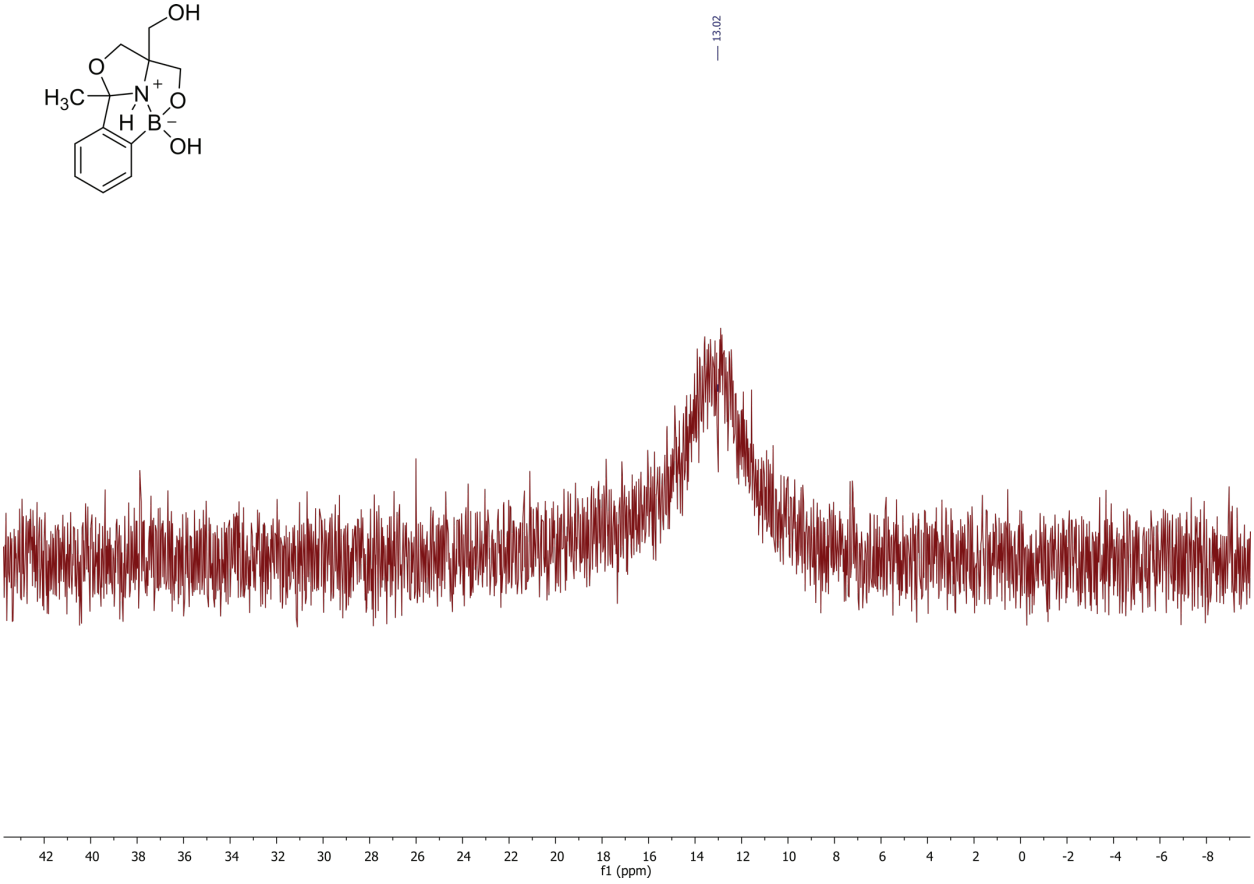

^{1}H-NMR Spectrum of Compound **2**

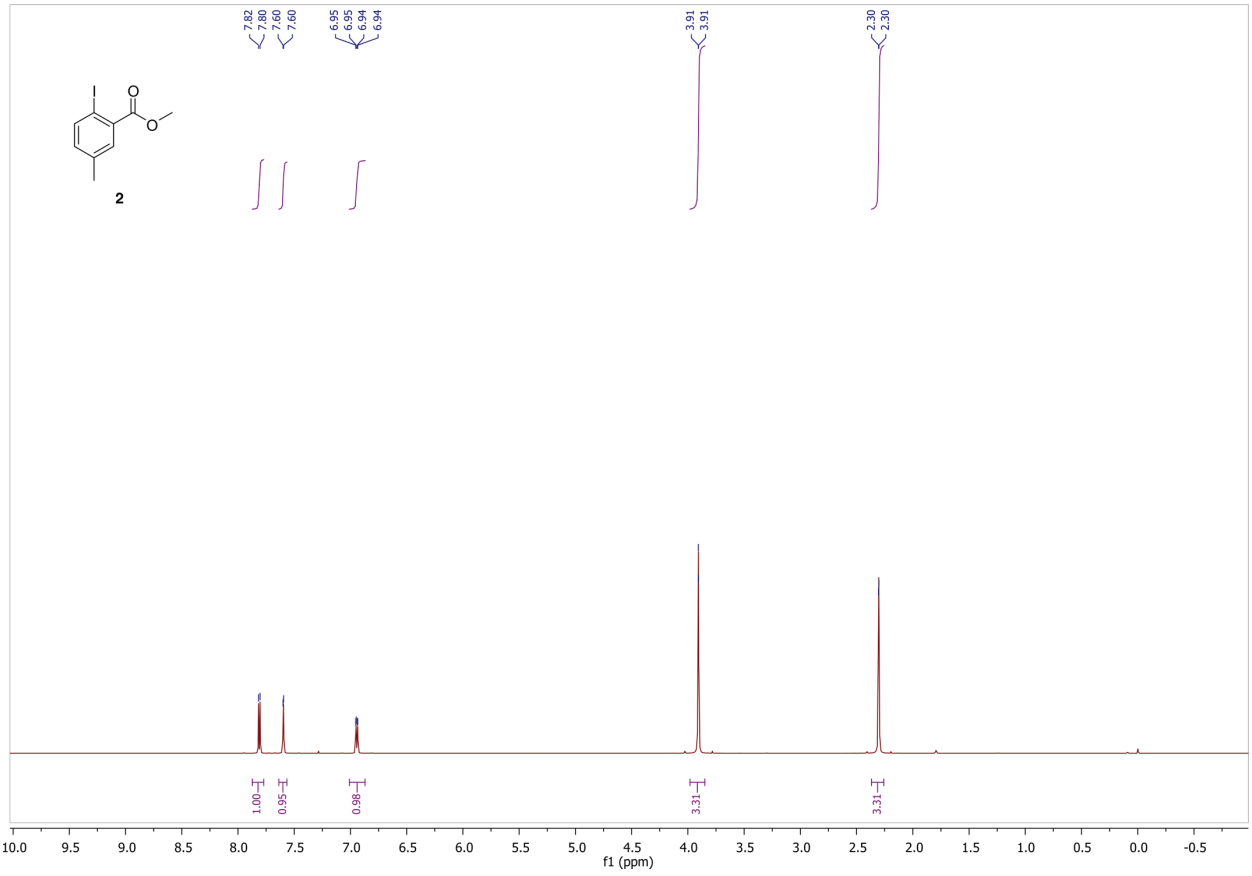

^{13}C-NMR Spectrum of Compound **2**

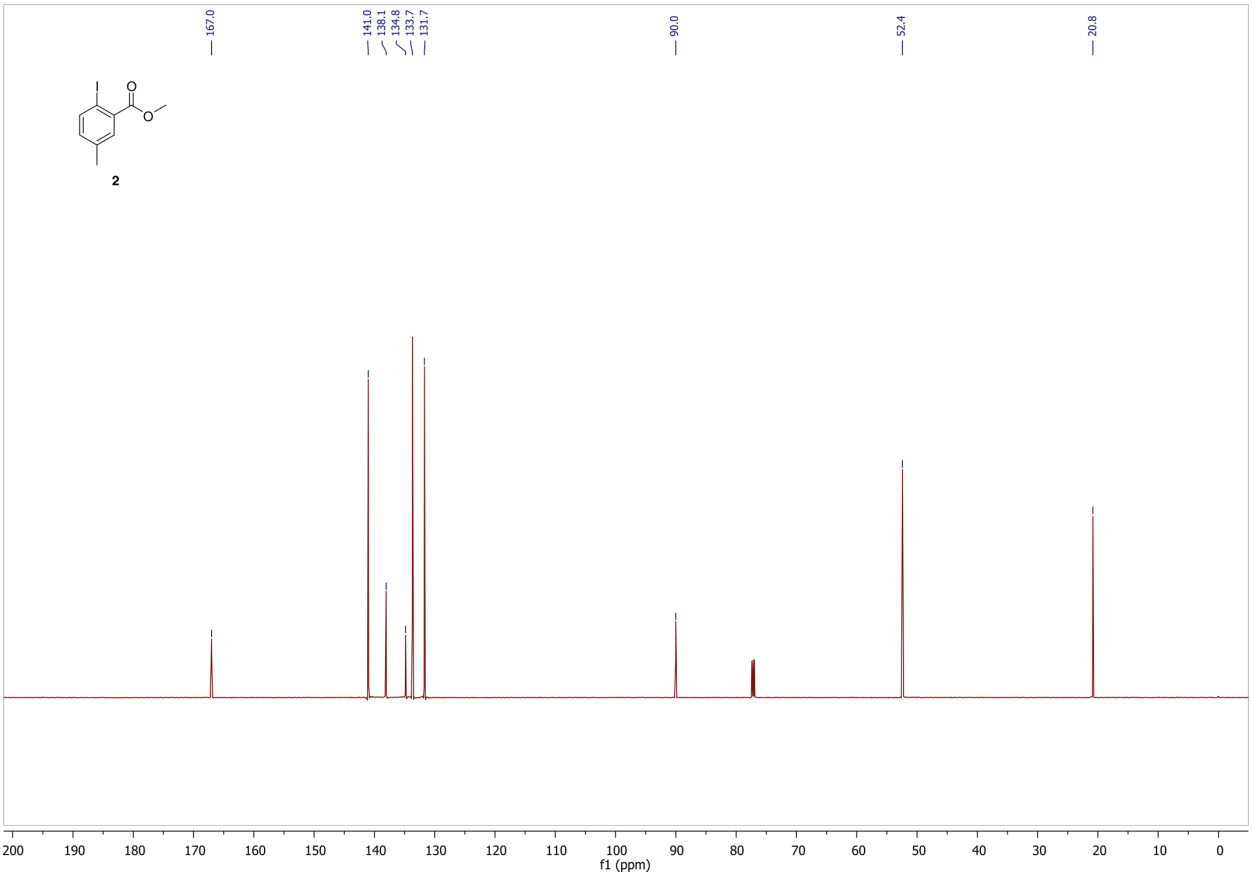

^{1}H-NMR Spectrum of Compound **3**

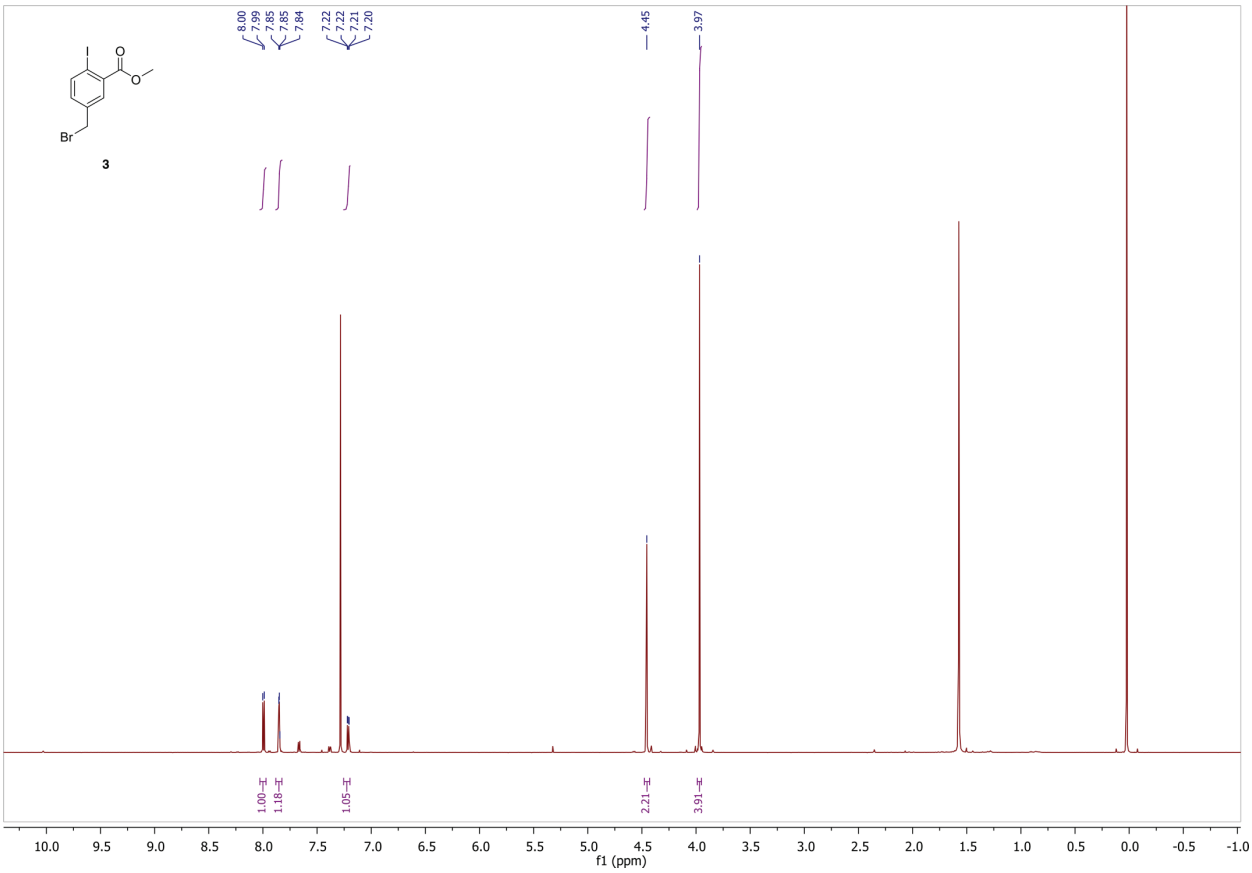

^{13}C-NMR Spectrum of Compound **3**

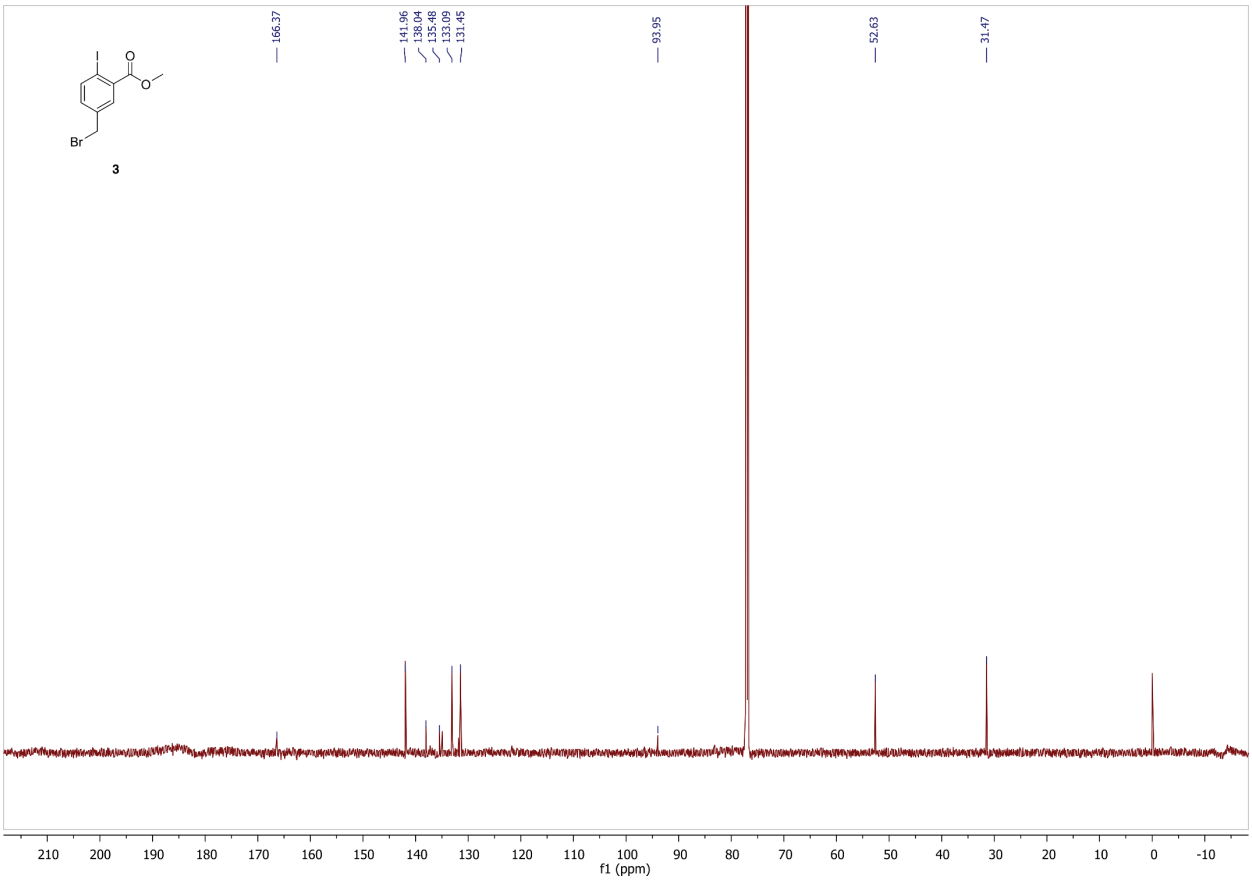

^{1}H-NMR Spectrum of Compound **4**

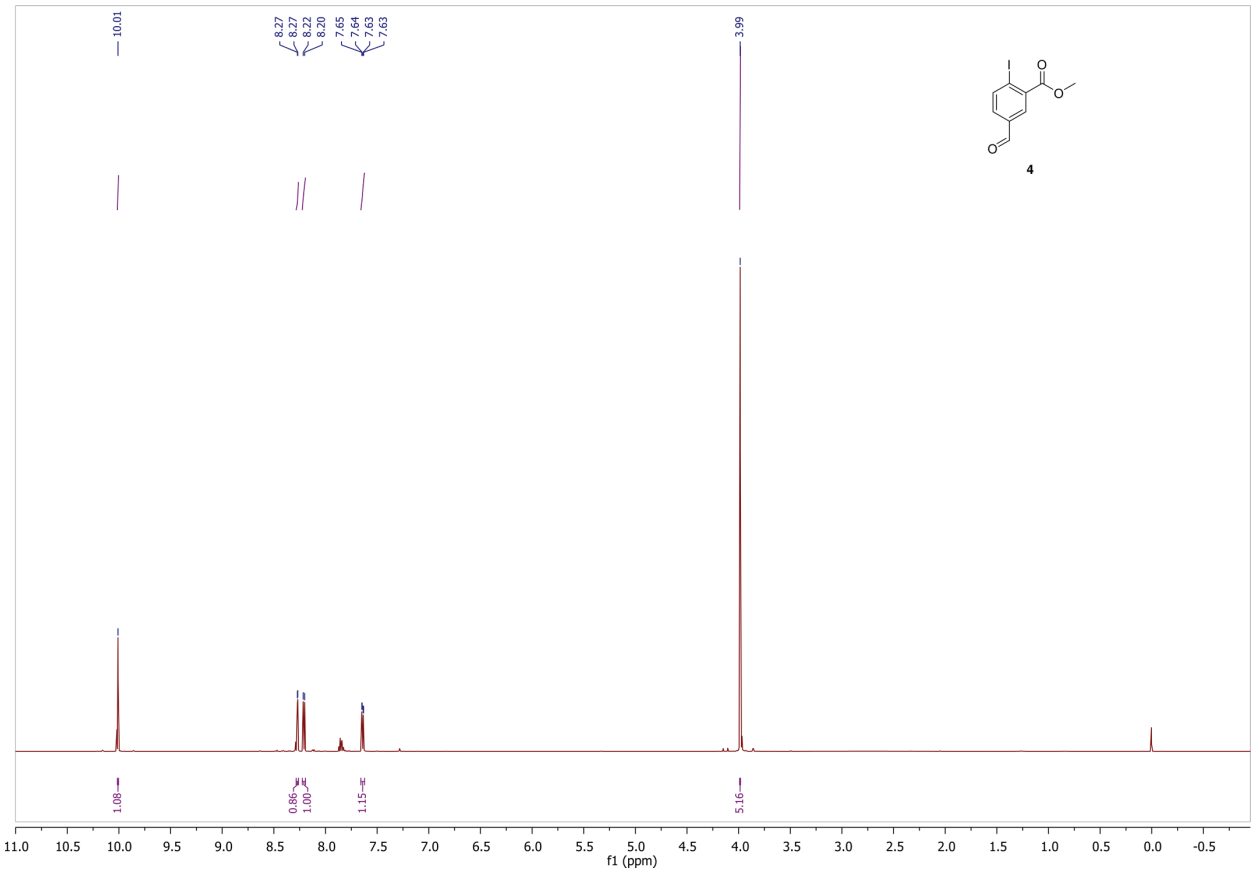

^{13}C-NMR Spectrum of Compound **4**

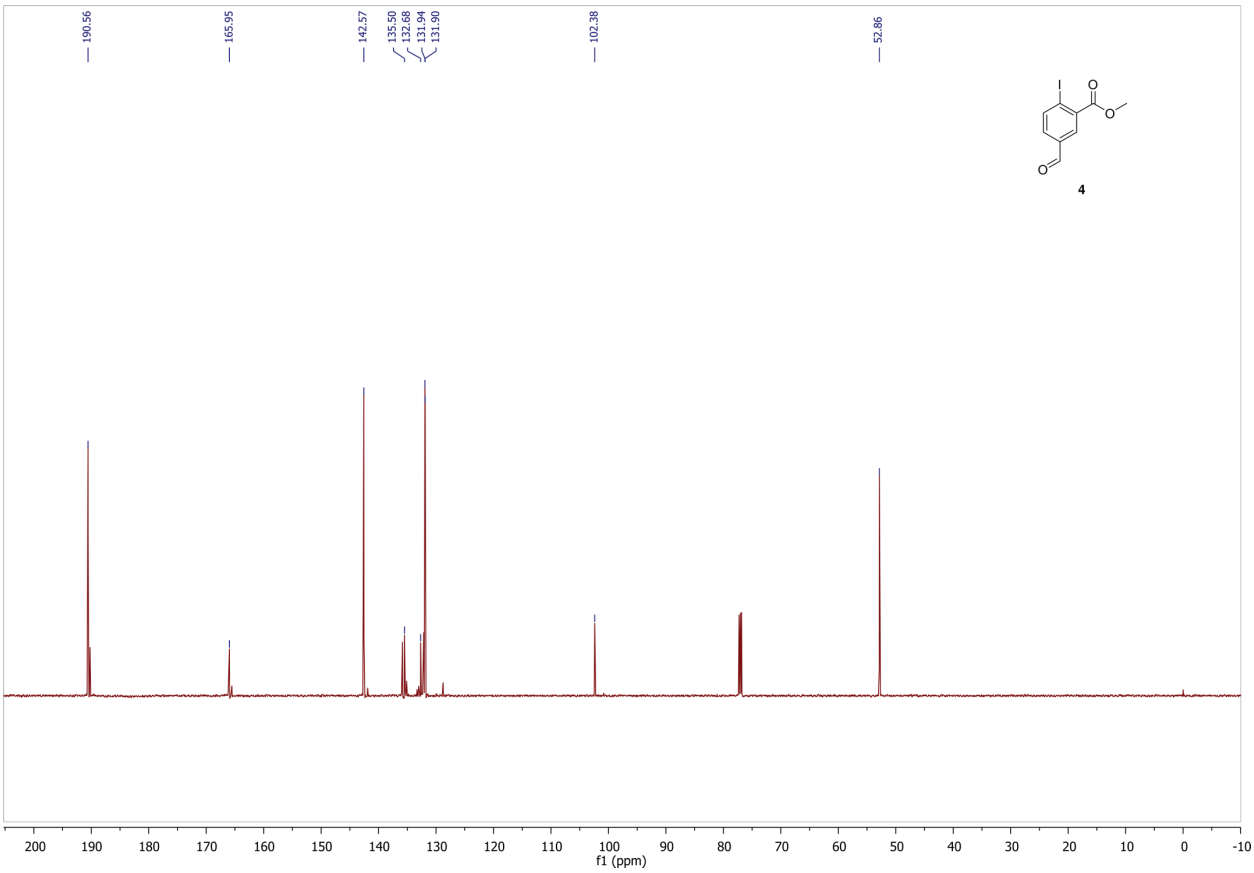

^{1}H-NMR Spectrum of Compound **5**

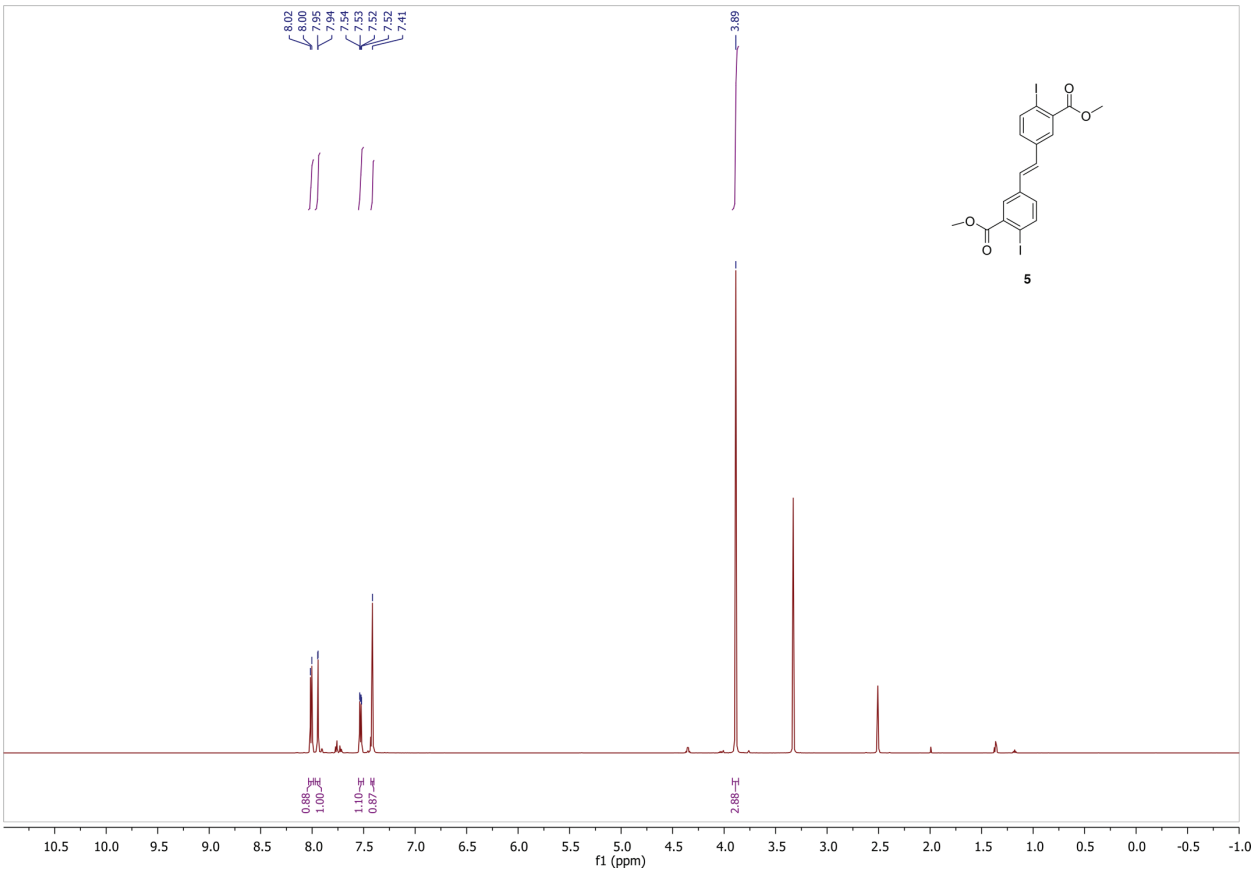

^{13}C-NMR Spectrum of Compound **5**

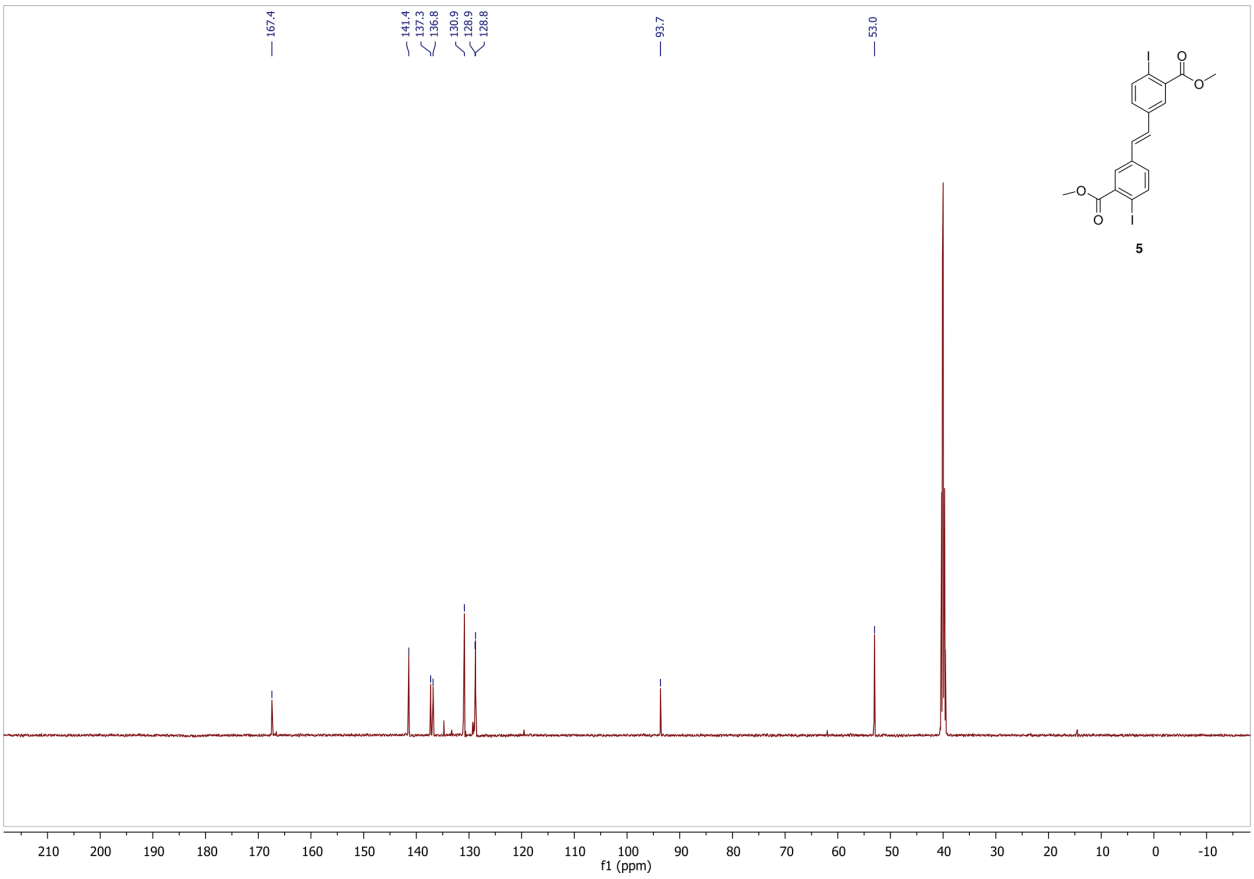

^{1}H-NMR Spectrum of Stilbene **1**

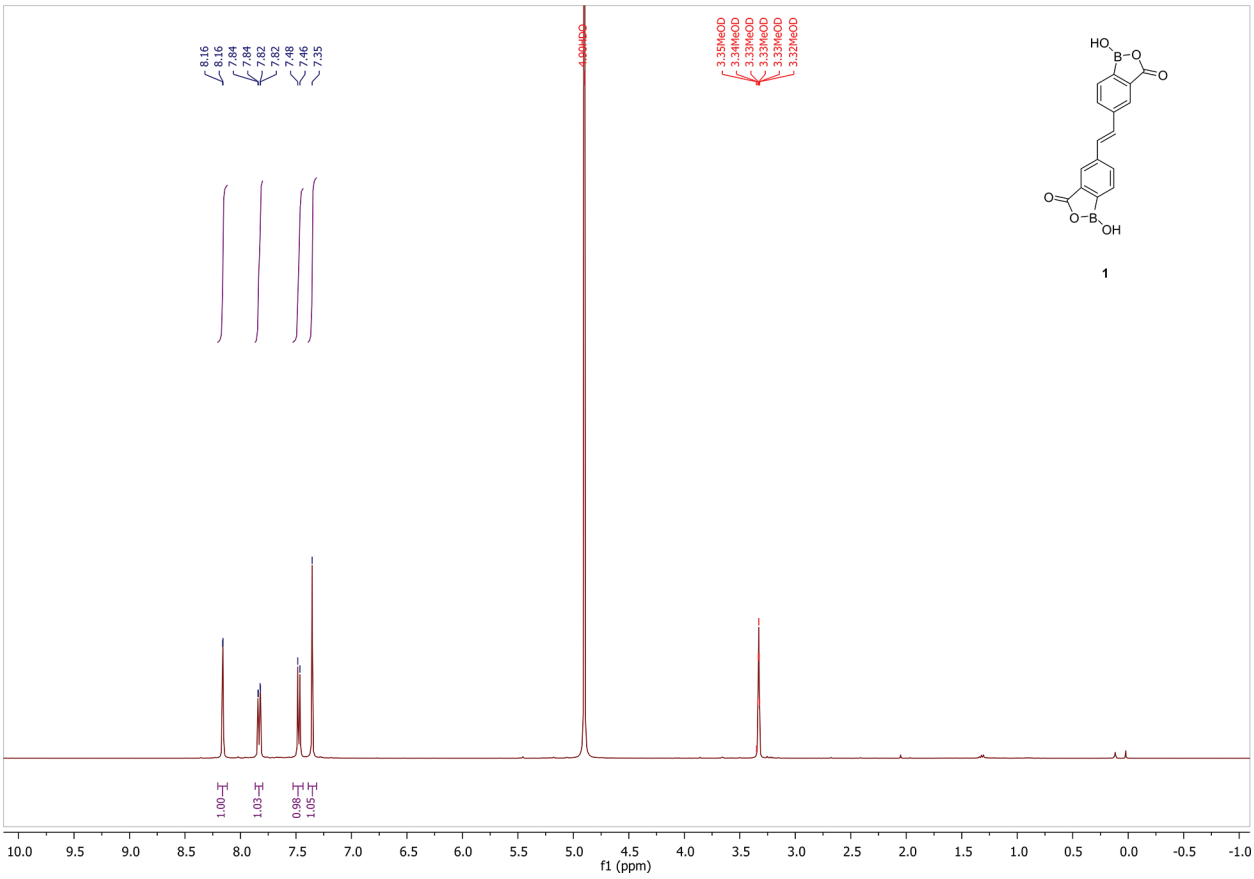

^{13}C-NMR Spectrum of Stilbene **1**

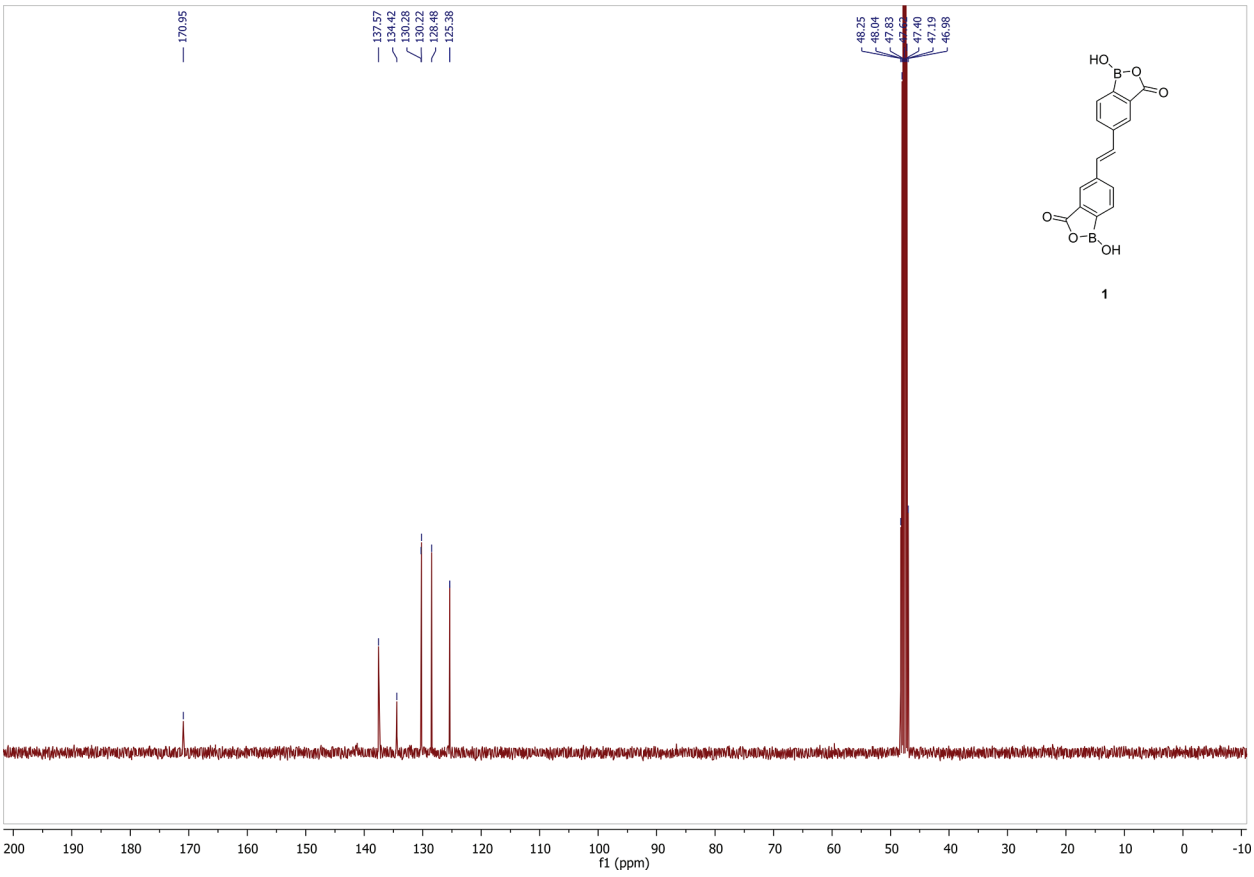

^{11}B-NMR Spectrum of Stilbene **1**

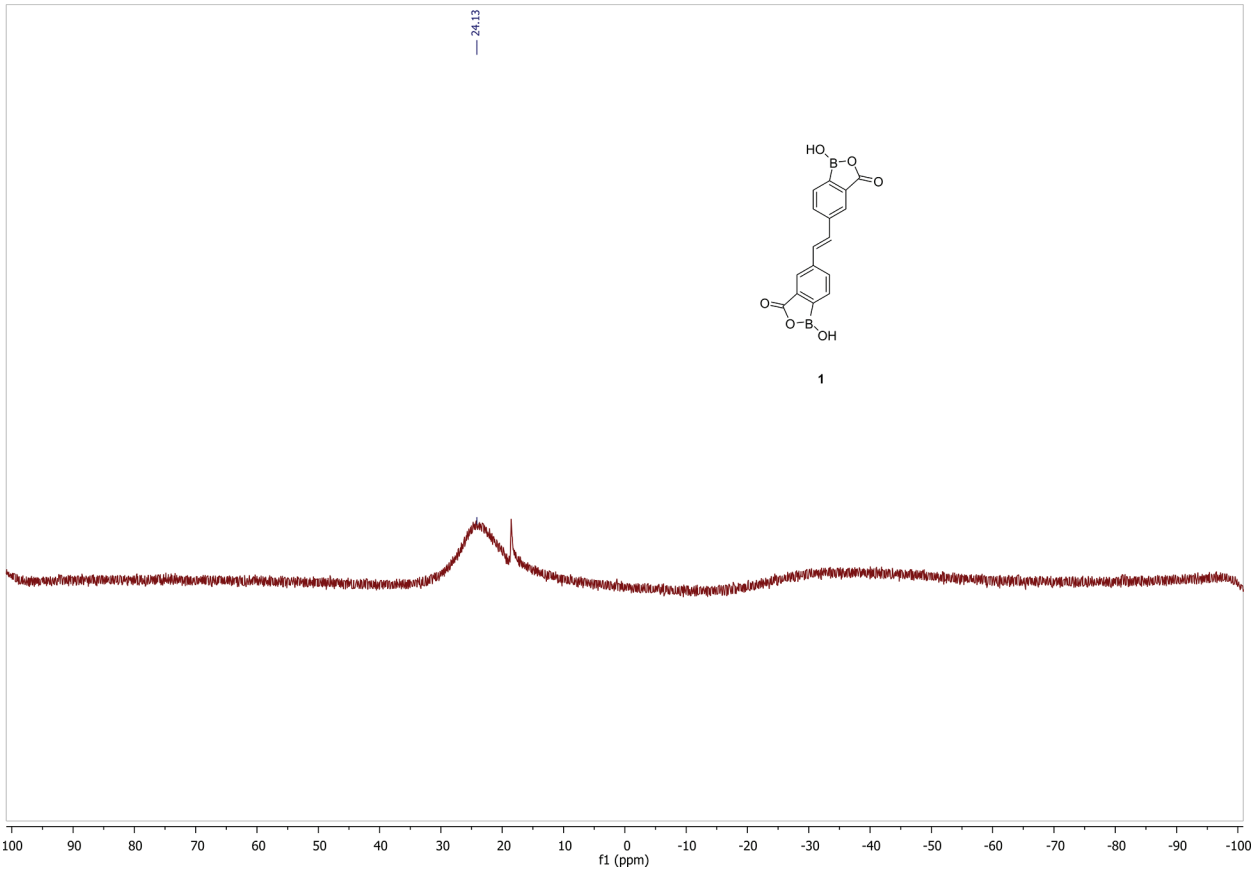

^{1}H-NMR Spectrum of Compound **6**

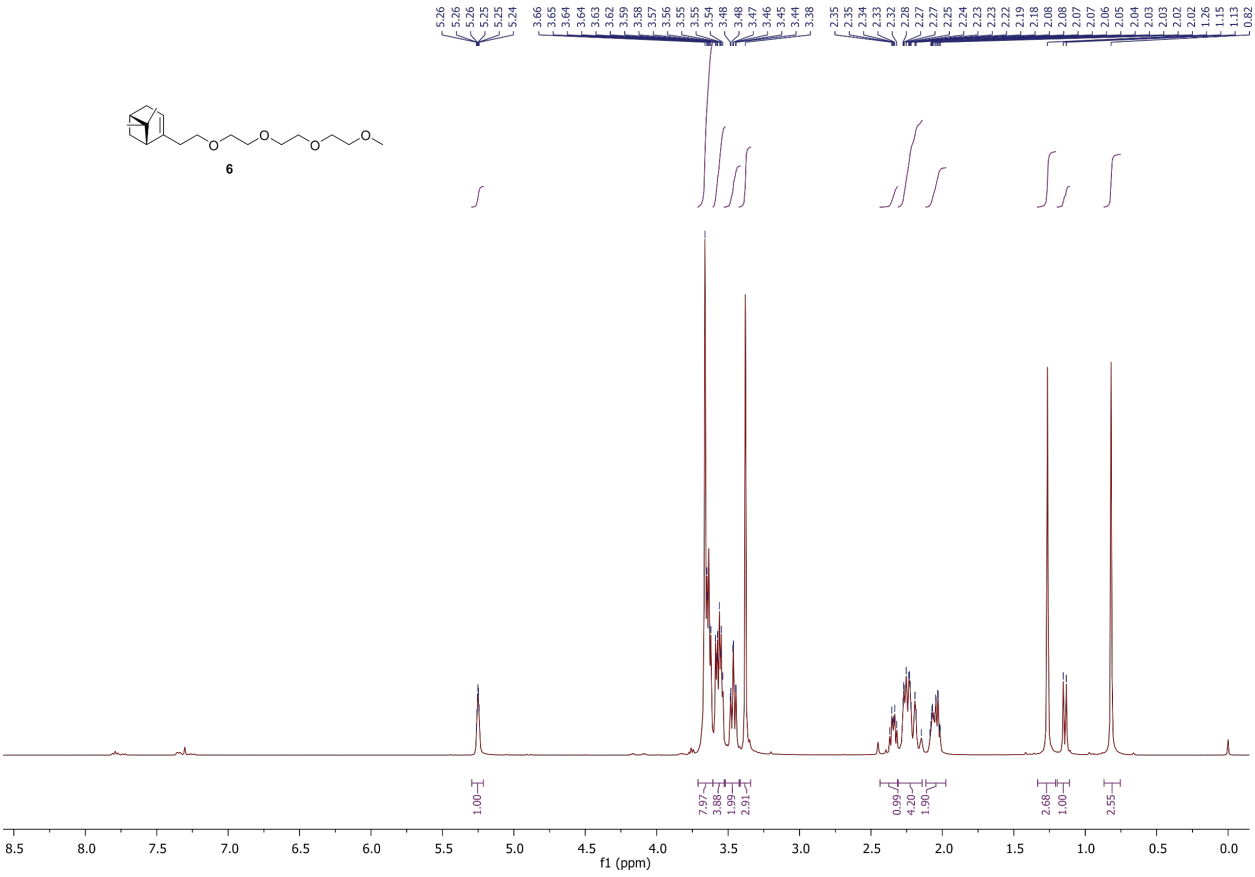

^{13}C-NMR Spectrum of Compound **6**

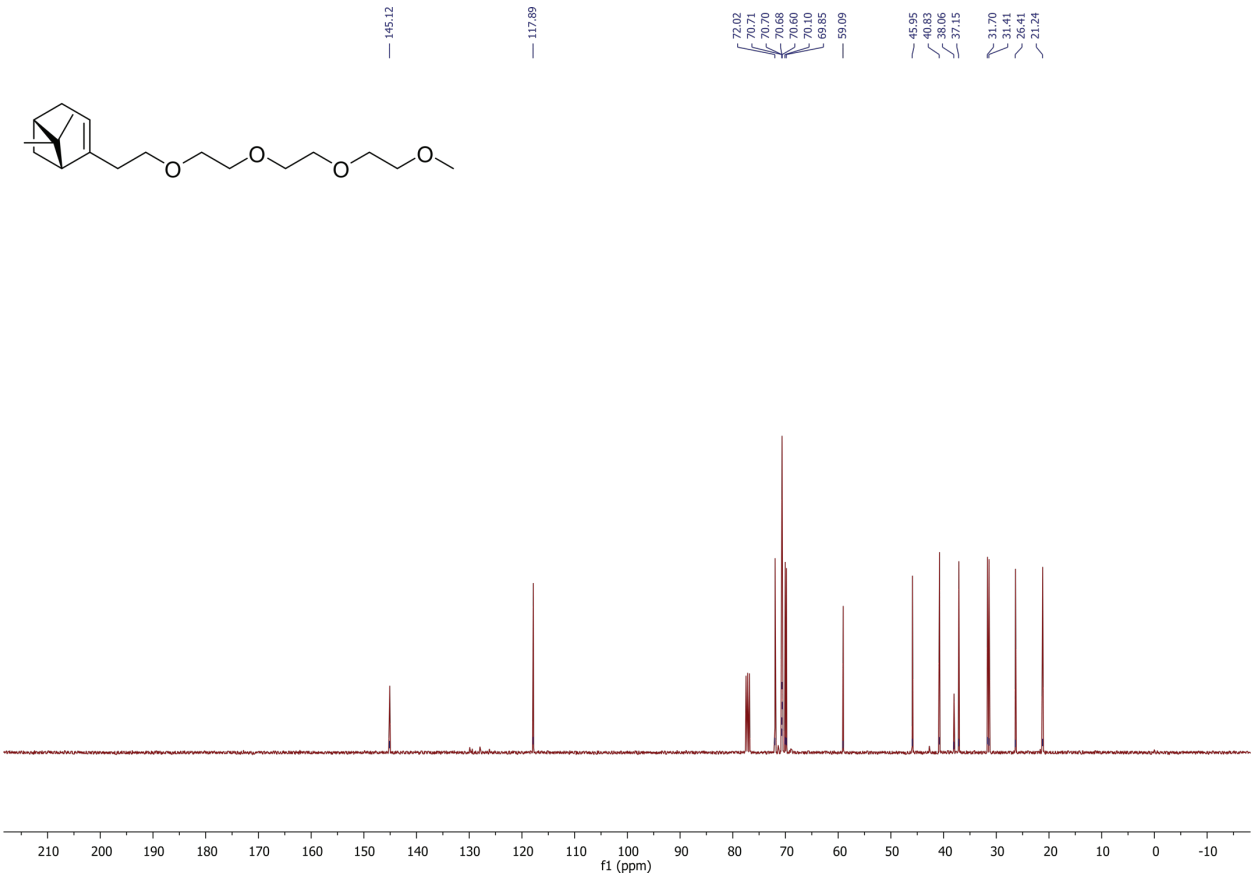

^{1}H-NMR Spectrum of Compound **7**

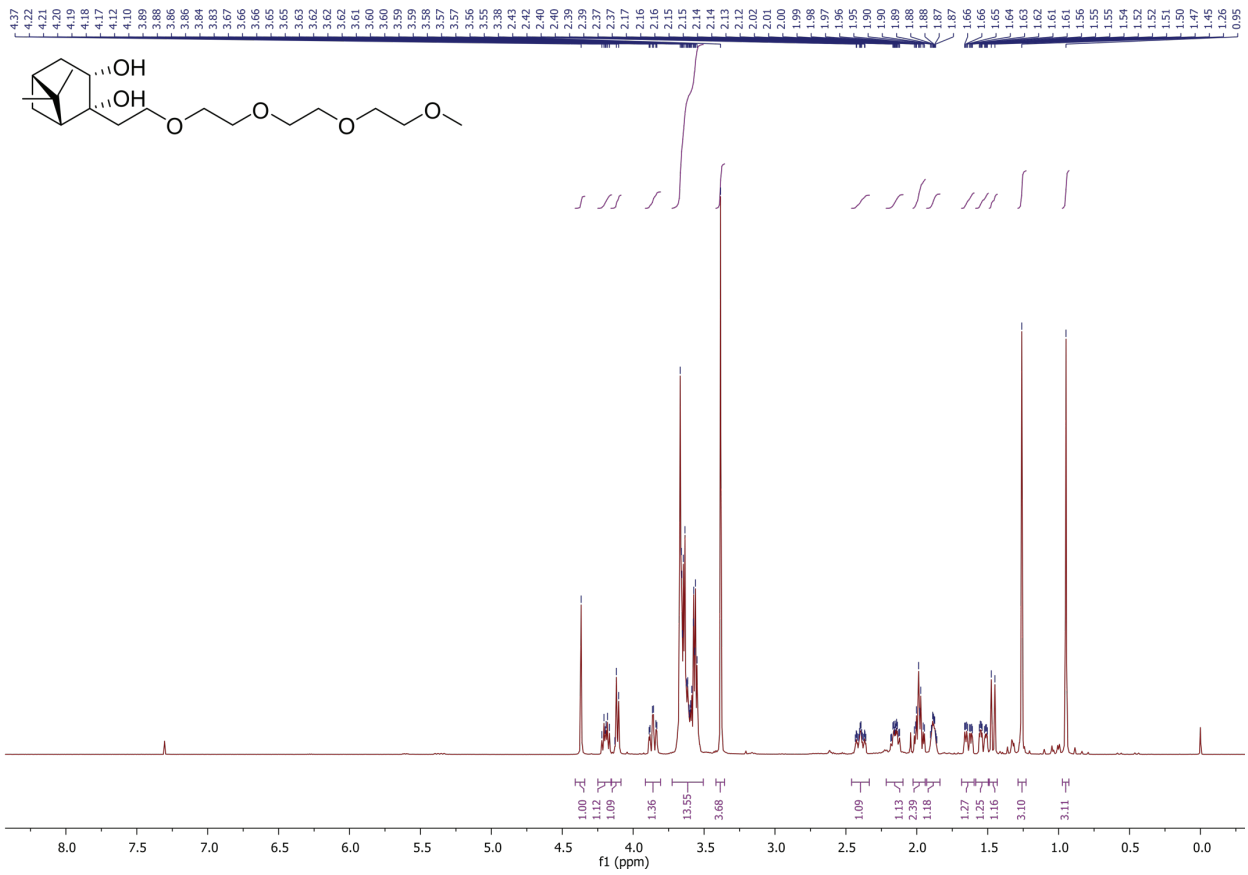
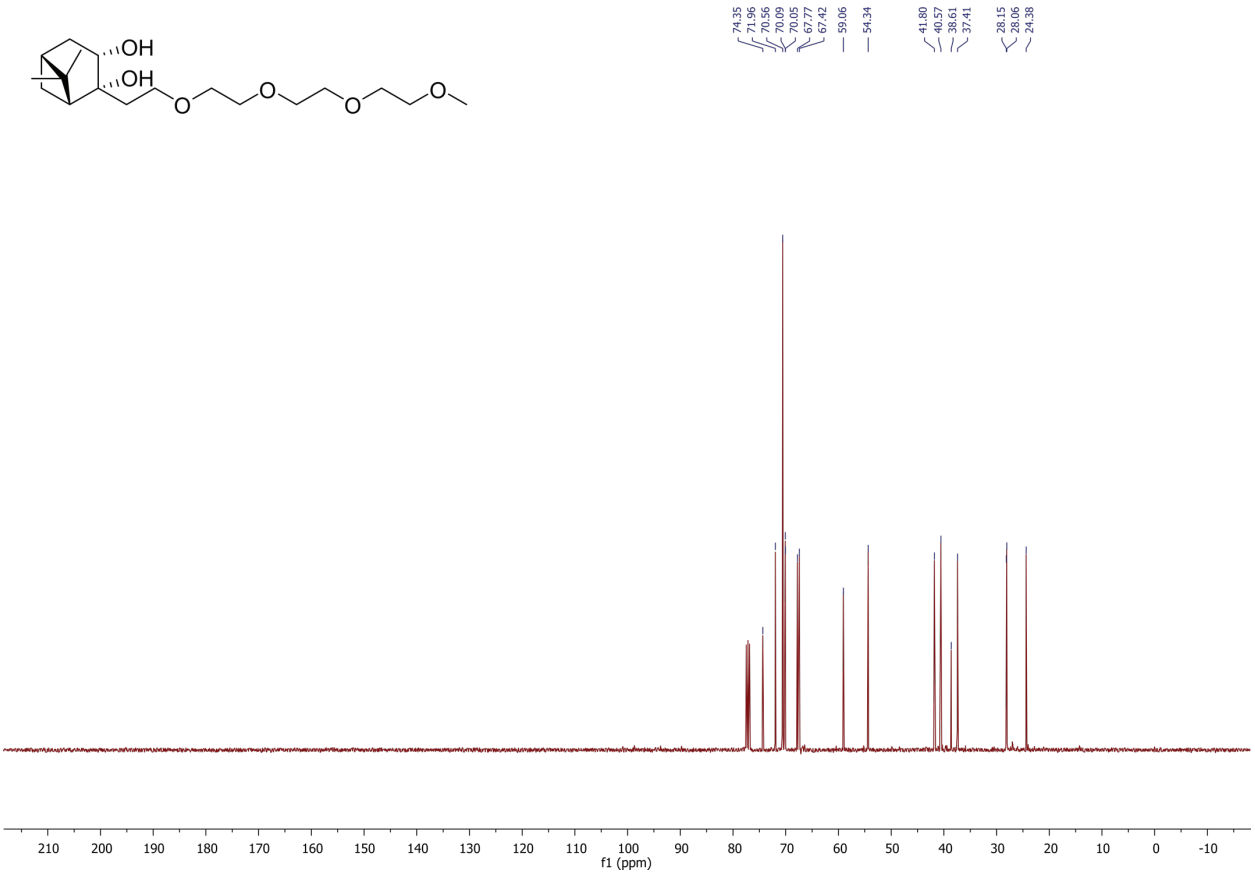
^{13}C-NMR Spectrum of Compound **7**